

# An overview of semiconductor photocatalysis

Andrew Mills \*, Stephen Le Hunte

*Department of Chemistry, University of Wales Swansea, Singleton Park, Swansea SA2 8PP, UK*

*Keywords:* Semiconductor photocatalysis; Heterogeneous photocatalysis

## 1. Introduction

The interest in heterogeneous photocatalysis is intense and increasing, as shown by the number of publications on this theme which regularly appear in this journal, and the fact that over 2000 papers have been published on this topic since 1981. This article is an overview of the field of semiconductor photocatalysis: a brief examination of its roots, achievements and possible future. Scheme 1 identifies some of the past and present guises of semiconductor photochemistry and associated major reviews [1–33]. The semiconductor titanium dioxide ( $\text{TiO}_2$ ) features predominantly in past and present work on semiconductor photocatalysis; as a result, in most of the examples selected in this overview to illustrate various points the semiconductor is  $\text{TiO}_2$ .

Most of the articles on semiconductor photocatalysis in this volume fit comfortably under at least one of the headings in Scheme 1. Thus the bulk of the papers in this volume fall largely under the heading of: “Semiconductor particles as photocatalysts for the oxidation of organic pollutants by oxygen”; this is not at all unrepresentative and simply reflects the prevalent strong research activity in this area; these papers include the work of: Singhal et al. (Photocatalytic degradation of cetylpyridinium over titanium dioxide powders), K.E. O’Shea et al. (Photocatalytic decomposition of organophosphonates in irradiated  $\text{TiO}_2$  suspensions), M. Bouchy et al. (Inhibition of the adsorption and the photocatalytic degradation of an organic contaminant in a  $\text{TiO}_2$  aqueous suspension), B. Viswanathan et al. (Synthesis, characterization and photocatalytic properties of iron-doped  $\text{TiO}_2$  catalysts), R.R. Hills et al. (Photocatalytic detoxification of aqueous 1,4-dioxane) and Maurette et al. (Photocatalytic degradation of 2,4-dihydroxybenzoic acid in water: efficiency, optimization and mechanistic investigations).

The work of Richard et al. (Photocatalytic transformations of aromatic compounds in aqueous zinc oxide suspensions: effect of substrate concentrations on the distribution of prod-

ucts) is an example of “Semiconductor particles as photosensitizers for organic photosynthetic processes”, and the work of B. Viswanathan et al. (Photocatalytic reduction of nitrite and nitrate ions to ammonia on  $\text{M}/\text{TiO}_2$  catalysts) is an example of “Semiconductor particles as photocatalysts for the removal of inorganic pollutants” (Scheme 1). Finally, the work of Lobedank et al. (Sensitized photocatalytic oxidation of herbicides using natural sunlight) has a close association with recent work on “Semiconductor colloids and Q-particles” (Scheme 1), as we shall see.

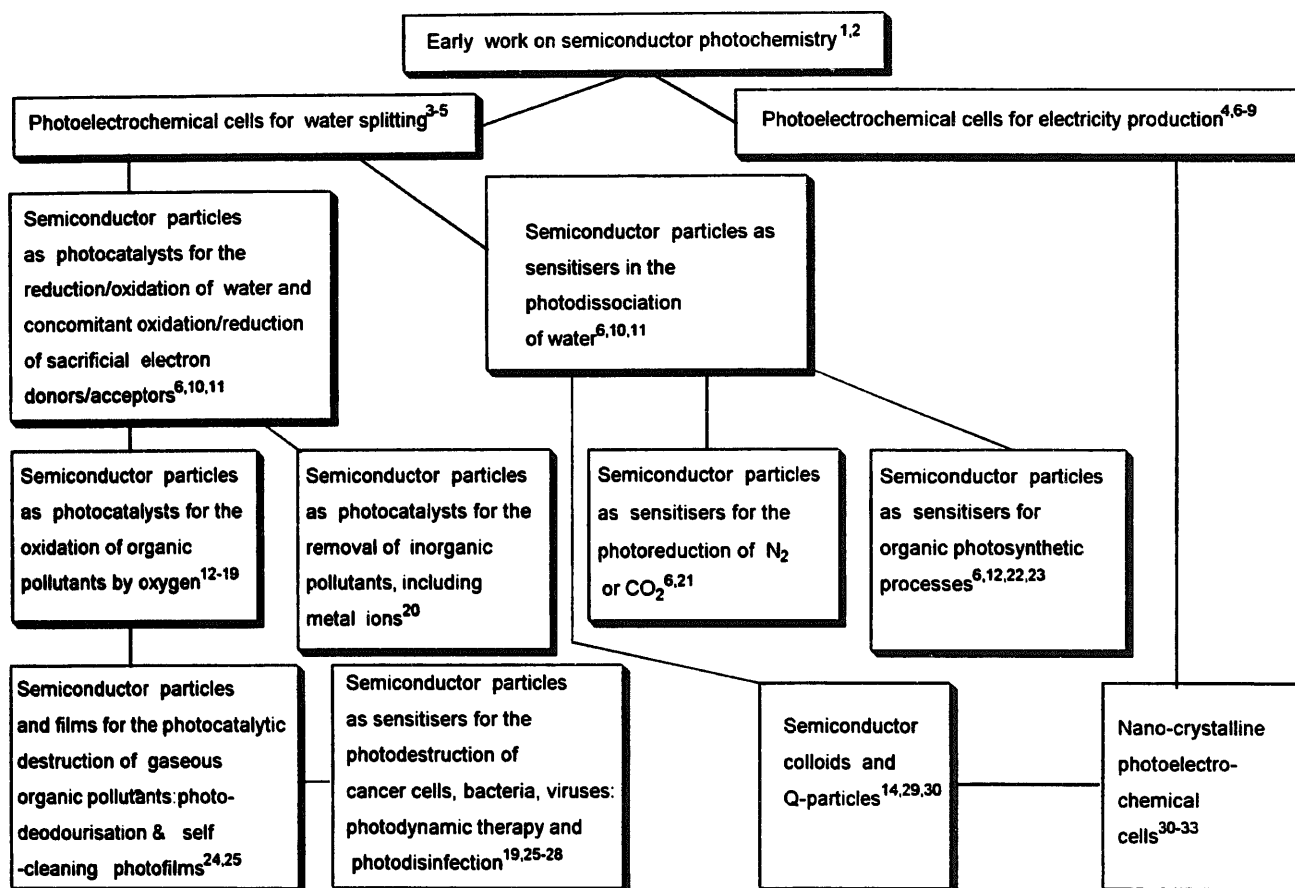
The work of D. Katakis et al. (New catalysts in the photo-oxidation of water) and Navio et al. (UV photoassisted degradation of phenyltin(IV) chlorides in water) are both examples of homogeneous photochemistry (the latter work is not an example of photocatalysis) and fall outside the scope of this overview.

Although Scheme 1 forms the basis of the main part of this overview, it seems appropriate to begin with a brief look at terms and basic principles.

## 2. Photocatalysis and photosynthesis

The term “photocatalysis” is still the subject of some debate. For example, it is argued [34] that the idea of a photocatalysed reaction is fundamentally incorrect, since it implies that, in the reaction, light is acting as a catalyst, whereas it always acts as a reactant which is consumed in the chemical process. In reality the term “photocatalysis” is in widespread use and is here to stay; it is not meant to, nor should it ever be used to, imply catalysis by light, but rather the “acceleration of a photoreaction by the presence of a catalyst”. The term “photoreaction” is sometimes elaborated on as a “photoinduced” or “photoactivated” reaction, all to the same effect. The above definition of “photocatalysis” includes the process of “photosensitization”, i.e. a process by which a photochemical alteration occurs in one chemical species as a result of the initial absorption of radiation by another chemical species called the photosensitizer.

\* Corresponding author. Tel.: +44 1792 295269; e-mail: A.Mills@swan.ac.uk



Scheme 1.

It follows from the above that heterogeneous photocatalysis involves photoreactions which occur at the surface of a catalyst. If the initial photoexcitation process occurs in an adsorbate molecule, which then interacts with the ground state of the catalyst substrate, the process is referred to as a "catalysed photoreaction". If, on the other hand, the initial photoexcitation takes place in the catalyst substrate and the photoexcited catalyst then interacts with the ground state adsorbate molecule, the process is a "sensitized photoreaction". In most cases, heterogeneous photocatalysis refers to semiconductor photocatalysis or semiconductor-sensitized photoreactions.

It is sometimes argued that the term "catalysis" should not be used unless it has been demonstrated that the turnover number (TN) for the process (i.e. the number of product molecules per number of active sites) is greater than unity; if this is not demonstrated, the term "heterogeneous (or semiconductor)-assisted photoreaction" should be used. In most examples of heterogeneous photocatalysis, the value of TN has not been demonstrated to be greater than unity because of the difficulty in determining the number of active sites on irradiation.

When titanium dioxide is used as the semiconductor sensitizer, it is sometimes assumed that the number of active sites can be taken as the product of the surface density of OH<sup>-</sup> groups (typically 10<sup>12</sup>–10<sup>15</sup> cm<sup>-2</sup>) and the specific surface

area of TiO<sub>2</sub>. However, the latter parameter is usually measured using the powder in the dry state (the Brunauer–Emmett–Teller (BET) surface area), and the actual surface area of the TiO<sub>2</sub> photocatalyst dispersed in solution will depend on the degree of aggregation. In addition, it does not follow that all the surface sites occupied by the OH<sup>-</sup> groups will be necessarily active. These approximations are likely to lead to a value for TN which is lower than the actual value; thus, if by carrying out such calculations it can be shown that TN is still greater than unity, it appears reasonable to assume that the process under examination is a "catalysed", rather than "assisted", reaction. For most research conducted in the area of semiconductor-assisted photoreactions, it is assumed that the process under study is an example of semiconductor-sensitized heterogeneous photocatalysis, especially if it can be shown, or it is known, that there is no evidence of a marked loss in semiconductor photoactivity with extended use.

The overall process of semiconductor-sensitized photoreactions can be summarized as follows



where  $E_{\text{bg}}$  is the bandgap of the semiconductor (see below). If, in the absence of semiconductor and light of energy greater than or equal to  $E_{\text{bg}}$ ,  $\Delta G^\circ$  for reaction (1) is negative, the

Table 1

Examples of TiO<sub>2</sub>-sensitized photosynthetic and photocatalytic processes

Reaction $A + D \rightarrow A^- + D^+$	Description	$\Delta G^\circ$ (kJ mol <sup>-1</sup> )	Reference
<b>Photosynthesis</b>			
$H_2O + H_2O \rightarrow 2H_2 + O_2$	Water splitting	475	[10,11]
$2CO_2 + 4H_2O \rightarrow 2CH_3OH + 3O_2$	Carbon dioxide reduction	1401	[6]
$2N_2 + 6H_2O \rightarrow 4NH_3 + 3O_2$	Nitrogen reduction	1355	[21]
$6CO_2 + 6H_2O \rightarrow C_6H_{12}O_6 + 6O_2$	Green plant photosynthesis	2895	[34]
<b>Photocatalysis</b>			
$3O_2 + 2CH_3OH \rightarrow 4H_2O + 2CO_2$	Methanol mineralization	-1401	[35]
$2HAuCl_4 + CH_3OH + H_2O \rightarrow 2Au + 8HCl + CO_2$	Deposition of precious metals	-	[36]
$6H_2O + C_6H_{12}O_6 \rightarrow 12H_2 + 6CO_2$	Biomass conversion to hydrogen	-32	[37]

semiconductor-sensitized photoreaction is an example of photocatalysis [5]. Alternatively, if  $\Delta G^\circ$  for reaction (1) is positive, the semiconductor-sensitized photoreaction is an example of photosynthesis [5]. Reported examples [6,10,11,21,35–38] of the two different semiconductor-sensitized photoreactions are given in Table 1.

### 3. Basic principles

As indicated in Fig. 1, for many compounds, as the number  $N$  of monomeric units in a particle increases, the energy necessary to photoexcite the particle decreases. In the limit when  $N \gg 2000$ , it is possible to end up with a particle which exhibits the band electronic structure of a semiconductor, as illustrated in Fig. 1, in which the highest occupied band (the valence band) and lowest unoccupied energy band (the conduction band) are separated by a bandgap  $E_{bg}$ , a region devoid of energy levels in a perfect crystal.

As indicated in Fig. 2, activation of the semiconductor photocatalyst for reaction (1) is achieved through the absorption of a photon of ultra-bandgap energy, which results in the promotion of an electron  $e^-$  from the valence band to the

conduction band, with the concomitant generation of a hole  $h^+$  in the valence band. For a semiconductor photocatalyst to be efficient, the different interfacial electron processes involving  $e^-$  and  $h^+$ , i.e. reactions (c) and (d) in Fig. 2, must compete effectively with the major deactivation processes involving  $e^- - h^+$  recombination, i.e. reactions (a) and (b) in Fig. 2.

### 4. Early work on semiconductor photochemistry [1,2]

In 1839, Becquerel [1] reported that a voltage and an electric current were produced when a silver chloride electrode, immersed in an electrolyte solution and connected to a counter electrode, was illuminated with sunlight. It was not until 1955, with the pioneering work of Brattain and Garret [39] on germanium semiconductor electrodes, that the origin of this photovoltaic phenomenon, called the ‘‘Becquerel effect’’, was understood and the modern era of photoelectrochemistry was born. It is not usually recognized that many examples of semiconductor photocatalysis had already been reported in the literature by the early part of this century. Most notably, the semiconductor zinc oxide had attracted a great deal of attention at the turn of this century as a photosensitizer for the decomposition of organic compounds and as a sensitizer for a number of inorganic photoreactions. Much of this early work has been summarized elsewhere [2].

As early as 1929 it was known that the pigment ‘‘titanium white’’, i.e. TiO<sub>2</sub>, was responsible for fading in paints [40], and several major studies into the photosensitizing action of TiO<sub>2</sub> followed [41]. The allure of TiO<sub>2</sub> as a pigment for the paint industry stems from its high refractive index (3.87 for rutile and 2.5–3 for anatase TiO<sub>2</sub>, whereas the refractive index for diamond is 2.42). Because of its photosensitizing action, TiO<sub>2</sub> appeared initially to be unsuitable as a pigment for paint, since it caused chalking, i.e. the photodegradation of the organic polymer binder of the paint [42]. However, this undesirable feature was largely eliminated by coating the pigment with a hydrous layer of an inert oxide, such as silica, alumina or zirconia. During the 1960s, much of the theory of semiconductor photoelectrochemistry was developed, most

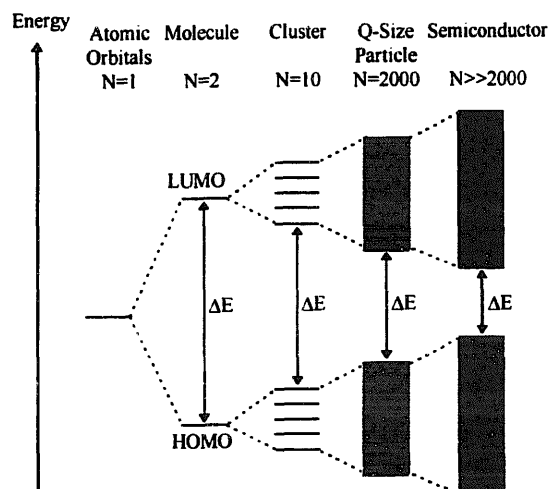


Fig. 1. Change in the electronic structure of a semiconductor compound as the number  $N$  of monomeric units present increases from unity to clusters of more than 2000 (after Ref. [16]).

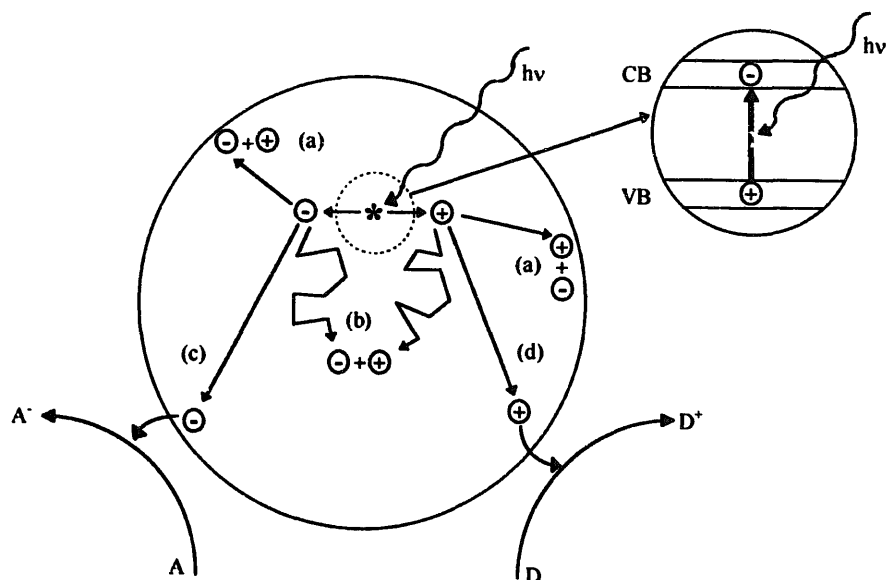


Fig. 2. Illustration of the major processes occurring on a semiconductor particle following electronic excitation. Electron-hole recombination can occur at the surface (reaction (a)) or in the bulk (reaction (b)) of the semiconductor. At the surface of the particle, photogenerated electrons can reduce an electron acceptor A (reaction (c)) and photogenerated holes can oxidize an electron donor D (reaction (d)). The combination of reactions (c) and (d) represents the semiconductor sensitization of the general redox reaction (1) given in the text (diagram after Ref. [16]).

notably through the contributions of Gerischer [43] and Pleskov and coworkers [44–46].

### 5. Photoelectrochemical cells [3–9]

As indicated in Fig. 2,  $e^-h^+$  pairs can be generated in a semiconductor by the absorption of light of energy greater than or equal to  $E_{bg}$ . In an  $n$ -semiconductor immersed in solution, an electric field forms spontaneously at the semiconductor-electrolyte interface;  $e^-h^+$  pairs generated in the region of the electric field, i.e. the space-charge region, are separated efficiently, rather than undergoing recombination. As a consequence, in an  $n$ -type semiconductor, the photogenerated electron moves into the bulk of the semiconductor, where it can be transferred either through a wire to a second, non-photoactive electrode (such as Pt) or through a surface site to a point where an electron acceptor A can be reduced, i.e.



In the meantime, the photogenerated hole, under the influence of the electric field, migrates towards the surface of the semiconductor to a surface site where it can oxidize a suitable electron donor D, i.e.



The energetics of such a macrophotoelectrosynthetic cell for driving reaction (1) are illustrated in Fig. 3, and Table 2 lists some examples [3,47–50]. From thermodynamic considerations, if the photogenerated electron in the conduction band can reduce water, the potential of the band ( $E_{CB}$ ) must be less than  $E(H^+/H_2)$ ; it also follows that, if the photo-

generated hole in the valence band can oxidize water,  $E_{VB}$  must be greater than  $E(O_2/H_2O)$ . Fig. 4 illustrates the band positions of various semiconductors, including rutile and anatase  $TiO_2$  and  $SrTiO_3$ , and the redox potentials of relevant redox couples.

The first photoelectrochemical cell for water splitting, i.e.  $2H_2O \rightarrow 2H_2 + O_2$  (see Table 1), was reported by Fujishima and Honda [3] in 1972 using a rutile  $TiO_2$  photoanode and Pt counter electrode. This work came at a time when there was increasing interest in developing artificial systems capable of converting solar to chemical or electrical energy. Such work was given greater impetus with the oil crisis of 1973, and from it arose a substantial research effort into photo-

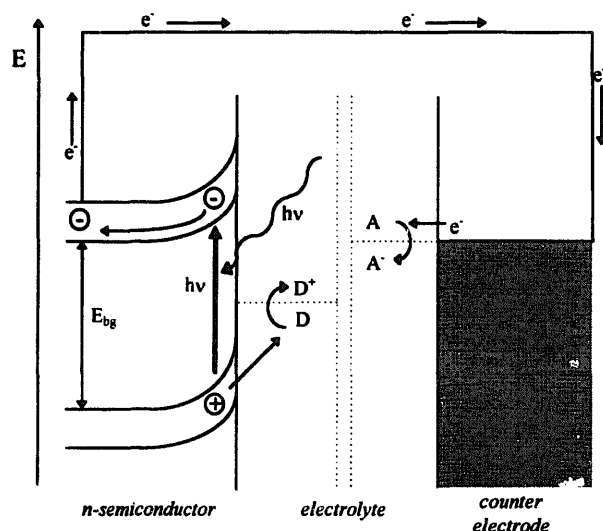


Fig. 3. Energetics of a macrophotosynthetic cell for driving reaction (1); in such a reaction,  $\Delta G^\circ > 0$ .

Table 2  
Examples of different macrophotosynthetic electrochemical cells

Semiconductor photoelectrode	Reaction $A + D \rightarrow A^- + D^+$	$E_{bg}$ (eV)	Reference
<i>n</i> -TiO <sub>2</sub>	$H_2O + H_2O \rightarrow 2H_2 + O_2$	3.0	[3]
<i>n</i> -SrTiO <sub>3</sub>	$H_2O + H_2O \rightarrow 2H_2 + O_2$	3.2	[47]
<i>n</i> -MoSe <sub>2</sub>	$SO_2 + 2H_2O \rightarrow H_2SO_4 + H_2$	1.09	[48]
<i>p</i> -GaAs	$2N_2 + 6H_2O \rightarrow 4NH_3 + 3O_2$	2.3	[49]
<i>p</i> -GaAs	$2CO_2 + 4H_2O \rightarrow 2CH_3OH + 3O_2$	2.3	[50]

electrochemical cells for water splitting and electricity production.

It is not often recognized that the Fujishima and Honda TiO<sub>2</sub>/H<sub>2</sub>O/Pt photoelectrochemical cell requires a degree of chemical or electrical bias to make it work [51]. This is not surprising given that  $E_{CB}$  (TiO<sub>2</sub>; rutile) is approximately 0.2 V more positive than  $E(H^+/H_2)$  (see Fig. 4). Indeed, it appears likely that the original short-circuit photocurrents observed in the Fujishima and Honda TiO<sub>2</sub>/H<sub>2</sub>O/Pt photoelectrochemical cell corresponded to the oxidation of water to oxygen at the TiO<sub>2</sub> photoanode, but not the concomitant reduction of water to hydrogen at the Pt-black cathode, rather the reduction of dissolved oxygen and/or some electrolyte impurity [4]; alternatively, these workers may have used a chemical bias (alkali in the TiO<sub>2</sub> photoanode half-cell and acid in the Pt cathode half-cell) which was not mentioned in their original paper [3]. In contrast, Wrighton et al. [47] were able to show subsequently that the SrTiO<sub>3</sub>/H<sub>2</sub>O/Pt photoelectrolysis cell worked with no bias and with a 25% efficiency with respect to UV photons ( $E_{bg} = 3.2$  eV;  $\lambda(\text{threshold}) = 388$  nm), but only 1% solar energy conversion efficiency  $\eta$ , since the proportion of UV light in the solar spectrum is very low (less than 5%). The reason for the success of the latter cell, compared with the Fujishima and Honda cell, is that in SrTiO<sub>3</sub>, unlike rutile TiO<sub>2</sub>,  $E_{CB}$  and  $E_{VB}$

straddle the hydrogen and oxygen evolution potentials, i.e.  $E(H^+/H_2)$  and  $E(O_2/H_2O)$  respectively [4] (see Fig. 4).

Although other *n*-type oxide semiconductors have been used as photoanodes for the photoelectrolysis of water, the inappropriate disposition of the conductance and valence bands and/or a bandgap which is too large makes these materials less than ideal for use in efficient solar photoelectrolysis cells. In addition, it is generally accepted that there is not a single non-oxide, *n*-type semiconductor which has been shown to be capable of sustaining the oxidation of water to oxygen when illuminated with ultra-bandgap light; all such semiconductors show a tendency towards photoanodic corrosion. In the case of *p*-type semiconductors, which are much rarer in nature, the bandgaps are usually too small and most suffer serious stability problems. As a result, *p*-type semiconductors are rarely used in semiconductor photocatalysis.

The energetics associated with a typical photoelectrochemical cell for electricity production are illustrated in Fig. 5. The photogenerated  $e^- - h^+$  pair, produced as a result of the absorption of a photon of ultra-bandgap light, is separated by the electric field within the semiconductor. The photogenerated holes migrate to the surface of the semiconductor where they oxidize redox species  $A^-$  to  $A$ . For the photoelectrochemical cell to work efficiently, the photogenerated electrons must move through an electrical circuit to the counter

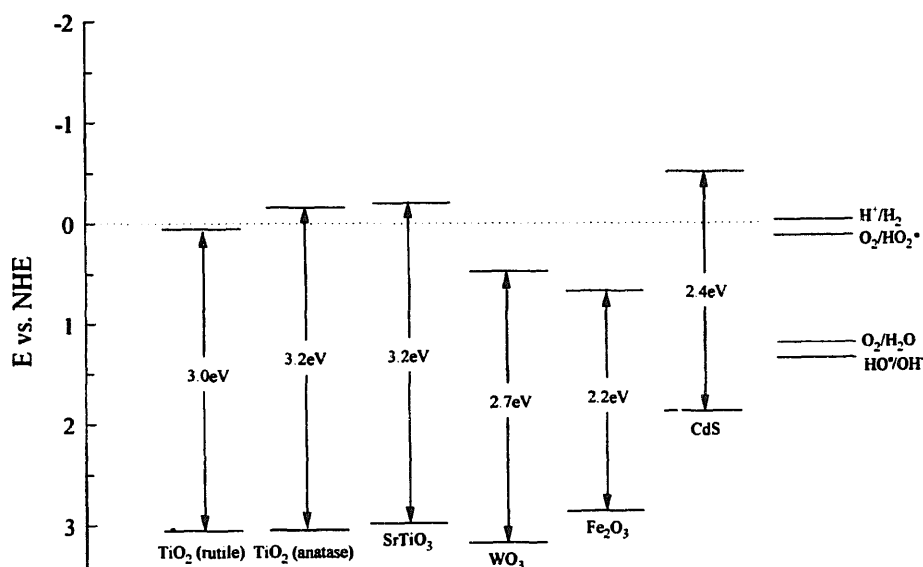


Fig. 4. Valence and conduction band positions for various semiconductors, and useful, relevant redox couples at pH 0. In order to photoreduce a chemical species, the conduction band of the semiconductor must be more negative than the reduction potential of the chemical species; to photo-oxidize a chemical species, the potential of the valence band of the semiconductor must be more positive than the oxidation potential of the chemical species.

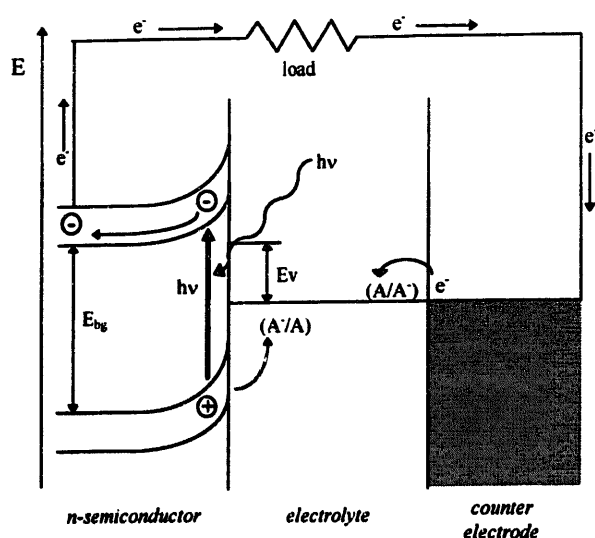


Fig. 5. Energetics of a typical, general macrophotoelectrochemical cell for electricity production employing an *n*-type semiconductor as the photoelectrode.

electrode and there reduce  $A$  to  $A^-$ . One of the major problems encountered in the development of an efficient photoelectrochemical cell for electricity production is to ensure that the semiconductor photoanode is stable towards photoanodic decomposition. It has already been mentioned that low bandgap, non-oxide semiconductors, such as CdS, GaAs and CdSe, which are more suitable than large bandgap oxide semiconductors for solar energy conversion, are prone to this latter process. In order to ensure the kinetic stability of such photoanodes, a careful choice of the  $A/A^-$  couple must be made so that the rate of oxidation of  $A$  by the photogenerated holes is much greater than that for the semiconductor. Table 3 lists a selection of photoelectrochemical cells for electricity production in which the semiconductors used were in single-crystal [52–55] or polycrystalline [56–58] form; the latter photoelectrochemical cells are more efficient, because of the reduced probability of  $e^-h^+$  pair recombination at grain boundaries, but more expensive because of the greater difficulty in fabricating single-crystal semiconductors.

The efficiency of polycrystalline photoelectrochemical cells can be improved by diffusing or co-adsorbing metal

ions, such as  $Ru^{3+}$ ,  $Os^{3+}$  and  $Pb^{2+}$ . It has been suggested [57] that the presence of such ions makes the surface and grain boundary recombination states less deep and therefore less likely to mediate the efficiency lowering process of  $e^-h^+$  recombination. An alternative explanation offered by others [52] is that this approach to chemical modification of the semiconductor primarily improves the interfacial hole transfer rate. More recently, others have produced very efficient single-crystal photoelectrochemical cells by addressing the problem of rapid semiconductor surface modification with use, which lowers the performance of the cell. Thus Licht and Peramunage [55], investigating the *n*-CdSe/[ $K_4Fe(CN)_6$ ]/[ $K_3Fe(CN)_6$ ] photoelectrochemical cell, found that its performance was greatly enhanced,  $\eta = 16.4\%$ , through the addition of excess cyanide. It is believed that the cyanide prevents passivation and chemical deposition at the CdSe surface, thereby keeping it clean and able to facilitate the necessary rapid charge transfer processes required for an efficient photoelectrochemical cell.

## 6. Semiconductor particles as sensitizers for water reduction, oxidation or dissociation [6,10,11]

Schematic illustrations of the mechanisms by which an *n*-type semiconductor is able to photosensitize the reduction, oxidation or cleavage of water are given in Fig. 6(a)–(c) respectively. A platinum group metal (PGM) redox catalyst, such as Pt, deposited on the surface of the semiconductor is invariably used to facilitate the reduction of water by the photogenerated electrons. Although a PGM oxide, such as  $RuO_2$ , is often used to mediate the oxidation of water by the photogenerated holes, this is often unnecessary when the semiconductor is a large bandgap metal oxide, such as  $TiO_2$ , since  $E_{VB} \gg E(O_2/H_2O)$  (see Fig. 4), i.e. there is a sufficiently large overpotential for the reaction to proceed readily without an oxygen redox catalyst. Table 4 provides some examples of the semiconductor-sensitized systems for water photoreduction [59–63] (incorporating a sacrificial electron donor), water photo-oxidation [61,64–67] (incorporating a

Table 3  
Some single-crystal and polycrystalline photoelectrochemical cells for electricity production<sup>a</sup>

Semiconductor	Redox electrolyte ( $D^+/D$ )	$\eta$	Reference
<i>Single-crystal photoelectrochemical cells</i>			
<i>n</i> -GaAs	1 mol dm <sup>-3</sup> $K_2Se$ /0.01 mol dm <sup>-3</sup> $K_2Se_2$ /1 mol dm <sup>-3</sup> KOH, $Os^{3+}$	15	[52]
<i>p</i> -InP	0.3 mol dm <sup>-3</sup> $V^{3+}$ /0.05 mol dm <sup>-3</sup> $V^{2+}$ /5 mol dm <sup>-3</sup> HCl	11.5	[53]
<i>n</i> -WS <sub>2</sub>	1 mol dm <sup>-3</sup> NaBr/0.01 mol dm <sup>-3</sup> Br <sub>2</sub>	6	[54]
<i>n</i> -CdSe	0.25 mol dm <sup>-3</sup> [ $K_4Fe(CN)_6$ ]/0.0125 mol dm <sup>-3</sup> [ $K_3Fe(CN)_6$ ]/0.1 mol dm <sup>-3</sup> KCN/pH 13.3	16.4	[55]
<i>Polycrystalline photoelectrochemical cells</i>			
<i>n</i> -CdSe <sub>0.65</sub> Te <sub>0.35</sub>	1 mol dm <sup>-3</sup> Na <sub>2</sub> S <sub>2</sub> /1 mol dm <sup>-3</sup> KOH	7.9	[56]
<i>n</i> -GaAs	1 mol dm <sup>-3</sup> $K_2Se$ /0.1 mol dm <sup>-3</sup> $K_2Se_2$ /1 mol dm <sup>-3</sup> KOH, $Ru^{3+}$ , $Pb^{2+}$	7.8	[57]
<i>n</i> -CdSe	1 mol dm <sup>-3</sup> Na <sub>2</sub> S <sub>2</sub> /1 mol dm <sup>-3</sup> NaOH	7.6	[58]

<sup>a</sup>The counter electrode is usually carbon.

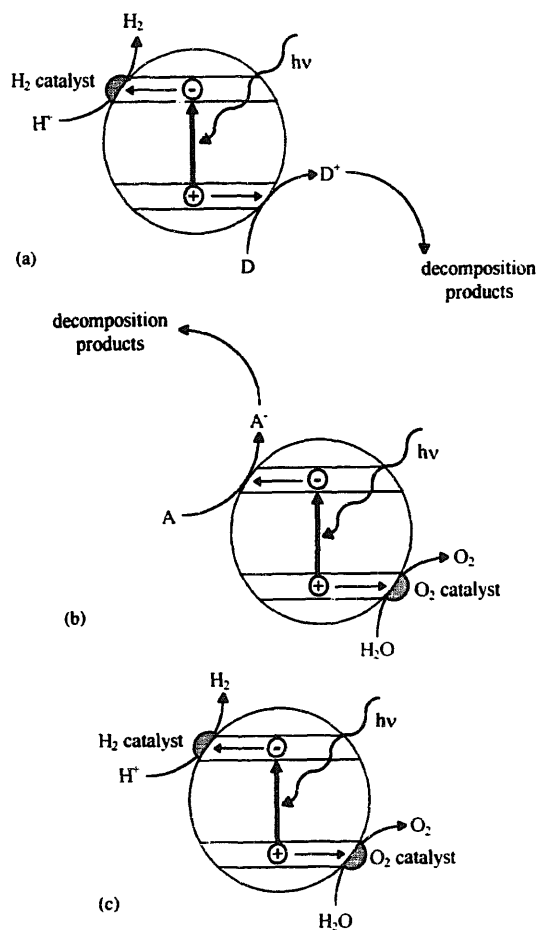


Fig. 6. Schematic illustration of the common form of typical systems for the following semiconductor-sensitized reactions: (a) photoreduction of water by a sacrificial electron donor, such as ethylenediaminetetraacetic acid (EDTA), enhanced by the presence of a hydrogen catalyst, such as platinum, on the semiconductor's surface; (b) photo-oxidation of water by a sacrificial electron acceptor, such as persulphate, possibly enhanced by the presence of an oxygen catalyst, such as ruthenium dioxide, on the semiconductor's surface; (c) photodissociation of water, which appears to be unlikely unless carried out under forced conditions.

sacrificial electron acceptor) and water photodissociation [68–72].

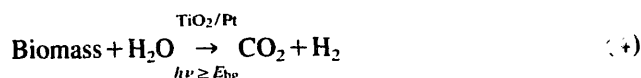
There is no doubt that it is possible to use semiconductors to sensitize the photoreduction [59–63] and photo-oxidation [61,64–67] of water through the use of sacrificial electron donors and acceptors respectively. The photocleavage of water is another matter. Most research groups have had to resort to using large bandgap metal oxide semiconductors, such as anatase TiO<sub>2</sub> or SrTiO<sub>3</sub>, and forcing conditions of high temperature and/or reduced pressure to observe both hydrogen and oxygen generation [11,68,70]. The early reports [69] of a "bifunctional catalyst", RuO<sub>2</sub>/TiO<sub>2</sub>/Pt, which photocleaved water efficiently ( $\Phi(\text{H}_2) = 0.3$  was reported; presumably  $\Phi(\text{O}_2) = 0.15$ , but the latter is usually not observed [73]) under ambient conditions, remain unsubstantiated and, with hindsight, doubtful. Indeed, it has now been suggested [73] that any oxygen observed on irradiation of the RuO<sub>2</sub>/TiO<sub>2</sub>/Pt bifunctional catalyst probably "leaked

in from outside". The claims that CdS can be used as a sensitizer for the photocleavage of water are highly dubious [71,72] given the well-recognized tendency of CdS to undergo photoanodic corrosion; certainly a number of major research groups have failed to reproduce these findings [67,73]. All the semiconductors listed in Table 4 are excellent sensitizers for the photoreduction of oxygen; it seems most likely that, under ambient conditions, if the photodissociation of water does occur it will not be sustainable, since any oxygen generated will be photoreduced and so short circuit the overall process.

It is worth making the following general points about semiconductor-sensitized systems for water photocleavage. Clearly, the observation of hydrogen evolution alone in such systems does not imply water cleavage and the concomitant generation of a stoichiometric amount of oxygen must not be assumed. Great care must be taken when working on such systems, since hydrogen can be photogenerated using most semiconductors if a sacrificial electron donor is present; likely sources of this sacrificial agent include electron donors, such as methanol or formaldehyde, used in the deposition of the PGM redox catalyst onto the surface of the semiconductor (repeated washing of such a treated photocatalyst does not ensure that all the electron donor is removed) and any polymer support used if the semiconductor is in colloidal form. Even the observation of the evolution of oxygen can be the result of air leaks; the oxygen/nitrogen ratio must not be taken as a guide to assess how much of the oxygen observed is photogenerated [67,73]. With all of these problems, it follows that many of the reports on semiconductor particle-sensitized systems for water cleavage should be viewed with a high degree of scepticism. A sustainable, reproducible, semiconductor particle-based sensitized system for water cleavage is still to be achieved.

## 7. Semiconductor particles as photocatalysts for the removal of organic and inorganic pollutants [12–20]

The first example in Table 4 is the oxidation of biomass with the concomitant reduction of water to hydrogen, i.e.



If experiments with this system had been carried out in aerated, rather than nitrogen-purged, solution, the reaction under study would have been one of the first, well-documented examples of the semiconductor-sensitized photomineralization of organic substrates by oxygen. The latter process may be summarized as follows

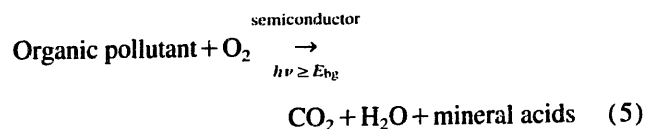


Table 4

Examples of semiconductor-sensitized systems for the photoreduction, photo-oxidation and photodissociation of water

Semiconductor-sensitized systems for the photoreduction of water		Hydrogen catalyst	$\Phi(\text{H}_2)$	Reference
Semiconductor	Sacrificial donor			
TiO <sub>2</sub>	Biomass (including grass, wood, algae, seaweed, cockroaches, urine and glucose)	Pt (4%)	0.02–0.004	[59]
TiO <sub>2</sub>	Methanol, propanol	Pt (10%–0.05%)	–	[60]
TiO <sub>2</sub>	EDTA	Pt (0.1%–2%)	0.03	[61]
CdS	EDTA	Pt	–	[62]
CdS	S <sup>2–</sup>	RuO <sub>2</sub> ·xH <sub>2</sub> O	–	[63]
Semiconductor-sensitized systems for the photo-oxidation of water		Oxygen catalyst	$\Phi(\text{H}_2)$	Reference
Semiconductor	Sacrificial acceptor			
TiO <sub>2</sub>	Fe(III) ions	None, or Rh, Ru, Ir, Au, Co	–	[61]
TiO <sub>2</sub>	[PtCl <sub>6</sub> ] <sup>2–</sup>	None	–	[64]
WO <sub>3</sub>	Fe(III) ions	None, or Pt, Rh, Ru, RuO <sub>2</sub> ·xH <sub>2</sub> O	0.03	[65]
CdS	[PtCl <sub>6</sub> ] <sup>2–</sup>	Pt	–	[66]
CdS	[PtCl <sub>6</sub> ] <sup>2–</sup>	RuO <sub>2</sub> ·xH <sub>2</sub> O	–	[67]
Semiconductor-sensitized systems for the photodissociation of water		Oxygen catalyst	$\Phi(\text{H}_2)$	Reference
Semiconductor	Hydrogen catalyst			
TiO <sub>2</sub>	Pt	None	–	[68]
TiO <sub>2</sub>	Pt	RuO <sub>2</sub> ·xH <sub>2</sub> O	0.3	[69]
SrTiO <sub>3</sub>	Pt, Ir, Pd, Os, Ru, Re or Co	None	–	[70]
TiO <sub>2</sub>	Pt	None	–	[70]
CdS	Pt	RuO <sub>2</sub> ·xH <sub>2</sub> O	0.005	[71]
CdS	Pt, Rh or Ir	RuO <sub>2</sub> ·xH <sub>2</sub> O with [Ru(OH)(EDTA) <sub>2</sub> O <sub>2</sub> ]	–	[72]

The energetics and primary processes associated with the semiconductor-sensitized photomineralization of organic substrates by oxygen, i.e. reaction (5), are illustrated in Fig. 7.

The first clear recognition and implementation of semiconductor sensitizers for organic pollutant oxidative mineralization came in 1983 with the work of Ollis and coworkers [74,75] on the photomineralization of halogenated hydrocarbons, including trichloroethylene, dichloromethane, chloroform and carbon tetrachloride, sensitized by TiO<sub>2</sub>. Subsequent work by these workers indicated that this approach

may be limited to non-aromatic compounds; however, these concerns were quickly dispelled through the work of others [76,77] using chlorobenzene and phenol as the organic substrates. A brief list of some of the many (over 200 to date) organic substrates which can be mineralized via reaction (5) is given in Table 5; more exhaustive lists, with references, can be found elsewhere [16,78,79].

The semiconductor sensitizer for reaction (5) must be:

1. photoactive;
2. able to utilize visible and/or near-UV light;
3. biologically and chemically inert;

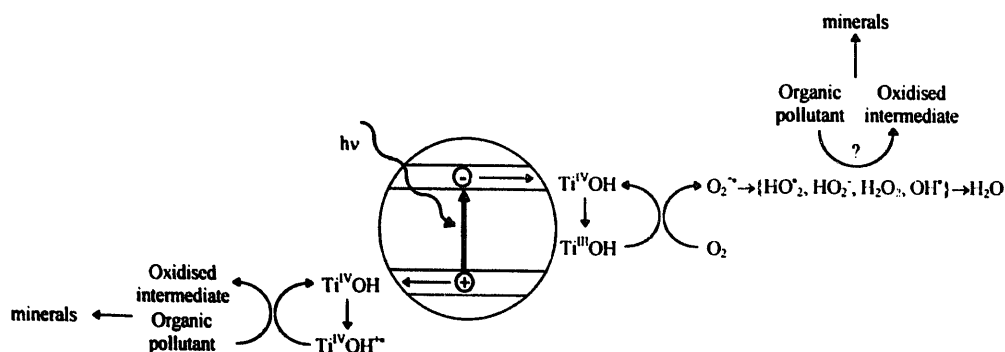


Fig. 7. Energetics and major general processes for the photo-oxidative mineralization of organic pollutants in aqueous solution by dissolved oxygen, sensitized by semiconductor particles. The role of oxygen in the overall process is a current source of debate [24] (see below); it may be that many of the different chemical species which can result from the reduction of oxygen, such as HO<sub>2</sub><sup>·</sup>, HO<sub>2</sub><sup>·</sup>, H<sub>2</sub>O<sub>2</sub> and, possibly, OH<sup>·</sup> radicals, play a major role in the oxidation of the organic substrate; it is already generally recognized that the trapped photogenerated hole species, Ti<sup>IV</sup>OH<sup>+</sup>, is very important in the latter process.



Table 5

Some examples of TiO<sub>2</sub>-sensitized photomineralization of organic substrates

Class	Example
Alkanes	Methane, isobutane, pentane, heptane, cyclohexane, paraffin
Haloalkanes	Mono-, di-, tri- and tetrachloromethane, tribromoethane, 1,1,1-trifluoro-2,2,2-trichloroethane
Aliphatic alcohols	Methanol, ethanol, isopropyl alcohol, glucose, sucrose
Aliphatic carboxylic acids	Formic, ethanoic, dimethylethanoic, propanoic, oxalic acids
Alkenes	Propene, cyclohexene
Haloalkenes	Perchloroethene, 1,2-dichloroethene, 1,1,2-trichloroethene
Aromatics	Benzene, naphthalene
Haloaromatics	Chlorobenzene, 1,2-dichlorobenzene, bromobenzene
Nitrohaloaromatics	3,4-Dichloronitrobenzene, dichloronitrobenzene
Phenols	Phenol, hydroquinone, catechol, 4-methylcatechol, resorcinol, <i>o</i> -, <i>m</i> -, <i>p</i> -cresol
Halophenols	2-, 3-, 4-Chlorophenol, pentachlorophenol, 4-fluorophenol, 3,4-difluorophenol
Aromatic carboxylic acids	Benzoic, 4-aminobenzoic, phthalic, salicylic, <i>m</i> - and <i>p</i> -hydroxybenzoic, chlorohydroxybenzoic acids
Polymers	Polyethylene, poly(vinyl chloride) (PVC)
Surfactants	Sodium dodecylsulphate (SDS), polyethylene glycol, sodium dodecyl benzene sulphonate, trimethyl phosphate, tetrabutylammonium phosphate
Herbicides	Methyl viologen, atrazine, simazine, prometon, propetryne, bentazon
Pesticides	DDT, parathion, lindane
Dyes	Methylene blue, rhodamine B, methyl orange, fluorescein

4. photostable (i.e. not liable to photoanodic corrosion for example);
5. inexpensive.

By common consent, the semiconductor TiO<sub>2</sub> satisfies criteria (1)–(5) and is one of the best semiconductors for sensitizing reaction (5). In order to improve the reproducibility of the results between groups, many have chosen to use a particular source of TiO<sub>2</sub>, with a recognized high photocatalytic activity, namely Degussa P25 TiO<sub>2</sub>, which is produced through the high temperature (greater than 1200 °C) flame hydrolysis of TiCl<sub>4</sub> in the presence of hydrogen and oxygen. The TiO<sub>2</sub> is treated with steam to remove HCl which is also produced as part of the reaction. The product is 99.5% pure TiO<sub>2</sub> (anatase : rutile ratio, 70 : 30), which is non-porous, with cubic particles with rounded edges. The P25 TiO<sub>2</sub> powder has a surface area of 50 ± 15 m<sup>2</sup> g<sup>-1</sup> and an average particle diameter by number count of 21 nm; 90% of the particles fall in the size range 9–38 nm; however, the particles do not exist in isolation, but rather as irreducible complex primary aggregates, typically approximately 0.1 µm in diameter.

It is no surprise that different samples of TiO<sub>2</sub> exhibit different photocatalytic activities towards the same organic substrate under otherwise identical reaction conditions [80,81]. Such differences can be qualitatively attributed to differences in morphology, crystal phase, specific surface area, particle aggregate size and surface density of OH groups in the TiO<sub>2</sub> samples. However, it may be considered surprising that a TiO<sub>2</sub> photocatalyst which is good at destroying one organic substrate may be ineffective at destroying another, and that for a different sample of TiO<sub>2</sub> the situation can be reversed. For example, Degussa P25 TiO<sub>2</sub> exhibits a photoactivity for reaction (5) which is 50% and 149% of that of Tioxide A-HR TiO<sub>2</sub> (surface area only 12 m<sup>2</sup> g<sup>-1</sup>, 100% anatase) when the organic substrates are phenol and hydro-

quinone respectively [81,82]. Such results highlight the importance of using a standard form of TiO<sub>2</sub>, such as Degussa P25, in order to make the general findings of one group reproducible by another.

The results of detailed laser flash photolysis experiments have enabled many of the primary processes associated with reaction (5), sensitized by TiO<sub>2</sub>, to be identified, together with their characteristic time domains [16]; the results of this work are summarized in Table 6. In general, it is usually assumed that the organic pollutant substrate does not undergo direct hole transfer, although there is some evidence that this process does occur in some cases (at least to some extent), but rather that oxidation takes place through a surface-bound hydroxyl radical (Ti<sup>IV</sup>OH<sup>•+</sup>). As we shall see later, and as indicated in Fig. 7, the results of recent work on the semiconductor-sensitized photomineralization of thin organic films [24], with electron acceptors other than oxygen, indicate that the role of oxygen in reaction (5) may be much greater than previously assumed. A full kinetic model for reaction (5) is far from complete and continued research in this area is more useful than further photomineralization studies on yet another, different, untried organic substrate.

In their investigations and modelling of reaction (5), using TiO<sub>2</sub> as the semiconductor sensitizer, Gerischer and Heller [82,83] have generated a substantial body of evidence indicating that the interfacial electron transfer process involving the reduction of oxygen (see Table 5) is the rate-limiting step in the TiO<sub>2</sub>-sensitized photodegradation of organics. In order to improve the kinetics of this process, catalytic sites must be placed on the TiO<sub>2</sub> surface; these sites can be of the form of islands of Pd<sup>0</sup>. These workers were able to show that, in the photosensitized oxidation of 2,2-dichloropropionate by TiO<sub>2</sub>, 0.01 wt.% and 2 wt.% loadings of the TiO<sub>2</sub> photocatalyst resulted in threefold and sevenfold improvements in the rate. Recently, Lewis and coworkers [84] have developed a flux-

Table 6

Primary processes and associated characteristic time domains in the TiO<sub>2</sub>-sensitized photomineralization of organic pollutants [16]

Primary process	Characteristic time
Charge carrier generation $\text{TiO}_2 + h\nu \rightarrow \text{h}^+ + \text{e}^-$	fs (very fast)
Charge carrier trapping $\text{h}^+ + >\text{Ti}^{\text{IV}}\text{OH} \rightarrow \{>\text{Ti}^{\text{IV}}\text{OH}^+\}$	10 ns (fast)
$\text{e}^- + >\text{Ti}^{\text{IV}}\text{OH} \rightarrow \{>\text{Ti}^{\text{III}}\text{OH}\}$	100 ps (shallow trap; dynamic equilibrium)
$\text{e}^- + >\text{Ti}^{\text{IV}} \rightarrow >\text{Ti}^{\text{III}}$	10 ns (deep trap)
Charge carrier recombination $\text{e}^- + \{>\text{Ti}^{\text{IV}}\text{OH}^+\} \rightarrow >\text{Ti}^{\text{IV}}\text{OH}$	100 ns (slow)
$\text{h}^+ + >\text{Ti}^{\text{III}}\text{OH} \rightarrow >\text{Ti}^{\text{IV}}\text{OH}$	10 ns (fast)
Interfacial charge transfer $\{>\text{Ti}^{\text{IV}}\text{OH}^+\} + \text{organic pollutant} \rightarrow >\text{Ti}^{\text{IV}}\text{OH} + \text{oxidized pollutant}$	100 ns (slow)
$\{>\text{Ti}^{\text{III}}\text{OH}\} + \text{O}_2 \rightarrow >\text{Ti}^{\text{IV}}\text{OH} + \text{O}_2^-$	ms (very slow)

matching model of semiconductor photocatalysis based on their work with a single-crystal rutile TiO<sub>2</sub> photoanode. In this model, three major carrier decay pathways were identified, namely electron–hole recombination (which is significant), reduction of oxygen by photogenerated electrons and hole transfer to the organic, water or any other acceptor. In this model, all three processes are intimately related and none can be stated as being ‘‘rate determining’’. However, they were also able to show that the presence of a Pt catalyst on the surface of the TiO<sub>2</sub> photocatalyst should lead to an enhancement in the rate, as would the use of more readily reduced acceptors, such as  $[\text{Fe}(\text{CN})_6]^{3-}$ .

However, the same workers also added, at the end of the paper [84], a cautionary note about extending their findings on single-crystal rutile TiO<sub>2</sub> to the anatase particulate TiO<sub>2</sub> photocatalytic systems which most people work with. They note that the added redox agents can act as recombination sites, and so the overall photocatalytic rate could increase, decrease or remain unchanged in the presence of such reagents. Gerischer and Heller [82,83] were able to deposit Pd<sup>0</sup> onto particulate TiO<sub>2</sub> to produce more active photocatalysts. In contrast, in an extensive investigation of TiO<sub>2</sub> photocatalysts with PGM deposits, we found [85] that the presence of PGMs had very little, if any, effect on the rate of photocatalysis, even at high (10 wt.%) loadings, and, if anything, decreased the rate at very high loadings. This work provides a small insight into the complex, sometimes contradictory, nature of TiO<sub>2</sub> particulate photocatalytic systems and the resulting difficulty in developing satisfactory general kinetic models.

In general, the kinetics of photomineralization of organic substrates by oxygen, sensitized by TiO<sub>2</sub>, on steady state illumination fit a Langmuir–Hinshelwood kinetic scheme, i.e.

$$R_i = -d[\text{S}]_i/dt = k(\text{S})K(\text{S})[\text{S}]_i/(1 + K(\text{S})[\text{S}]_i) \quad (6)$$

where  $R_i$  is the initial rate of substrate removal,  $[\text{S}]_i$  is the initial concentration of the organic substrate and, traditionally,  $K(\text{S})$  is taken to be the Langmuir adsorption constant of species S on the surface of TiO<sub>2</sub> and  $k(\text{S})$  is a proportionality constant which provides a measure of the intrinsic reac-

tivity of the photoactivated surface with S. Generally, the value of  $K(\text{S})$  derived from a kinetic study is not directly equivalent to the dark Langmuir adsorption isotherm for S on the semiconductor; the latter values are usually much smaller. It is found that  $k(\text{S})$  is proportional to  $I_a^\theta$ , where  $I_a$  is the rate of light absorption and  $\theta$  is a power term which is equal to 0.5 or unity at high or low light intensity respectively. It is also found that  $k(\text{S})$  is proportional to the fraction of O<sub>2</sub> adsorbed on TiO<sub>2</sub>, i.e.  $f(\text{O}_2)$ , where

$$f(\text{O}_2) = K_{\text{O}_2}[\text{O}_2]/(1 + K_{\text{O}_2}[\text{O}_2]) \quad (7)$$

$K_{\text{O}_2}$  is the Langmuir adsorption coefficient for O<sub>2</sub> on the semiconductor, which appears to be non-competitively adsorbed at Ti<sup>III</sup> sites. Several kinetic models of semiconductor photocatalysis have been developed which generate working forms of Eqs. (6) and (7); most notably, Turchi and Ollis [86] have proposed four possible different mechanistic schemes involving OH<sup>•</sup> radical attack of the organic substrate as the rate-determining step. Two of the most likely schemes focus on adsorbed hydroxyl radical attack on the adsorbed organic substrate and adsorbed hydroxyl radical attack on the free organic substrate as the rate-determining steps [86].

Eqs. (6) and (7) are often found to be applicable to ‘‘batch’’ irradiation systems, i.e. those in which the semiconductor is dispersed in an aqueous solution containing the organic substrate for photomineralization. Many ‘‘flow’’ systems have also been developed, in which the semiconductor is immobilized on an inert support and the aqueous solution containing the organic substrate for photomineralization is passed over it. The semiconductor photocatalyst has been attached to a variety of supports including Nafion film, ceramic, silica gel, glass tubing, beads and mesh. A summary of many of the flow and batch photocatalytic reactors has been reported elsewhere [87]. In such systems, Eqs. (6) and (7) usually still apply, but often with  $k(\text{S})$  exhibiting a dependence on the flow rate, indicating a mass transfer dependence which is not found with batch systems [88]. As a result, flow reactors are not considered to be as helpful as batch photoreactors in the evaluation of the fundamental

kinetic parameters associated with semiconductor-sensitized photoprocesses, such as reaction (5).

The overall process of semiconductor photocatalysis is not usually found to be particularly temperature sensitive; reported activation energies usually lie in the range 5–16 kJ mol<sup>-1</sup>. In reaction (5), increasing the temperature may increase the rate of oxidation of the organic substrate at the interface, but it will also have the effect of lowering the adsorption isotherms associated with the substrate and O<sub>2</sub>, and lowering [O<sub>2</sub>]. Most photocatalyst experiments are carried out under conditions in which  $f(\text{O}_2) \approx 1$  (i.e.  $P_{\text{O}_2} = 1$  atm;  $K_{\text{O}_2}$  is typically 0.025 atm<sup>-1</sup>) and [S]<sub>i</sub> is low. Under these conditions, the effect of an increase in temperature on the kinetics of reaction (5) will be largely dominated by the effect on the rate of oxidation of the organic substrate at the interface. If [S]<sub>i</sub> is made large (greater than 10<sup>-3</sup> mol dm<sup>-3</sup>; typically  $K(\text{S}) = 4.5 \times 10^4$  dm<sup>3</sup> mol<sup>-1</sup>) and  $P_{\text{O}_2}$  small (e.g. 0.05 atm or less), the effect of an increase in temperature on the rate of reaction (5) may be dominated by the rate of interfacial electron transfer to oxygen. Thus in a study [89] of the effect of temperature on the kinetics of reaction (5), using 4-chlorophenol as S, we were able to show that the activation energy for the reaction was small and positive (approximately 6.4 kJ mol<sup>-1</sup>) at low [S]<sub>i</sub> and high  $P_{\text{O}_2}$ , and large and negative (approximately -15 kJ mol<sup>-1</sup>) at high [S]<sub>i</sub> and low  $P_{\text{O}_2}$ .

The rate of photomineralization of an organic substrate S, sensitized by a semiconductor, not only depends on the nature of the semiconductor photocatalyst,  $I_a$  (and therefore the incident light intensity and [TiO<sub>2</sub>]), [O<sub>2</sub>], the nature and concentration of S and temperature, as indicated by Eqs. (6) and (7), but also on the pH and presence of interfering adsorbing species. The pH of an aqueous solution significantly affects all oxide semiconductors, including the surface charge on the semiconductor particles, the size of the aggregates formed and the energies of the conductance and valence bands. Despite this, the rate of reaction (5), sensitized by TiO<sub>2</sub>, is not usually found to be strongly pH dependent; typically  $R_i$  varies by less than one order of magnitude from pH 2 to pH 12. Higher reaction rates for various TiO<sub>2</sub>-sensitized photomineralizations have been reported at both low and high pH [16]. Generally, it is found that perchlorate and nitrate anions have little effect on the kinetics of reaction (5), photosensitized by TiO<sub>2</sub>, whereas sulphate, chloride and phosphate ions, especially at concentrations of greater than 10<sup>-3</sup> mol dm<sup>-3</sup>, can reduce the rate by 20%–70% due to competitive adsorption at the photoactivated reaction sites [90].

This particular branch of semiconductor photocatalysis has many possible applications, including an advanced oxidation process (AOP) for the purification of water and air. As such, efforts have begun to devise measurable parameters which will aid in the comparison of results between groups and those derived from other waste treatment technologies. It has been suggested [91] that, when [S]<sub>i</sub> is high (and the kinetics are zero order), an appropriate figure-of-merit is the “electrical energy per unit mass”, i.e. EE/M, which is defined as the

electrical energy (kWh) needed to degrade 1 kg of S. When [S]<sub>i</sub> is low (and first-order kinetics prevail), it has been suggested [91] that the “electrical energy per order”, i.e. EE/O, is an appropriate figure-of-merit, where EE/O is defined as the electrical energy (kWh) needed to degrade [S] by one order of magnitude in 1 m<sup>3</sup> of contaminated water.

The above figures-of-merit will help to compare and contrast the efficacy of whole AOP systems; however, they do not provide a direct indication of the efficiency of an ultra-bandgap photon to drive the semiconductor-sensitized process of reaction (5). The latter quantity is provided by the overall quantum yield for the process ( $\Phi_{\text{overall}}$ ) and is defined as follows

$$\Phi_{\text{overall}} = \text{rate of reaction} / (\text{rate of absorption of radiation}) \quad (8)$$

In heterogeneous semiconductor photocatalysis, the measurement of  $\Phi_{\text{overall}}$  is very difficult and, as a consequence, rare. The most obvious reason is that the rate of absorption of ultra-bandgap photons is very difficult to assess, since the semiconductor particles will absorb, scatter and transmit light. A more useful term [81,92] is the “photonic efficiency”  $\xi$ , which is defined as the number of reactant molecules transformed or product molecules formed divided by the number of photons of monochromatic light incident inside the front window of the irradiation cell. In simple photochemist’s terms,  $\xi$  may be defined as follows

$$\xi = \text{rate of reaction} / (\text{incident monochromatic light intensity}) \quad (9)$$

It follows from Eqs. (8) and (9) that, for a given reaction (5),  $\Phi_{\text{overall}} \geq \xi$ . It has been suggested [93] that the fraction of light scattered or reflected by a semiconductor dispersion may be 13%–76% of the incident light intensity. Thus the difference between  $\Phi_{\text{overall}}$  and  $\xi$  may be significant.

Many workers in the field use polychromatic light sources, such as Xe arc lamps, medium pressure mercury lamps and blacklight bulbs; the typical relative emission profiles associated with these three popular light sources are illustrated in Fig. 8, together with the measured absorption spectrum of a typical (100 mg dm<sup>-3</sup>) Degussa P25 TiO<sub>2</sub> dispersion. The latter illustrates the extensive degree of incident light scattering/reflection by a typical TiO<sub>2</sub> dispersion; thus, in the region 400–500 nm, in which TiO<sub>2</sub> does not absorb, the results in Fig. 8 indicate that the TiO<sub>2</sub> particles at this modest concentration scatter/reflect over 90% of the incident light and that this effect increases with decreasing wavelength. If a polychromatic light source is used, a value for  $\xi$  cannot be calculated and, under these circumstances, we can calculate the formal quantum efficiency (FQE) [94], which is defined as

$$\text{FQE} = \text{rate of reaction} / (\text{incident light intensity}) \quad (10)$$

If monochromatic light is used,  $\text{FQE} = \xi$ , otherwise  $\text{FQE} < \xi$ ; for multielectron-photoinduced reactions, FQE values will

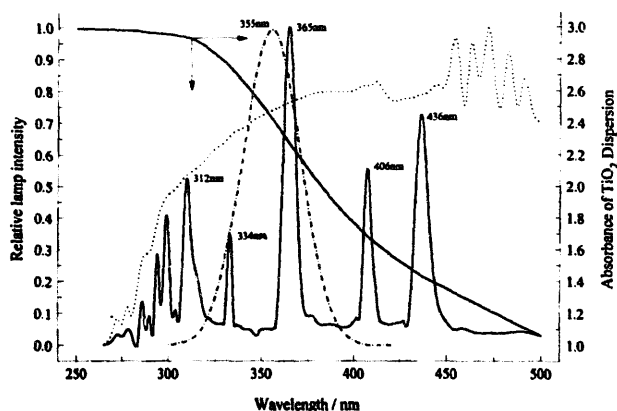


Fig. 8. Typical normalized emission spectra of a medium pressure mercury lamp (full line), blacklight bulb (chain line) and Xe arc lamp (dotted line) (light sources commonly used in semiconductor photocatalysis studies) and UV-visible reflectance-scattering-absorption spectrum of a typical ( $100 \text{ mg dm}^{-3}$ ) dispersion of Degussa P25  $\text{TiO}_2$  in doubly distilled deionized water in a 1 cm cell.

usually be much less than unity, unless, for example, a chain reaction is in operation.

The parameters FQE and  $\xi$  at least provide some idea of the efficiency of a photocatalytic process. However, it must be remembered that, in semiconductor photocatalysis, the rate of reaction depends on many parameters, including the reactor geometry, nature and concentration of the semiconductor,  $[\text{O}_2]$ ,  $[\text{S}]$ , light intensity, temperature, pH, the presence of competitive interfering species and stirrer speed. As a result, in a study of the same system, the values of FQE and  $\xi$  obtained by one research group may be very different from those obtained by another.

It has been proposed [81,92,95–97] that the extent of the difference in the photochemical irradiation systems used by different groups could be identified if, in addition to the studies on the substrate under test, each group reported the initial rate of a standard test system, such as phenol/Degussa P25/ $\text{O}_2$  or 4-chlorophenol/Degussa P25/ $\text{O}_2$ . In such a standard system, many of the experimental parameters, which could be made common to each research group, would be defined, e.g.  $[\text{4-chlorophenol}] = 10^{-3} \text{ mol dm}^{-3}$ ,  $[\text{TiO}_2] = 500 \text{ mg dm}^{-3}$ ,  $[\text{O}_2] = 1.3 \times 10^{-3} \text{ mol dm}^{-3}$  ( $P_{\text{O}_2} = 1 \text{ atm}$ ), pH 2,  $T = 30^\circ\text{C}$ . The FQE for carbon dioxide evolution for the latter standard test system has been reported as 0.0112 by our group [97]. A comparison of the rate of the heterogeneous semiconductor-sensitized photochemical reaction under test with that obtained for the standard test system would provide some idea of the efficiency of the former process and allow some degree of comparison of results between groups.

Others [81,91] have gone further and suggested that the use of relative photonic efficiencies  $\xi_r$  would be useful, where  $\xi_r$  is defined as

$$\xi_r = \frac{\text{rate of disappearance of substrate/}}{\text{(rate of disappearance of phenol)}} \quad (11)$$

where both (initial) rates are obtained under exactly the same conditions. It follows from Eq. (11) that the quantum yield

of the process under test ( $\Phi_{\text{overall}}$ ) is  $\xi_r \Phi_{\text{standard}}$ , where  $\Phi_{\text{standard}}$  is the quantum yield of the disappearance of phenol under exactly the same reaction conditions. There is no advantage to this compared with measuring  $\Phi_{\text{overall}}$  on its own (which, as we have noted, is very difficult and rarely performed), since  $\Phi_{\text{standard}}$  will vary enormously with different reaction conditions, and a value will have to be determined for each set of special reaction conditions (this task is no less difficult than the measurement of  $\Phi_{\text{overall}}$ ).

There is also a danger in quoting  $\xi_r$  values, since a  $\xi_r$  value of much greater than unity will be taken as an indication of a very efficient photochemical process, which it may not be. For example, a  $\xi_r$  value of two for a process under test indicates simply that it is twice as fast as the degradation of phenol carried out under the same reaction conditions; however, it provides no indication of how efficient the process is with respect to photons; thus, if the reaction was carried out in the presence of a high phosphate concentration, both the photo-process under test and the photodegradation of phenol would be very slow and photochemically inefficient, and yet a  $\xi_r$  value of two could easily be returned and misunderstood as implying an efficient photoreaction. As a result, the suggestion [92] that “the term photonic efficiency, together with  $\xi_r$ , should be used only when the number of incident photons impinging on the front window of the photolysis cell is known by actinometry (or by other means)”, represents a very sound and important safeguard when  $\xi_r$  values are used.

Semiconductors have also been used to sensitize the photoconversion of toxic inorganic substrates to harmless or less toxic ones. A number of examples of such photoreactions, sensitized by  $\text{TiO}_2$ , are listed in Table 7 [98–110]. The photoreduction of metal ions by semiconductor photocatalysts, usually using a hole-trapping, sacrificial electron donor such as methanol or formaldehyde to help promote the photoreduction process, is a popular approach to the preparation of metallized semiconductor photocatalysts, such as platinized  $\text{TiO}_2$ , i.e.  $\text{Pt/TiO}_2$ , and metal-supported catalysts [111]. The photoreduction of mercury(II) chloride and methyl mercury ( $\text{CH}_3\text{Hg(II)Cl}$ ) to  $\text{Hg}^0$ , sensitized by  $\text{TiO}_2$ , has been reported; the latter photoreaction requires the presence of methanol as a sacrificial electron donor [112].  $\text{TiO}_2$  can be used to remove, nearly sequentially, platinum, gold and rhodium in a mixed solution of their chlorides using a finite level of dissolved oxygen to delay rhodium reduction [113]. In most industrial gold recovery processes, cyanide is present and must be removed before semiconductor photocatalysis can be used to extract the gold [114].

One of the cornerstone technologies in the production of potable water is chlorination; however, it is now recognized that this process produces potential carcinogens as disinfection byproducts (DBPs), such as the trihalomethanes. Ozonation offers an attractive alternative, since it avoids the formation of most of the hazardous DBPs associated with chlorination. However, it has now been discovered that ozonation generates small levels of bromate ions, a recognized cancer suspect agent. At the moment, the major environmen-

Table 7

TiO<sub>2</sub>-sensitized photosystems for the removal of toxic inorganics

Reaction $A + D \rightarrow A^- + D^+$	Reference
$O_2 + 2NO_2^- \rightarrow 2NO_3^-$	[98]
$O_2 + 2SO_3^{2-} \rightarrow 2SO_4^{2-}$	[99]
$2O_2 + H_2O + S_2O_3^{2-} \rightarrow 2SO_4^{2-} + 2H^+$	[100]
$O_2 + 2CN^- \rightarrow 2OCN^-$	[101]
$5O_2 + 4H^+ + 4CN^- \rightarrow 2H_2O + 4CO_2 + 2N_2$	[102]
$M^{n+} + (n/2)H_2O \rightarrow M^0 + nH^+ + (n/4)O_2$	[99,103]
$M^{n+} + (n/6)CH_3OH + (n/6)H_2O \rightarrow M^0 + nH^+ + (n/6)CO_2$	[103,104]
(Ag > Pd > Au > Pt > Rh > Ir > Cu = Ni = Fe = 0 using the following metal salts: AgNO <sub>3</sub> , PdCl <sub>2</sub> , AuCl <sub>3</sub> , H <sub>2</sub> PtCl <sub>6</sub> , RhCl <sub>3</sub> , H <sub>2</sub> IrCl <sub>6</sub> , Cu(NO <sub>3</sub> ) <sub>2</sub> , Ni(NO <sub>3</sub> ) <sub>2</sub> and Fe(NO <sub>3</sub> ) <sub>3</sub> )	
$M^{2+} + 1/2O_2 + H_2O \rightarrow MO_2 + 2H^+$ ( $M^{2+} \equiv Mn^{2+}$ and $Pb^{2+}$ (needs Pt/TiO <sub>2</sub> ))	[105,106]
$O_2 + 2H_2O \rightarrow 2H_2O_2$	[107]
$2BrO_3^- \rightarrow 2Br^- + 3O_2$ (works best with Pt/TiO <sub>2</sub> )	[108,109]
$5O_2 + 6NH_3 \rightarrow 2N_2 + N_2O + 9H_2O$	[110]

tal regulatory agencies have set a maximum bromate level in potable water of 10 ppb, although there are indications that this level will be reduced to 0.5 ppb very shortly. Typically, potable water which has been treated with ozone will have a bromate level in the range 3–68 ppb; thus there is a great deal of interest in inexpensive methods for the removal of bromate ions in ozonated water. In a recent paper [109], we established that TiO<sub>2</sub> was able to sensitize the photodecomposition of bromate, i.e.



at the parts per billion level (typically  $[BrO_3^-]_0 = 50$  ppb) using 254 nm light, and that platinization of the TiO<sub>2</sub> photocatalyst (0.5% Pt w/w) enhanced the effectiveness of the photocatalyst by a factor of 4.2.

Research in the area of semiconductor-sensitized photodegradation of organic and inorganic materials has been extensive and, as a result, we have a greater understanding of the fundamental processes involved. Following on from this work, some commercial products have already been generated, e.g. a small-scale TiO<sub>2</sub> photocatalytic reactor system for the destruction of organic pollutants in air and water is commercially available from Nutech Energy Systems (London, Ont.), and SGE (UK Ltd.) have launched ANATOC™, an analyser for the rapid determination of total organic carbon (TOC) in water, which utilizes semiconductor photocatalyst technology.

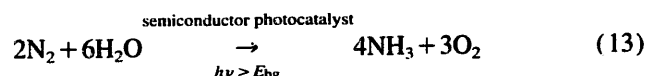
It may appear surprising at first that there are not more commercial water purification systems available based on semiconductor photocatalysis given the impressive, extensive range of organic pollutants which can be destroyed by this method and the fact that it can be turned on and off with the flick of a light switch. However, it should also be recognized that deactivation of the semiconductor photocatalyst is possible, especially by the deposition of solid inert oxides, such as iron(III) oxide, on the photocatalyst's surface and by the binding of strongly adsorbed inert anions, such as phosphate ions, to the surface. In addition, the most active

semiconductor photocatalysts, such as TiO<sub>2</sub>, require UV photons and, therefore, are unlikely to find application in water purification systems using sunlight. In addition, the formal quantum yields of most semiconductor-sensitized photocatalytic reactions associated with water purification are less than 1% and, therefore, are quite inefficient. Furthermore, major developments in this area are required, such as the production of more active semiconductor photocatalysts, or photocatalysts which can utilize effectively, and without wear, visible light as well as UV light, in order to make this approach to water purification a realistic competitor to the current traditional methods of chlorination, ozonation, air stripping and granulated activated carbon adsorption.

### 8. Semiconductor particles as sensitizers for the photoreduction of nitrogen and carbon dioxide (and concomitant oxidation of water to oxygen) [6,21]

If the photocleavage of water, sensitized by semiconductor particles, under ambient conditions of temperature and pressure, is considered to be controversial, this pales into insignificance when we examine the semiconductor-sensitized photoreduction of nitrogen and carbon dioxide, under ambient conditions, which may be considered to be decidedly unproven, despite some 20 years of research and many claims to the contrary.

The photocatalytic synthesis of ammonia and oxygen from nitrogen and water, i.e.

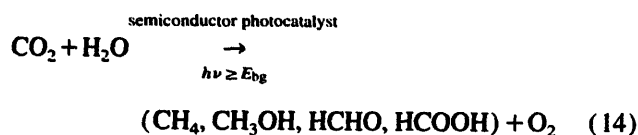


was first claimed in 1977 by Schrauzer and Guth [115] using water vapour and generating gaseous ammonia. Over the last 20 years, a plethora of semiconductor-sensitized photosystems for reaction (13), usually using liquid phase water and purporting to generate dissolved ammonia, have been described [21]. Various semiconductors have been used, including TiO<sub>2</sub>, SrTiO<sub>3</sub>, Fe<sub>2</sub>O<sub>3</sub>, FeO(OH), WO<sub>3</sub> and CdS;

however, in all the systems studied, invariably the yields of ammonia have been very low, typically nanomoles, and around the limit of detection. Indeed, Davies et al. [21], in their outstanding and challenging review on the subject, state that with all the reports of ammonia synthesis with titania-based photocatalysts “no paper reports the photosynthesis of ammonia from water and nitrogen at a level that was shown to be significantly different from levels of ammonia that might result from contamination”. Contamination can come from breath (ammonia can be exhaled at a rate of up to  $375 \mu\text{g h}^{-1}$ ) and many laboratory sources. For example, the latter workers found that water placed in contact with silicone rubber septa, high vacuum grease, traces of acetone (commonly used to clean glassware) and Teflon tape gave false positive indications of ammonia when subjected to the popular Nessler’s method for ammonia analysis [21].

In their detailed examination of the literature associated with reaction (13), Davies et al. [21] found no report in which the experiments involving reaction (13) had been carried out a significant number of times in order to determine both the yield of ammonia and its standard deviation. In their own studies of reaction (13), sensitized by Fe-doped  $\text{TiO}_2$ , these workers found no statistically significant experimental evidence for ammonia synthesis, despite previous reports indicating that this system operates under a wide range of experimental conditions [21,116–118]. It should also be pointed out that the views of Davies and coworkers [21,116–118], i.e. that the achievement of reaction (13) remains, as yet, unproven through the lack of statistically significant results, are hotly contested by some of those working in this field [119,120]. However, the case made by Davies and coworkers [21,116–118] is strong and the call for the use of isotope ratio mass spectrometers in correctly designed, significant experiments, repeatable by more than one research group, appears to be a reasonable approach to settle the matter. Time will tell whether 20 years of research in this area is up to this simple task. As Davies and coworkers [21,116–118] point out “the concept of a major discovery, such as reaction (13), that remains continually on the borderline of demonstration is internally inconsistent” and that “results which cannot be reproduced are of no scientific interest”.

The photocatalytic reduction of carbon dioxide by semiconductor particles, under ambient conditions of temperature and pressure, to reduced carbon products, such as methanol, methane, formaldehyde and formic acid, in water, with the concomitant oxidation of water to oxygen, i.e.



has been less well studied [6] compared with the reduction of nitrogen. However, the few reports of reaction (15) which do exist [6] have the common features of very low yields and the real possibility of contamination.

It should also be noted that, in most reported cases of reactions (13) and (14), the semiconductor photocatalyst has been pre-treated, e.g. by doping with iron or high temperature firing in an inert or reduced atmosphere, and this may create reduction sites (such as  $\text{Ti}^{\text{III}}$  in  $\text{TiO}_2$  or  $\text{SrTiO}_3$ ) which may be able to undergo a photoinduced, stoichiometric reaction with nitrogen or carbon dioxide in which the ammonia or reduced carbon products are generated. Such a process is not photocatalysis and yet would initially give the appearance of it. The generation of  $\text{Ti}^{\text{III}}$  sites, and their subsequent photoinduced stoichiometric reaction with carbon dioxide, certainly provides an alternative explanation to the results of Hemminger et al. [121] on the reduction of carbon dioxide to methane by water vapour using a clean, reduced  $\text{SrTiO}_3$  single crystal. In this system, methane production is low (quantum yield, 0.01%) and ceases after 10 min of irradiation, but is restored after cleaning by argon ion bombardment and short periods of heating in oxygen. In the same system, methane production, “at rates comparable with the photo-assisted reaction”, can also be observed in the dark using the same “photocatalyst” heated to 450 K. It is also worthwhile noting that, although reactions (13) and (14) may not occur, the semiconductor-sensitized reverse reactions do. Indeed, the oxidation of ammonia by oxygen, photocatalysed by  $\text{TiO}_2$ , to form nitrite and nitrate ions is a well-recognized process [110,118], and the photomineralization of organics by oxygen, sensitized by  $\text{TiO}_2$ , is the basis of a large amount of the work described in the previous section.

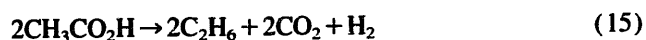
It was suggested as long ago as 1913 by Benjamin Moore [122] that “the first step towards the origin of life must have been the synthesis of organic matter from inorganic by agency of inorganic colloids acting as transformers or catalysts for radiant solar energy”. This theme was followed up extensively some 28 years later by Dahr et al. [123] working on nitrogen fixation in soils. As part of this work, Dhar et al. [123] used naturally occurring minerals, such as hydroxides of iron and oxides of iron, titanium and manganese, as catalysts/photocatalysts for nitrogen fixation. The results of this work are inconclusive as they do not eliminate the possibility of contamination and the photodegradation of nitrogen-containing compounds. However, the theme of nitrogen fixation by inorganic photocatalysts was picked up by Schrauzer et al. [124] in their work on nitrogen fixation using desert sands. These workers suggested that nitrogen is reduced photochemically on the surfaces of minerals containing titanium dioxide, and nitrogen fixed in this manner represents a significant contribution to the nitrogen cycle, particularly in arid regions of the earth [124]. Although positive results were reported by Schrauzer et al. [124] on some of the desert sands tested, Davies et al. [21] suggest that the results are inconclusive and may be interpreted in terms of either contamination or variations in background levels.

Dunn et al. [125] have shown that platinized  $\text{TiO}_2$ , when placed in contact with a mixture of methane, ammonia and water and irradiated with ultra-bandgap light, can generate small amounts of the amino acids glycine, alanine, serine,

aspartic acid and glutamic acid. Experiments with nitrogen-15-labelled ammonia showed that the nitrogen in the amino acids originated from the ammonia rather than from contaminants. It is tempting, therefore, to believe that such abiotic processes may have played a role in the production of amino acids from the primordial atmosphere many millions of years ago. However, the same workers note [125] that the unplatinized minerals,  $\text{Fe}_2\text{O}_3$  and ilmenite, do not photocatalyse the production of amino acids at detectable levels and that the primordial atmosphere [126] may not have been reducing, but more oxidizing, containing  $\text{CO}_2$  and  $\text{N}_2$ .

### 9. Semiconductor particles as sensitizers for organic photosynthetic processes [6,12,22,23]

The use of semiconductors as sensitizers for various organic photosynthetic processes stems from the early work of Kraeutler and Bard [127] on the use of platinized  $\text{TiO}_2$  as a sensitizer for the conversion of acetic acid to methane and carbon dioxide: an alternative photoinduced Kolbe reaction. These workers were able to show subsequently that the conventional Kolbe reaction involving acetic acid



could be photoinduced using a rutile  $\text{TiO}_2$  photoanode. It was quickly recognized that, if water was used as the solvent, reaction (5), the complete oxidative mineralization of the organic substrate, would usually predominate due to the generation of highly oxidizing hydroxyl radicals. Thus most work in the area of semiconductor-sensitized organic photosynthesis has been carried out either in an inert solvent, such as acetonitrile (MeCN), or in the neat organic substrate. The semiconductor-sensitized organic photosynthetic reactions which have been carried out to date can be fitted into the following broad categories: oxidations and oxidative cleavages, reductions, isomerizations and polymerizations.

Most work in this area has been carried out on oxidation and oxidative cleavage photoreactions sensitized by  $\text{TiO}_2$ , and a number of examples are collected in Table 8 [127–135]. For most of the reactions in Table 8,  $\Delta G^\circ$  is negative, and therefore they are technically examples of photocatalytic, rather than photosynthetic, reactions (see above). An interesting example of an oxidative cleavage photoreaction sensitized by a semiconductor is the photo-oxidation of toluene to benzaldehyde and then to benzoic acid, sensitized by  $\text{TiO}_2$  in MeCN [131] (see Table 8). Fig. 9 illustrates the observed temporal variations in [toluene], [benzaldehyde] and [benzoic acid] on illumination of the system with ultra-bandgap light when a small amount of sulphuric acid ( $50 \mu\text{dm}^3$ ;  $5 \text{ mol dm}^{-3}$ ) is added to the reaction mixture; in the absence of the acid, the photosensitized reaction is considerably slower. It is believed [131] that the  $\text{HSO}_4^-$  anion promotes the reaction by mediating the oxidation of the organic substrate by reacting with the photogenerated hole to form the highly oxidizing radical  $\text{HSO}_4^\bullet$ . Further work using substituted toluenes has

shown that the addition of a small amount of sulphuric acid also enhances the kinetics of oxidation of the organic substrate and that the formation of benzoic acid is favoured with more strongly electron-withdrawing substituents.

Examples of reduction, isomerization and polymerization photoreactions sensitized by  $\text{TiO}_2$  are given in Table 9 [136–141]. Work in this area and in the field of oxidation and oxidative cleavage photoreactions has shown that the product distribution can be markedly affected by a wide variety of parameters, including the nature of the semiconductor (in particular, its conductance and valence band positions), crystal phase, particle size, surface morphology, light intensity and presence of surface catalysts (such as Pt) [6,12,22,23].

### 10. Semiconductor particles and films as sensitizers for the destruction of gaseous and thin film organic pollutants [24,25]

The use of semiconductors as sensitizers for organic photosynthetic reactions in the condensed phase has also been extended to work in the gas phase. For example, Djeghri and Teichner [142] reported the details of the oxidation of 2-methylbutane by oxygen, sensitized by  $\text{TiO}_2$ , in which the main initial products were carbon dioxide (15%), ethanal (16%), acetone (36%), butanone (12%) and 3-methylbutanone (10%). However, in this work, only 2% of the initial substrate was converted. Many more studies have investigated the initial selectivity of  $\text{TiO}_2$  as a sensitizer for the photo-oxidation of gaseous organic substrates by oxygen. In most of the systems studied to date, although a relatively stable intermediate (or intermediates) is (are) often generated, eventually all the initial gaseous organic substrate is completely degraded to carbon dioxide, water and mineral acids, i.e.

Gaseous organic substrate

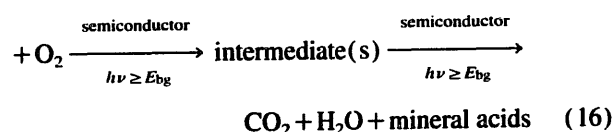
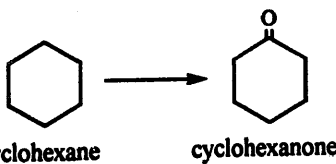

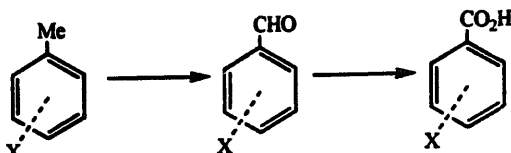
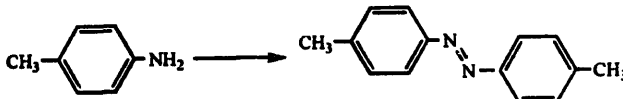
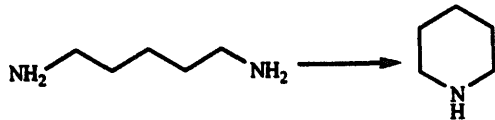
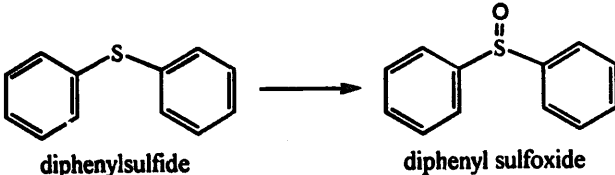


Table 10 [143–159] lists some examples of the use of  $\text{TiO}_2$  as a semiconductor sensitizer for the oxidation of gaseous organic substrates by oxygen, together with the major intermediates and formal quantum efficiencies, where the data are given. For some simple, usually halogenated, organic substrates, such as trichloroethylene or perchloroethylene, FQE values for reaction (16), sensitized by  $\text{TiO}_2$ , approaching unity have been reported and are taken as an indication of the operation of a radical chain reaction mechanism. In contrast, when other, non-halogenated organic substrates are used, such as benzene, toluene, xylene, ethylene, propylene, tetramethylethylene, acetone, propanol and ethanol, FQE values of less than 0.1 are found [143,145].

These FQE values are usually more than tenfold greater than those found for the photodestruction of the same organic



Table 8  
Oxidation and oxidative photoreactions sensitized by TiO<sub>2</sub>

Semiconductor	Reaction	Solvent plus additives	Reference
TiO <sub>2</sub> (anatase) / Pt	CH <sub>3</sub> CO <sub>2</sub> H → CH <sub>4</sub> + CO <sub>2</sub> (alternative photo-Kolbe reaction)	Aqueous acetic acid	[127]
TiO <sub>2</sub> (rutile) macroelectrode	2CH <sub>3</sub> CO <sub>2</sub> H → 2C <sub>2</sub> H <sub>6</sub> + 2CO <sub>2</sub> + H <sub>2</sub> (photo-Kolbe reaction)	Aqueous acetic acid, MeCN	[128]
TiO <sub>2</sub>	 cyclohexane → cyclohexanone	Neat cyclohexane	[129]
TiO <sub>2</sub>	 1,1 diphenyl ethylene → benzophenone (reaction rate sensitive to ring substitution, with electron-withdrawing groups decreasing and electron-donating groups increasing the rate) (71% yield)	MeCN, O <sub>2</sub>	[130]
TiO <sub>2</sub>	 (toluene substituted substrates tested included: X = H, <i>p</i> -CF <sub>3</sub> , <i>p</i> -NO <sub>2</sub> , <i>p</i> -Cl, <i>p</i> -F, <i>p</i> -Me, <i>p</i> -tert-butyl, <i>m</i> -NO <sub>2</sub> , <i>m</i> -Cl, <i>m</i> -F; benzoic acid formation favoured the more electron withdrawing the substituent)	MeCN, H <sub>2</sub> SO <sub>4</sub> , O <sub>2</sub>	[131]
TiO <sub>2</sub>		H <sub>2</sub> O, O <sub>2</sub>	[132]
TiO <sub>2</sub> /Pt		H <sub>2</sub> O	[133]
TiO <sub>2</sub> /Pt	C <sub>7</sub> H <sub>15</sub> CH <sub>2</sub> OH → C <sub>7</sub> H <sub>15</sub> CHO (poor yields obtained with secondary aliphatic or aromatic alcohols) (70% yield)	Benzene	[134]
TiO <sub>2</sub>	 diphenylsulfide → diphenyl sulfoxide	MeCN, O <sub>2</sub>	[135]

substrates dissolved in aqueous solution, e.g. the FQE value for trichloroethylene in aqueous solution is approximately 0.01 [145]. As a consequence, the use of semiconductor photocatalysis as a method of purifying air has begun to attract increasing attention. Such a system could find application in the following:

1. the remediation of contaminated soils and groundwater (through the use of air stripping, coupled with a photocatalytic air purification process);
  2. the purification of industrial gaseous effluent;
  3. the treatment of indoor or closed system air.
- The latter is believed to be a potentially very important market



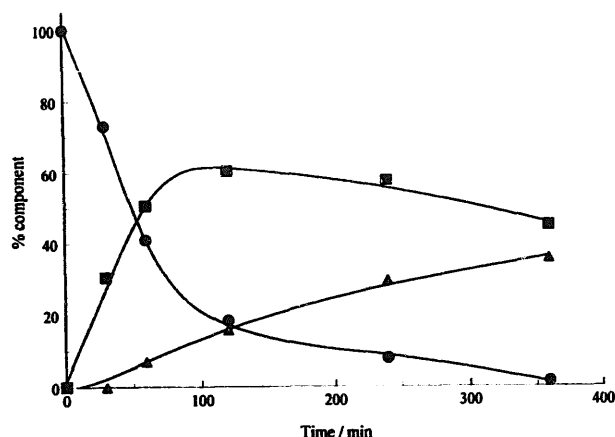


Fig. 9. Observed variations with time of the concentrations of toluene (●) (the initial substrate), benzaldehyde (■) (an intermediate) and benzoic acid (▲) (the major final product) after prolonged illumination of 100 cm<sup>3</sup> of acetonitrile containing TiO<sub>2</sub> (50 mg), O<sub>2</sub> (100% saturation), toluene (0.1 mmol) and H<sub>2</sub>SO<sub>4</sub> (25 μmol) at 30 °C.

as the public becomes more aware of the effect of the quality of indoor air, at work and at home, on general health. An important class of offensive odour chemicals are oxygenates, such as aldehydes, ketones and alcohols, many of which can be degraded via semiconductor photocatalysis, as indicated by the examples in Table 10.

However, Ollis and coworkers [160–162], and others, have highlighted possible weaknesses in the use of semiconductor photocatalysis as a means of purifying air. For example, it is recognized that some organic substrates are very difficult to photomineralize completely (e.g. certain aromatics and haloethanes), and that complete mineralization of the organic substrate is not always established unequivocally. In addition, there is the possibility that this method of purification may generate a relatively stable intermediate (such as phosgene from trichloroethylene; see Table 10) which is much more toxic than the initial organic substrate. Finally, and probably most crucially, the destruction of many organic substrates via reaction (16) appears to generate byproducts

Table 9  
Other organic synthesis photoreactions sensitized by TiO<sub>2</sub>

Semiconductor	Reaction	Solvent plus additives	Reference
<b>Reduction reactions</b>			
TiO <sub>2</sub> /Pt		Aqueous HNO <sub>3</sub>	[136]
TiO <sub>2</sub> /Pt		EtOH	[137]
<b>Isomerizations</b>			
TiO <sub>2</sub>		MeCN	[138]
<b>Substitutions</b>			
TiO <sub>2</sub>	(C <sub>6</sub> H <sub>5</sub> ) <sub>3</sub> CH → (C <sub>6</sub> H <sub>5</sub> ) <sub>3</sub> CF (57% yield) (also selective photofluorination reaction for olefins, phosphines and phosphites)	AgF in MeCN	[139]
TiO <sub>2</sub>		MeCN, H <sub>2</sub> O, NaCN	[140]
<b>Polymerizations</b>			
TiO <sub>2</sub> /Pt	γ-Methyl methacrylate → poly(methyl methacrylate)	MeCN	[141]

Table 10  
Examples of TiO<sub>2</sub>-sensitized oxidation photoreactions of gaseous organic substrates

Semiconductor	Organic substrate	Major intermediates	Comments	FQE	Reference
<i>Halogenates</i>					
TiO <sub>2</sub>	CCl <sub>4</sub> , CH <sub>3</sub> Cl	None	No degradation observed	0	[143]
TiO <sub>2</sub>	Trichloroethylene (TCE)	Dichloroacetaldehyde chloride (DCAC) and phosgene	TCE can be used to increase the degree of destruction of toluene from 0.1–0.15 to 1.0 through a chlorine radical chain reaction mechanism	–	[144]
TiO <sub>2</sub> on alumina	TCE	DCAC and phosgene	Chlorine and carbon monoxide are also formed as significant intermediates; the TiO <sub>2</sub> was supported on a high surface area alumina foam	0.5–0.8	[145]
TiO <sub>2</sub> pellets	TCE	–	No phosgene is generated by this photocatalyst	0.4–0.9	[146]
<i>Alkanes</i>					
TiO <sub>2</sub>	Isobutane	Acetone and CO <sub>2</sub>	Typically about 6 times more acetone than CO <sub>2</sub> is produced in the initial stages	0.1	[147,148]
TiO <sub>2</sub>	Methane	None	If the photocatalyst is loaded with tungstosilicate, CO, CO <sub>2</sub> and H <sub>2</sub> O are produced	–	[149]
<i>Alcohols</i>					
TiO <sub>2</sub>	1-Butanol	1-Butanal (89%) and 1-butene (11%)	Low (2%) oxygen levels were used	–	[150]
TiO <sub>2</sub>	2-Propanol	Acetone	Ethanol and methanol were also studied and their aldehydes were observed as major intermediates	–	[151]
<i>Aldehydes</i>					
TiO <sub>2</sub>	Propionaldehyde	–	The effect of different supports (zeolites, alumina, silica and activated carbon) on the kinetics was studied; can make a factor of approximately four difference	–	[152]
TiO <sub>2</sub>	Acetaldehyde	Acetic acid	A smooth, semi-transparent highly active film photocatalyst was used	0.13–0.35	[153]
<i>Aromatics</i>					
TiO <sub>2</sub> on glass fibre	Benzene	–	Little degradation at high levels (143000 ppm), but appreciable at lower levels (2200 ppm; approximately 70% conversion)	–	[154]
TiO <sub>2</sub>	Toluene	–	Degree of conversion: 0.15–0.25	–	[143]
<i>Heterocycles</i>					
TiO <sub>2</sub> on zeolite	Pyridine	–	–	0.11	[155]

which lead to the deactivation of the semiconductor photocatalyst (usually TiO<sub>2</sub>). For example, Peral and Ollis [160] have found that the photocatalysed degradation of certain volatile organic substrates containing an Si or N heteroatom (such as dimethylsiloxane and pyrrole respectively) deactivates irreversibly a TiO<sub>2</sub> photocatalyst by the surface deposition of species which inhibit and deactivate photoactive sites. There is also evidence that some alcohols when used in reaction (16) will lead to photocatalyst deactivation, presumably through the formation of strongly adsorbing, deactivating carboxylic acids. Fig. 10 illustrates the loss of photocatalytic activity observed by Peral and Ollis [161] in the photodegradation of 1-butanol by oxygen sensitized by TiO<sub>2</sub>. The photocatalyst could only be reactivated by contin-

ued illumination in clean flowing dry air. It was suggested that a certain strongly adsorbed intermediate species was responsible for the loss of photocatalytic activity and that, with prolonged irradiation, the intermediate could be slowly oxidized [161]. In a recent paper, Sauer and Ollis [162] surveyed the current literature on the semiconductor-sensitized photodegradation of gaseous organics, and found that photocatalyst deactivation was almost always found in single-pass, fixed-bed photoreactors for cumulative contamination conversions in excess of 1–10 equivalent monolayers, whereas no evidence of catalyst deactivation was found for batch reactor studies. The lack of evidence of photocatalyst deactivation in batch reactors is thought to be because it would only be detected with repeated runs, without catalyst

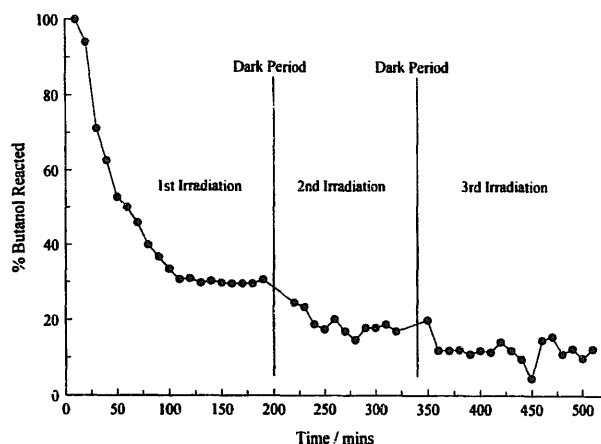


Fig. 10. Observed temporal variation in the level of gaseous 1-butanol (initial concentration,  $260 \text{ mg m}^{-3}$ ; light intensity (above  $300 \text{ nm}$ ),  $5.0 \times 10^{-7} \text{ einstein cm}^{-2} \text{ min}^{-1}$ ) in the presence of a  $\text{TiO}_2$  photocatalyst on repeated irradiation. There is a discernible loss in photocatalytic activity as the reaction proceeds and after each dark period (a loss which could not be regenerated by keeping the semiconductor in the dark). The amount of 1-butanol consumed equals the amount of butaldehyde produced, and thus the concentration of any other (interfering) product is near zero (data from Ref. [161]).

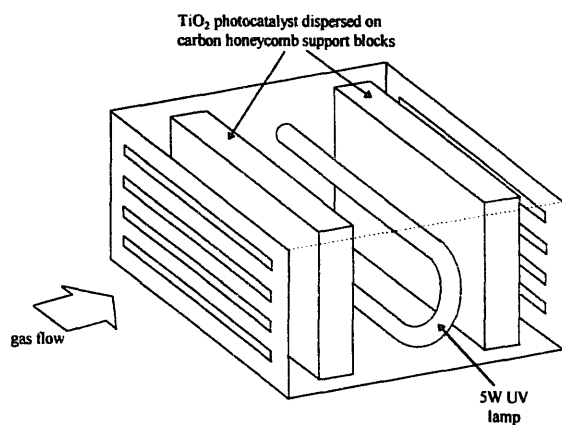


Fig. 11. Schematic illustration of the basic components of a prototype photocatalytic air purifier made by Toyota (diagram after Ref. [168]).

pretreatment or regeneration between runs, and such experiments do not appear to have been carried out. Clearly, more research must be performed in this area if thin film semiconductor photocatalysts for the destruction of gaseous (or thin film) organic pollutants are to be of real commercial value.

The role of water vapour in the photocatalytic degradation process, as well as the photodeactivation process, will be a key area of focus for future research. In some studies, water vapour appears to inhibit (isopropanol [163], trichloroethylene [163,164], acetone [149,161]) photocatalytic activity, whereas in others it promotes (toluene [165]) or has little effect (1-butanol [149,161]) on photocatalytic activity; in others (toluene [144], *m*-xylene [161]), it promotes and inhibits photocatalytic activity at low and high water vapour levels respectively. In some studies, photocatalyst deactivation occurs when there is no water vapour (toluene [166], methyl-tert-butyl ether [156], acetone [156]); in others (trichloroethylene [167]), the photocatalyst appears to work

indefinitely under dry conditions. The current situation is confused and needs to be resolved.

Commercial prototype photocatalytic systems for the purification of air indoors and in the car are already being created. Thus Suzuki [168], working for Toyota Central R and D Laboratories, has reported a  $\text{TiO}_2$  photocatalyst, on a honeycomb carbon support, for the purification of air in cars. Fig. 11 illustrates the typical features of the prototype photocatalytic air purifier, and Fig. 12 shows some of the results obtained using the photoreactor in a stirred box. From the latter results, it appears that the carbon support helps to purify the air, but the presence of the semiconductor photocatalyst makes for a more effective air purifier with prolonged use. However, there is some evidence of photocatalyst deactivation when ammonia is used as the test substrate rather than isoprene (see Fig. 12), although the semiconductor photocatalyst can be rejuvenated by exposure to clean air. Feasibility tests were carried out using this system on 25 new cars with positive results.

It has also been suggested that a thin layer semiconductor photocatalyst, dispersed on an inert support such as window glass, ceramic tiles or a honeycomb carbon monolith, as described above, could be used as photoactivated deodorizers

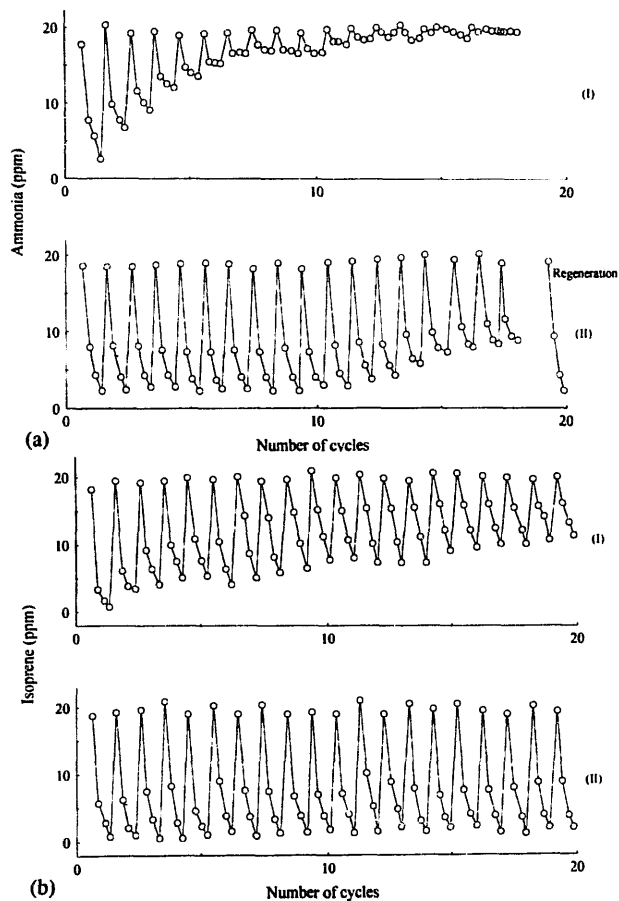


Fig. 12. Observed removal of gaseous ammonia (a) and isoprene (b) by carbon adsorption (I) and carbon adsorption and semiconductor photocatalysis (II). The photocatalytic system used to perform these experiments employed the major components in Fig. 11 and the experiments were conducted in a stirred box (data after Ref. [168]).

in the kitchen and bathroom, as well as in cars [168]. Indeed, with respect to the former application, TOTO, Japan's largest bathroom fixture producer, is currently selling photoactive  $\text{TiO}_2$ -coated ceramic tiles for this purpose [169]. Various recipes have been reported [166,169–171] for creating semi-transparent, thin (10  $\mu\text{m}$  to 50 nm)  $\text{TiO}_2$  films with photocatalytic activities which appear to be greater than that of Degussa P25  $\text{TiO}_2$  (although it is debatable whether such comparisons between a thin film and a powder (Degussa P25) are meaningful).

Of relevance to the use of thin  $\text{TiO}_2$  films as photodeodorizers in the house environment is the observation [169] that the photocatalyst appears to be only six times more active in the destruction of methyl mercaptan when illuminated by a blacklight bulb than when illuminated by a regular fluorescent light, even though the UV component of a regular fluorescent light is 1%–3% relative to that of a blacklight bulb. This surprising result is attributed to the dramatic increase in the photocatalytic efficiency with decreasing light intensity [169]. Further work is needed to see whether such an effect is reproducible and sustainable for this and other test organic substrates, such as alcohols, ketones, aldehydes and aromatics, which represent the wide range of gaseous organic substrates responsible for unwanted household odours. The problem of photocatalyst deactivation is the family ghost which haunts this area of research and which must be exorcized fully if commercial devices based on semiconductor photodeodorization are to have a future as enduring air purification systems.

The semiconductor-sensitized oxidation of the  $\text{NO}_x$  gases, NO and  $\text{NO}_2$ , by oxygen, to nitric acid does not really fit under this heading, but the recent developments in this area are such that they should be mentioned, albeit briefly [172,173] and slightly out of context. Research in this area has advanced sufficiently such that Mitsubishi Materials Laboratory have applied a semi-permanent layer of  $\text{TiO}_2$  to the surface of concrete paving blocks and are testing them on a busy stretch of road in Osaka as a method of reducing the  $\text{NO}_x$  gases produced by cars [173].

There is a growing interest in the use of thin, transparent films of  $\text{TiO}_2$  as a sensitizer for the photodestruction of not only gaseous organic species, thereby generating a photodeodorizing surface, but also thin organic films, thereby generating a self-cleaning surface. The latter films could find application in self-cleaning windows and automotive windshields. Such  $\text{TiO}_2$  films need to be clear (i.e. they must not scatter visible light), adherent (with an abrasion resistance which is sufficient to withstand cleaning or impact by dust particles) and photoactive. The photoactivity must be such that it is able to destroy the thin film organic substrate under ambient conditions at a rate which is greater than the rate of deposition, otherwise it will become fouled with UV-absorbing non-volatile partial oxidation products. Clear  $\text{TiO}_2$  films require  $\text{TiO}_2$  particles which must be much smaller than the wavelength of visible light, i.e. typically less than 30 nm (nanocrystalline  $\text{TiO}_2$ ), and this largely rules out the use of

Degussa P25 particles which have aggregate particle diameters of approximately 0.1  $\mu\text{m}$ . Heller and coworkers [24,166,174,175], and others [169–171], have developed several methods for the creation of such films, usually via a sol-gel process in which, typically, a titanium alkoxide (e.g. titanium isopropoxide) is hydrolysed, coated onto a glass substrate, previously treated with sulphuric acid to produce a sodium-depleted layer, and calcined at a high temperature (usually 500  $^\circ\text{C}$ ) for a short time (approximately 20 min) [175]. Such films usually comprise anatase  $\text{TiO}_2$  crystallites of 3–6 nm in diameter and therefore are clear. Layers of  $\text{TiO}_2$  can be built up using the sol-gel procedure to produce films approximately 60–100 nm thick which are not abraded when scribed with pencils of hardness H2 or softer and cannot be removed using Scotch Tape or rubbing with paper towels. In contrast, when similar, but scattering, P25  $\text{TiO}_2$  films are deposited onto the same glass substrate, although they appear very photoactive, they are easily detached by wiping, applying Scotch Tape and scribing with very soft B pencils. Photonic efficiency values (see Eq. (9)) for the degradation of stearic acid films of  $(2.6\text{--}7.2) \times 10^{-4}$  have been reported by Paz et al. [175] for thin, non-scattering  $\text{TiO}_2$  films using 365 nm light at intensities similar to that of the UV component of sunlight at sea level at zenith, i.e. approximately 3.5  $\text{mW cm}^{-2}$  ( $10^{-8}$  einstein  $\text{cm}^{-2} \text{s}^{-1}$ ). Calculations show that the  $\text{TiO}_2$  thin films can photodegrade stearic acid at a rate of 20  $\text{nm h}^{-1}$  in sunlight, which implies that it may be possible to use such films to remove, over a period of a day, the glare-causing organic film, typically more than 100 nm, which deposits on automobile windscreens.

It has also been proposed by Heller et al. [24,176] that oil and organic spills on water can be cleaned up through the use of  $\text{TiO}_2$ -coated hollow glass or glass-ceramic microbeads floating at the air-oil interface, as illustrated in Fig. 13. The  $\text{TiO}_2$ -coated buoyant photocatalytic microbubbles created are typically 50–200  $\mu\text{m}$  in diameter and are rendered oleophilic by reactive coating with an organosilicone, for example. Addition of the microbeads (2 g) to a thin layer of crude oil (2 ml) in a small Petri dish causes the oil to rapidly aggregate around the oleophilic photocatalytic microbeads and, with lengthy (2000 h) exposure to UV light (40  $\text{mW cm}^{-2}$  of 365 nm light), the black crude oil is degraded, leaving the fine, white, sand-like microbeads floating on the surface. Calculations show that the photocatalyst microbeads would be able to sensitize the photo-oxidation of a mass of oil equal to their own weight in 10–30 days under solar irradiation. The thickness of an oil layer on water is reduced, when fully covered with bubbles and when irradiated by AM 1 sunlight, by about  $5 \times 10^{-4}$  cm each day. Heller et al. [24,176] believe that this rate of photo-oxidation is adequate to maintain the water free of the oily sheen often seen around harbours and where there is a lot of boat traffic.

Although the microbead photocatalysts are not suitable for the removal of thick (2–10 cm) layers of oil, they do help such layers to be burnt down to a thickness at which semiconductor photocatalytic action could be applicable. There is

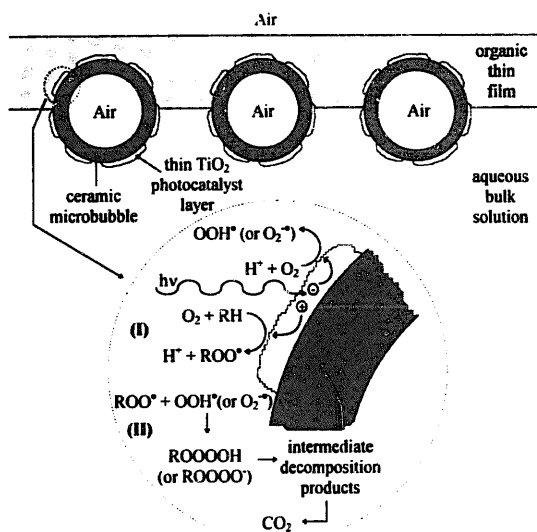
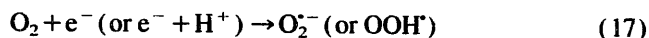


Fig. 13. Schematic illustration of the photocatalytic microbubbles used by Heller et al. [24,176] to sensitize the photodestruction of thin organic films on water. The beads are typically 50–200  $\mu\text{m}$  in diameter. The proposed mechanism of photocatalysis operating in these systems is illustrated in the expanded diagram of one of the beads. The mechanism involves: (I) reduction of  $\text{O}_2$  to superoxide by photogenerated electrons; the photogenerated holes participate in hydrogen abstraction from the organic substrate, coupled with reaction with  $\text{O}_2$ , to form an organoperoxide species; (II) the reaction of the organoperoxide species with the superoxide radical to form an organic tetraoxide species, which decomposes to form intermediate decomposition products which are then further oxidized to  $\text{CO}_2$ .

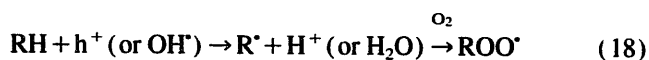
evidence [177] to suggest that the products of the semiconductor-sensitized photodegradation of oil are less harmful than those associated with the destruction of oil by weathering; this is not surprising given that the latter process produces phenols, polyphenols and, eventually, tar. However, to many, the photocatalyst itself represents a pollutant and, it might be argued, a more permanent and visible pollutant than the surfactants currently used to disperse oil spills. In addition, it seems probable, given the broad range of aromatic compounds in oil, that photocatalyst deactivation by UV-absorbing, polymeric, photogenerated intermediates will be a problem. Thus much more work is needed on the environmental impact and long-term efficacy of microbead photocatalyst technology if this approach to the cleaning up of oil and organic spills in environmental waters is to have a real future.

Schwitzgebel et al. [178] have also used a hydrophilic form of the photocatalyst microbubbles to investigate the air oxidation of *n*-octane, 3-octanol, 3-octanone and *n*-octanoic acid in aqueous  $0.5 \text{ mol dm}^{-3}$  NaCl with and without  $2 \times 10^{-2} \text{ mol dm}^{-3}$  of  $\text{FeCl}_3$ . The major gaseous- and organic phase-soluble products per 100 einstein of 365 nm light, after 12 h of irradiation in ambient air, for each of the organic substrates, with and without  $\text{FeCl}_3$ , are summarized in Fig. 14. The observed products and intermediates, as well as the inhibition of the degradation process by  $\text{FeCl}_3$ , have been interpreted by Schwitzgebel et al. [178] as evidence that not only holes, but also electrons and oxygen, participate in the oxidative degradation process for hydrocarbon, alcohol,

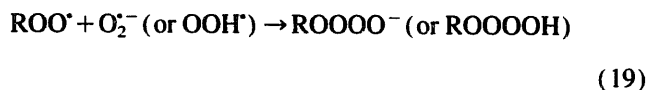
ketone and carboxylic acid organic substrates. In addition, the results suggest that the photogenerated holes, or  $\text{OH}^\bullet$  radicals, although necessary, are by themselves inadequate oxidizers. In particular, these workers propose that the  $\text{TiO}_2$  electron reduces  $\text{O}_2$  to superoxide ( $\text{p}K_a = 4.8$ ), i.e.



the hole reacts with an aliphatic compound through a hydrogen abstraction process, followed by reaction with dissolved oxygen to form an organoperoxide radical, i.e.



and the organoperoxide radical reacts with the superoxide radical to form a tetraoxide, i.e.



which decomposes to products. In the absence of oxygen, but in the presence of  $\text{FeCl}_3$ , the yield of  $\text{CO}_2$  and all the other oxidation products of *n*-octane, 3-octanol, 3-octanone and *n*-octanoic acid is reduced by at least one order of magnitude. This finding is taken as proof that holes, or  $\text{OH}^\bullet$  radicals, are by themselves much less able to oxidize the reactants than a combination of the holes, or  $\text{OH}^\bullet$  radicals, and dissolved oxygen. It is also suggested [178] that the reduced level of  $\text{CO}_2$  generated in ambient air with  $\text{FeCl}_3$  is due to the capture of electrons by ferric chloride and the oxidation of superoxide to oxygen, leading to a reduction in the overall steady state concentration of superoxide.

The above ‘‘Russell-like’’ mechanism [179] is simple and, if correct, is likely to find general application in many of the photocatalytic systems developed for the photodegradation of organic thin films and gaseous organic substrates.

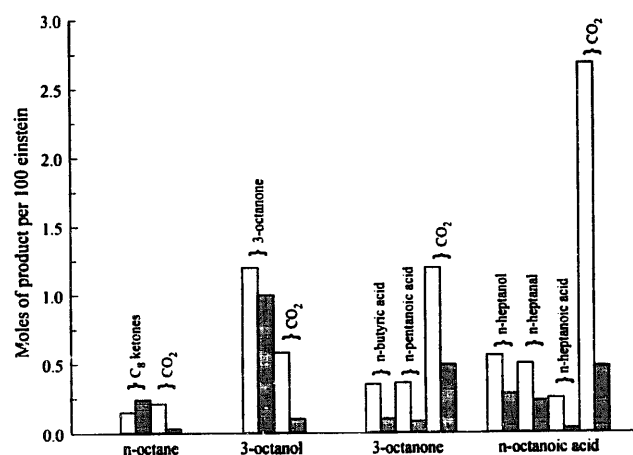


Fig. 14. Histogram representation of the measured [178] yields of the major gaseous- and organic phase-soluble oxidation products after 12 h irradiation with 365 nm light of a dispersion of hydrophilic  $\text{TiO}_2$ -coated microbubbles in  $0.5 \text{ mol dm}^{-3}$  NaCl aqueous solution covered with a thin layer of organic substrate (*n*-octane, 3-octanol, 3-octanone and *n*-octanoic acid were used in this work) (see Fig. 13). The irradiations were performed in the presence (shaded columns) or absence (open columns) of  $0.02 \text{ mol dm}^{-3}$   $\text{FeCl}_3$  in the aqueous solution. In this work, the photosystems were in ambient air.

An important part of this work focuses on the effect of the addition of  $\text{FeCl}_3$  at a high concentration ( $2 \times 10^{-2} \text{ mol dm}^{-3}$  and 80 times that of dissolved oxygen) on the product distribution in the absence and presence of oxygen. The assumption made is that  $\text{FeCl}_3$  will dissolve in water to give  $\text{Fe}^{3+}$  ions, which are excellent electron scavengers. However,  $\text{FeCl}_3$  undergoes extensive hydrolysis and forms yellow–orange–coloured complexes in aqueous solution; indeed, for all the  $\text{Fe(III)}$  to be present as  $\text{Fe}^{3+}$  ions, the pH must be approximately zero. Thus the addition of  $\text{FeCl}_3$  to an aqueous  $0.5 \text{ mol dm}^{-3}$   $\text{NaCl}$  solution will produce a solution with many different, highly UV-absorbing  $\text{Fe(III)}$  species, including multinuclear species; we found, typically, that such a solution had an absorbance maximum of approximately 3.0 in a 1 mm cell at 333 nm and that, after 2 days, the solution appeared cloudy as precipitation of some of the more chlorinated/hydroxylated species took place. The hydrolysis process occurs at different rates for the different species involved, and thus the exact ionic composition of the  $\text{FeCl}_3$  solution will change with time. The kinetics of electron transfer from the semiconductor to these different species may not be as rapid as that to  $\text{Fe}^{3+}$  ions. The UV-screening action of these different  $\text{Fe(III)}$  species, and their deposition/adsorption onto the surface of the  $\text{TiO}_2$  photocatalyst, may play a part in reducing the amount of  $\text{CO}_2$  generated. In addition, with the hydrolysis of  $\text{FeCl}_3$ , there will be an accompanying dramatic drop in pH (we found that the final pH dropped below  $\text{pH} < 2$  from an initial pH of 5.2 before  $\text{FeCl}_3$  was added). It is not clear what the effect of such a change in pH would be on the product distributions illustrated in Fig. 14 for the photocatalytic destruction of *n*-octane, 3-octanol, 3-octanone and *n*-octanoic acid in aqueous  $0.5 \text{ mol dm}^{-3}$   $\text{NaCl}$  in the absence of  $\text{FeCl}_3$  sensitized by the  $\text{TiO}_2$  microbeads.

In the work of Butler and Davis [180] on the photodegradation of toluene in the absence and presence of different metal ions at different pH values, it was reported that, at pH 3, high concentrations ( $10^{-2} \text{ mol dm}^{-3}$ ) of  $\text{Fe(III)}$  inhibited the rate of toluene photodegradation sensitized by  $\text{TiO}_2$ . This inhibition was interpreted as being due to UV screening of the photocatalyst by the highly coloured  $\text{Fe(III)}$  species, such as  $\text{Fe(OH)}^{2+}$  and  $\text{Fe(OH)}_2^+$ . This latter effect has been proposed by others [181], but was rejected by Schwitzgebel et al. [178] on the grounds that the photocatalyst microbubbles are buoyant and, as a result, the absorption of light by dissolved  $\text{Fe(III)}$  could not account for the suppression of the yields. This rejection may not be reasonable given that the molar absorptivities of hydrolysed  $\text{Fe(III)}$  species in the 300–400 nm region are very large, coupled with the concern that some of these species may deposit or adsorb on the surface of the photocatalyst. Intriguingly, Butler and Davis [180], in the photodegradation of toluene sensitized by  $\text{TiO}_2$  dispersed in aqueous solution at pH 3, found that although a  $10^{-2} \text{ mol dm}^{-3}$  solution of  $\text{Fe(III)}$  inhibited the rate, a much less UV-absorbing  $10^{-5} \text{ mol dm}^{-3}$  solution of  $\text{Fe(III)}$  enhanced the rate, relative to that found for no  $\text{Fe(III)}$  added.

It should also be noted that Schwitzgebel et al. [178] found that the addition of  $\text{FeCl}_3$  did not affect the rate of  $\text{CO}_2$  production when *n*-octanal was used as the organic substrate; they suggest that this is because, unlike the other substrates tested, the oxidation reaction does not involve the photogenerated electron or its product, the hydroperoxyl radical; instead, they propose that *n*-octanal is oxidized through a hole-initiated, or  $\text{OH}^\bullet$  radical-initiated, autocatalytic air oxidation process. The suggestion made here that, when *n*-octane, 3-octanol, 3-octanone or *n*-octanoic acid in aqueous  $0.5 \text{ mol dm}^{-3}$   $\text{NaCl}$  are used as the organic substrates in the presence of  $2 \times 10^{-2} \text{ mol dm}^{-3}$  of  $\text{FeCl}_3$ , the yields of  $\text{CO}_2$  may be suppressed as a result of UV screening or adsorption of  $\text{Fe(III)}$  species on the surface of  $\text{TiO}_2$  does not agree with the findings of Schwitzgebel et al. [178] for *n*-octanal. In addition, if, alternatively, the suppression of  $\text{CO}_2$  is due to the substantial drop in pH associated with the addition of  $\text{FeCl}_3$ , it is surprising that the yield of  $\text{CO}_2$  generated by the oxidation of *n*-octanal is not depressed by the addition of  $\text{FeCl}_3$ . Thus, as is often the case, the results of a few ‘simple’, apparently clarifying, experiments produce more questions than answers. The ‘Russell-like’ mechanism [179] proposed by Schwitzgebel et al. [178] may well be valid, but some of the simple experiments used to provide supporting evidence for the mechanism appear, on close inspection, to be of debatable value, and further work is needed to resolve this issue.

## 11. Semiconductor particles as sensitizers for the photodestruction of cancer cells, bacteria and viruses [19,25–28]

In photodynamic therapy (PDT) [182,183], dye sensitizers, such as haematoporphyrin, are used, which ideally localize selectively in the cancerous tumour. Typically, the triplet state of the dye sensitizer can react directly with the biological material associated with the cancerous tumour, or transfer its electronic excitation energy to oxygen to form singlet oxygen, which can then react with and damage such biological material. A cancer cell will die if its membrane is damaged or the oxidation–reduction agents needed in the cell for the production of adenosine triphosphate (ATP), such as reduced glutathione, reduced nicotinamide adenine dinucleotide phosphate, coenzyme A (CoA) and flavine adenine dinucleotide, are depleted or exhausted. We have seen that semiconductors, such as  $\text{TiO}_2$ , can sensitize the photogeneration of  $\text{OH}^\bullet$  and  $\text{O}_2^{\bullet-}$  (or  $\text{OOH}^\bullet$ ) radicals, as well as hydrogen peroxide, and such species should be able to cause oxidative damage similar to that found in traditional PDT, leading to death of cancerous cells. Only a few examples of this novel approach to PDT have been reported in the literature, and most of these are collected in Table 11 [25,26,184–186], together with relevant details and comments.

Quite early on in this work, it was found [25] that P25  $\text{TiO}_2$  particles were incorporated into the cancerous cells by

Table 11  
TiO<sub>2</sub> particles as sensitizers for the photodestruction of cancer cells

Semiconductor	Cancer cells	Comments	Reference
TiO <sub>2</sub>	HeLa cells (50 µm diameter)	An in vitro study in which the TiO <sub>2</sub> particles are not toxic, but the cancer cells are completely killed with 10 min of irradiation (see Fig. 15). Electron microscopy shows that TiO <sub>2</sub> particles exist at the cell membrane and in the cytoplasm of the cells through phagocytosis, but not in the cell nuclei	[25]
TiO <sub>2</sub>	HeLa cells	An in vitro study shows that L-tryptophan and catalase, both scavengers of H <sub>2</sub> O <sub>2</sub> , inhibit the photokilling action of the TiO <sub>2</sub> particles. The TiO <sub>2</sub> particles show no toxicity when administered (orally or through injection) to nude mice. In an in vivo study, some mice were injected with HeLa cells and the cancerous tumour was allowed to grow for 2 weeks before being injected with TiO <sub>2</sub> particles. Three days after the latter injection, the skin covering the tumour was opened surgically, the tumour was irradiated with UV (300–400 nm) light and the skin was then closed. The results of this work indicate that the presence of TiO <sub>2</sub> particles, coupled with UV irradiation, suppresses significantly the growth of the cancerous tumour	[26]
TiO <sub>2</sub>	HeLa cells	An in vitro study in which superoxide dismutase enhances the photokilling action of the TiO <sub>2</sub> particles towards HeLa cells. The addition of EDTA-Fe (Fenton's reagent) also enhances the photokilling action of TiO <sub>2</sub>	[184]
TiO <sub>2</sub>	T24 cells (human bladder carcinoma line)	An in vitro study which shows that the cell membrane permeability towards Ca <sup>2+</sup> ions is increased, possibly by peroxidation of the lipid membrane, prior to cell death, but is not the main cause of cell death promoted by the TiO <sub>2</sub> photocatalyst particles. As with HeLa cells, electron microscopy shows that the TiO <sub>2</sub> particles exist at the cell membrane and in the cytoplasm of the cell through phagocytosis, but not in the cell nuclei	[185]
TiO <sub>2</sub> microelectrode (10 µm diameter)	T24 cells	An in vitro study which shows that selective photokilling of a single cancer cell by a TiO <sub>2</sub> microelectrode is possible if placed within 10 µm distance from the cell and illuminated with UV light	[186]

phagocytosis over a 24 h incubation period—this represents a very useful feature. The TiO<sub>2</sub> particles showed no toxicity to cancer cells, such as HeLa cells, but a significant ability to sensitize the photokilling of such cells, as illustrated by some of the results of Cai et al. [25], which are shown in Fig. 15. Other work [186] showed that the photokilling action of the TiO<sub>2</sub> particles could be enhanced through the addition of superoxide dismutase, which converts superoxide radicals into hydrogen peroxide. Overall, this approach to PDT is limited, since the penetration of UV light through skin is very small (less than 1 mm), and therefore fibreoptics or surgery

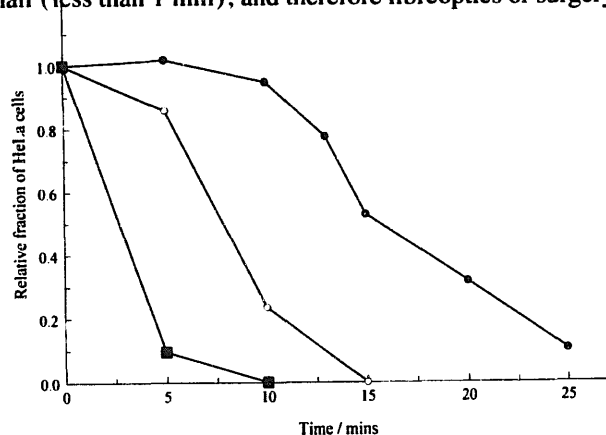


Fig. 15. Observed change in the relative surviving fraction of HeLa cells as a function of irradiation time using the following levels of TiO<sub>2</sub>: none (■); 12 µg cm<sup>-3</sup> (○); 120 µg cm<sup>-3</sup> (●). Irradiations were performed using a 500 W high pressure Hg lamp coupled with a UV filter to ensure that 300–400 nm light only was used (diagram after Ref. [25]).

[26] would be needed to use TiO<sub>2</sub> particles to destroy most cancerous tumours.

Bacteria and viruses can be destroyed by a number of different techniques, including heat, UV radiation, antibiotics (for bacteria: selective but slow) and chemical oxidation. One of the most popular current chemical oxidants for water disinfection is chlorine. However, as mentioned earlier, chlorination, although effective in inactivating bacteria and most viruses, generates unwanted disinfection byproducts, such as trihalomethane and other carcinogens. As a result, there are already moves within the water purification industry to limit the use of free chlorine as a disinfectant for high quality groundwater or water treated to reduce its TOC content. Other water disinfection technologies are becoming of increasing importance, such as chlorine dioxide, ozone, UV irradiation and advanced filtration processes.

One of the earliest examples of the application of semiconductor photocatalysis as a method of disinfection was the work of Matsunaga et al. [27]. These workers were able to show that TiO<sub>2</sub> particles were effective in sensitizing the photokilling of bacteria, such as *Lactobacillus acidophilus*, *Saccharomyces cerevisiae* and *Escherichia coli*, and that the photokilling action was associated with the reduction in the level of intracellular CoA through photo-oxidation. The results reported by these workers for the photokilling of *Saccharomyces cerevisiae*, sensitized by TiO<sub>2</sub> particles, are illustrated in Fig. 16. Surprisingly, the photodisinfection action of TiO<sub>2</sub> particles has not been extensively researched, and

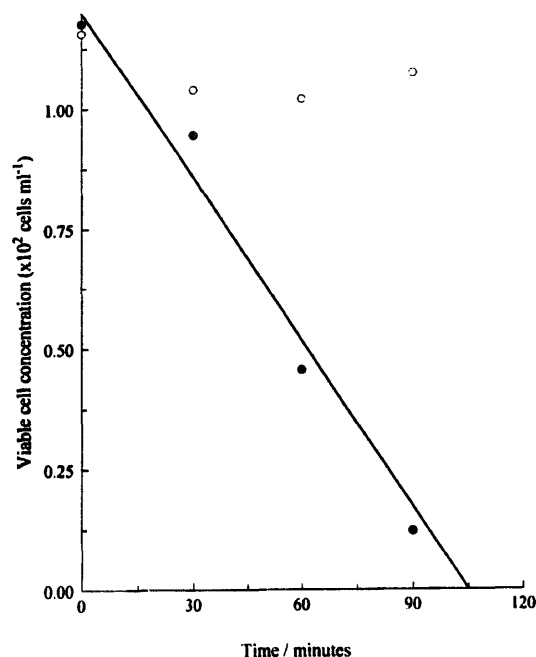


Fig. 16. Observed change in the viable cell concentration of the bacterium *Saccharomyces cerevisiae* with irradiation time when cell suspensions ( $10^3$  cells  $\text{cm}^{-3}$ ) were irradiated with an Xe arc lamp ( $0.012 \text{ einstein m}^{-2} \text{ s}^{-1}$ ) with (●) and without (○) platinized  $\text{TiO}_2$  ( $1 \text{ mg cm}^{-3}$ ) (data after Ref. [27]).

Table 12 [27,28,187–193] lists many of the major reports on the photodestruction of bacteria and viruses, with relevant details and comments.

A brief inspection of the literature on the photodisinfection action of  $\text{TiO}_2$  particles shows that, in the majority of cases, the bacterium under study was *Escherichia coli* (as reflected by the examples in Table 12) which can generally be considered as an easy target bacterium to destroy. Much more challenging, and yet to be addressed, is the application of  $\text{TiO}_2$  photodisinfection to the destruction of more resistant bacteria, e.g. pathogenic protozoans such as *Giardia lamblia* and *Cryptosporidium*, or persistent algae. The full breadth of the photodisinfection ability of  $\text{TiO}_2$  particles has yet to be established and if it is significant it may well find application as a disinfection technique at remote sites. If sunlight is to be used, given that it comprises less than 5% UV photons,  $\text{TiO}_2$  photodisinfection will only find application where long contact times can be tolerated and where there is plentiful sunlight, e.g. in rural areas with arid climates. The lack of residual disinfection capacity and the generally slow kinetics of disinfection represent two major disadvantages of photodisinfection sensitized by  $\text{TiO}_2$  compared with conventional chemical disinfection techniques.

Although most of the work carried out in this area has focused on the use of  $\text{TiO}_2$  particles as sensitizers for the photodestruction of bacteria and viruses in water, there is growing interest [194] in their use in the form of thin films as a method of keeping surfaces free of such species and fungi. Such self-disinfecting surfaces would be of particular value where sterile surfaces are essential, such as in operating

theatres in hospitals. Such a role opens up another possible market for the  $\text{TiO}_2$ -coated ceramic tiles currently being manufactured and sold by the Japanese company TOTO (see above).

## 12. Semiconductor colloids and Q particles [14,29,30]

Alongside the extensive research into semiconductor macroparticles, i.e. particles with diameters typically greater than 100 nm, there has also been much work performed on semiconductor colloids; both research areas are dominated by investigations into the photocatalytic properties of semiconductors. As noted earlier, dispersions of semiconductor powders often scatter and reflect, as well as absorb, excitation light and thus appear opaque. As a consequence, photocatalysis studies involving semiconductor macroparticles have been limited, to a large extent, to obtaining mechanistic information from the results of steady state irradiation. The scattering and reflection exhibited by semiconductor colloid particles is usually much less than that by macroparticles and, as a result, the colloids often appear clear. The fundamental photochemical and chemical processes which occur at the semiconductor colloid–electrolyte interface can be readily investigated in such clear, light-absorbing dispersions, using not only steady state techniques, but also time-resolved techniques, such as pulse radiolysis, flash photolysis and, if the colloid material luminesces, single-photon counting. The fundamental photochemical studies of semiconductor colloids have often provided the necessary insight into the photochemical processes which occur on semiconductor macroparticles. In general, in colloidal semiconductors, the band bending is small and charge separation occurs via diffusion. The dimensions of colloidal particles are such that the time taken for photogenerated electrons or holes to diffuse to the surface is a few picoseconds, and is usually considered to be more rapid than recombination in the bulk of the semiconductor. Thus it is possible to obtain higher quantum yields with such particles than with macroparticles of the same semiconductor.

Most of the semiconductor colloids which have been produced for photocatalytic studies are metal oxides, such as  $\text{TiO}_2$ ,  $\text{WO}_3$ ,  $\text{ZnO}$ ,  $\text{CdO}$  and  $\text{In}_2\text{O}_3$ , and metal chalcogenides, such as  $\text{CdS}$ ,  $\text{CdSe}$ ,  $\text{MoS}_2$  and  $\text{WS}_2$ , and usually involve the controlled precipitation of the colloid particles by hydrolysis, or anion or cation release respectively. Thus  $\text{TiO}_2$  colloids are often prepared by the forced hydrolysis of titanium(IV) tetraisopropoxide [195] or titanium(IV) tetrachloride [196]; such colloidal particles of  $\text{TiO}_2$  are typically 5–20 nm in diameter, need to be sterically stabilized with poly(vinyl alcohol) (PVA) above pH 3, and appear to be mainly amorphous, with a small percentage of anatase.  $\text{CdS}$  colloids can be simply prepared through the addition of  $\text{H}_2\text{S}$  to a cadmium salt; often they are electrostatically stabilized using sodium hexametaphosphate [197]. It should be noted that very little is known about the interaction between semiconductor par-



Table 12  
TiO<sub>2</sub> particles as sensitizers for the photodestruction of bacteria and viruses

Semiconductor	Biological material	Comments	Reference
<b>Bacteria</b>			
Pt/TiO <sub>2</sub>	<i>Lactobacillus acidophilus</i> (gram-positive bacterium), <i>Saccharomyces cerevisiae</i> (yeast), <i>Escherichia coli</i> (gram-negative bacterium), <i>Chlorella vulgaris</i> (green algae)	The Pt/TiO <sub>2</sub> particles were able to sensitize effectively the photokilling of the bacteria <i>Lactobacillus acidophilus</i> , <i>Saccharomyces cerevisiae</i> and <i>Escherichia coli</i> . In a more detailed study of the photocatalysed destruction of <i>Saccharomyces cerevisiae</i> , it was found that intracellular CoA is photo-oxidized by the TiO <sub>2</sub> particles, and this inhibits cell respiration and leads to cell death. Photodisinfection sensitized by TiO <sub>2</sub> had less effect on the green alga <i>Chlorella vulgaris</i> , which has a thick cell wall of polysaccharides and pectin	[27]
TiO <sub>2</sub> in a flow system	<i>Escherichia coli</i>	The TiO <sub>2</sub> particles were immobilized on acetyl cellulose to create a photodisinfecting film which was then incorporated into a flow system. The resulting photodisinfection flow system was suitable for the handling of samples containing a low concentration (less than 10 <sup>3</sup> cells cm <sup>-3</sup> ) of bacteria, but was less effective at higher bacterial levels. The flow photodisinfection system was operated for 1 week, at a bacterial input level of 10 <sup>2</sup> cells cm <sup>-3</sup> , showed no indication of a deterioration in performance and reduced the bacterial levels to less than 1% of the input level	[28]
TiO <sub>2</sub>	<i>Streptococcus mutans</i> , <i>Streptococcus rattus</i> , <i>Streptococcus cricetus</i> , <i>Streptococcus sobrinus</i> AHT	The TiO <sub>2</sub> particles were able to sensitize effectively the photokilling of the bacteria <i>Streptococcus mutans</i> , <i>Streptococcus rattus</i> , <i>Streptococcus cricetus</i> and <i>Streptococcus sobrinus</i> AHT within 3 min of irradiation with UV photons. In a detailed study of the photodestruction of <i>Streptococcus sobrinus</i> AHT, sensitized by TiO <sub>2</sub> , rapid leakage of K <sup>+</sup> ions was observed, together with a slow protein and RNA release and pH drop (pH 6.8 to pH 4.5), which occurred in parallel with the decrease in cell viability. Although K <sup>+</sup> leakage occurred in a short time and in parallel with the loss of cell viability, other results indicate that it is not the single cause of bacterial death	[187]
TiO <sub>2</sub> in a flow system	<i>Escherichia coli</i>	A sleeve of fibre glass mesh coated with TiO <sub>2</sub> covered the UV lamps, and water for photodisinfection was flowed past. In addition to studying the photodestruction of <i>Escherichia coli</i> , the flow system was used to treat coloured, algae-containing pond water. In this work, it was found that, although the total coliform level was reduced, the heterotrophic plate count was not, unless H <sub>2</sub> O <sub>2</sub> was added to enhance the photokilling action of TiO <sub>2</sub>	[188]
TiO <sub>2</sub>	<i>Escherichia coli</i>	A study of the kinetics of photokilling of the bacterium <i>Escherichia coli</i> , sensitized by TiO <sub>2</sub> , as a function of [O <sub>2</sub> ] (the process does not proceed without oxygen), [TiO <sub>2</sub> ] (half order) and incident light intensity (first order)	[189]
TiO <sub>2</sub>	<i>Escherichia coli</i>	Sunlight was used as the light source in the photokilling of the bacterium <i>Escherichia coli</i> sensitized by TiO <sub>2</sub>	[190]
TiO <sub>2</sub>	<i>Escherichia coli</i>	Diffuse light-emitting optical fibres were found to be more effective as a light source than conventional light fibres in the photokilling of the bacterium <i>Escherichia coli</i> sensitized by TiO <sub>2</sub>	[191]
<b>Viruses</b>			
TiO <sub>2</sub>	Phage MS2 (a single-stranded RNA bacteriophage)	A 2 × 10 <sup>-6</sup> mol dm <sup>-3</sup> FeSO <sub>4</sub> solution was used to promote (1.7 times) the photodestruction ability of the TiO <sub>2</sub> particles. From the results of this work, it appears that viral components, such as protein capsids and nucleic acids, are susceptible to direct attack by photogenerated OH <sup>•</sup> radicals. The Fe(II) solution is thought to enhance the steady state concentration of OH <sup>•</sup> radicals via a Fenton-type process	[192]
TiO <sub>2</sub>	Poliovirus 1 (also coliform bacteria for comparison)	The photodestruction of poliovirus 1, sensitized by TiO <sub>2</sub> , was complete in 30 min of irradiation, whereas it took 150 min to destroy the coliform bacteria. This work was carried out in secondary wastewater effluent. When either sunlight or blacklight bulbs were used as the light source, the photocatalytic disinfection rates were very slow. It should be recognized that wastewater is a complex matrix and there may be significant differences between disinfection rates in wastewater and deionized water; the latter is the medium most workers in this area use at the present time. In addition, although previous work in this area used low bacterial levels (typically less than 10 <sup>3</sup> CFU cm <sup>-3</sup> ), in wastewater effluent bacteria and virus levels can be as high as 10 <sup>3</sup> –10 <sup>6</sup> CFU cm <sup>-3</sup> and need to be reduced by over 10000 times to meet effluent discharge requirements	[193]

ticles and the added stabilizing agents, and that this interaction can affect the final shape, size and photochemical behaviour of the semiconductor colloidal particles [29]. The physical and photochemical characteristics of semiconductor colloids appear to be highly dependent on the exact experimental conditions used in their preparation. Most semiconductor colloid dispersions for photocatalysis work have been prepared in aqueous solution; however, it is not unusual to find reports on semiconductor colloidal photochemistry in non-aqueous media; thus Kormann et al. [198] have reported the preparation and characterization of  $\text{TiO}_2$  colloids in water, isopropanol, ethanol and acetonitrile. There is also a substantial body of work [14] focused on the photochemical characteristics of ultrasmall semiconductor colloidal material, usually CdS, in microcages, such as micelles, vesicles, bilayer membranes, zeolites, polymer films, clays and silicate glasses; such microcage environments allow fundamental photochemical studies to be performed under well-defined and often restricted conditions.

As indicated in Fig. 1, as the size of a semiconductor particle is decreased, it is expected that there will be a gradual transition from semiconductor properties to molecular properties. This quantization effect should become apparent when the size of the semiconductor particle becomes comparable with the de Broglie wavelength of the charge carriers in the semiconductor and, although this size will depend on the particular semiconductor, it typically lies in the range 5–25 nm. Semiconductor particles which exhibit quantum size effects are often called “Q particles”, although other names include quantum boxes or spheres, quantum dots and nanocrystals (a very popular term at the moment) [199]. In Q-sized particles, the wavefunction of the charge carrier spreads over the whole semiconductor particle; thus the charge carriers do not need to diffuse to accomplish reactions with species present at the surface and, as a consequence, it is possible to obtain quantum yields approaching unity.

One of the predicted effects of quantization is an increase in  $E_{\text{bg}}$ , and therefore a blue shift in the absorption edge, with decreasing particle size. Fig. 17 illustrates the predicted variation in the absorption threshold wavelength as a function of particle size for  $\text{TiO}_2$  (rutile), CdS and PbS. The change in the absorption spectrum of a semiconductor colloid with decreasing particle size can be very striking; thus CdS colloidal particles of approximately 6 nm exhibit an absorption spectrum typical of macrocrystalline CdS, with an absorption edge at 515 nm, and produce bright yellow-coloured solutions. With decreasing particle size, the absorption spectrum is blue shifted and becomes more structured (see below). With CdS particles of less than 2.2 nm in diameter, the dispersions appear colourless and a white powder of colloidal CdS particles can be extracted [24,200]. The size quantization effects, such as the blue shift in the absorption spectrum, are more marked the smaller the bandgap of the semiconductor material. From the data in Fig. 17, size quantization effects will become important in rutile  $\text{TiO}_2$  when the particle size is less than 5 nm. Because large single crystals of anatase

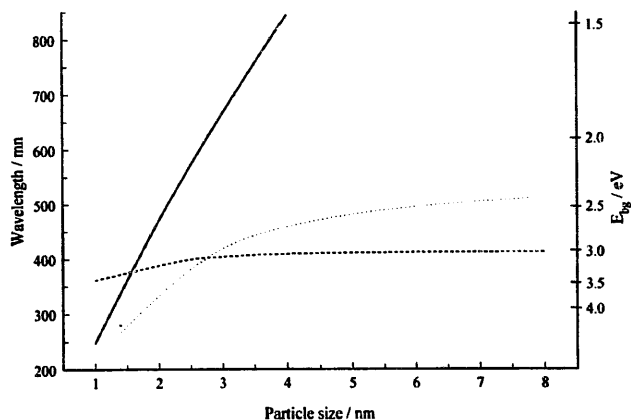


Fig. 17. Predicted variations in the absorption threshold wavelength (nm) or bandgap (eV) for colloidal particles of PbS [24] (full line), CdS [24] (dotted line) and  $\text{TiO}_2$  (rutile) [199] (broken line) as a function of particle size.

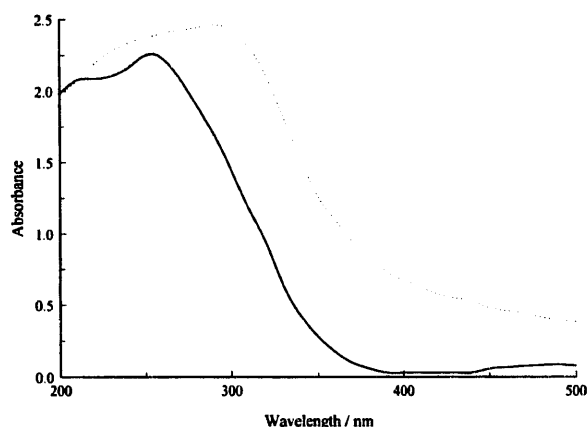


Fig. 18. Measured UV-visible absorption spectra of two thin films containing nanocrystalline anatase  $\text{TiO}_2$  particles of 3 nm (full line) and 50 nm (dotted line) (after Ref. [175]).

$\text{TiO}_2$  are very difficult to produce, less is known about their electronic properties, and the reliable data needed to predict the variation in the absorption threshold wavelength as a function of particle size for this material are not yet available [199]. However, the wavelength shift due to size quantization for anatase  $\text{TiO}_2$  is likely to be similar to that for rutile  $\text{TiO}_2$ . Fig. 18 illustrates the observed absorption spectra for two thin films (A and B) containing anatase  $\text{TiO}_2$  particles of 3 nm and 50 nm respectively [175].

Another of the predicted effects of size quantization is the increasing appearance of structure in the absorption spectrum associated with the increasing possibility of discrete transitions (see Fig. 1) with decreasing particle size. In order to achieve the predicted series of discrete peaks in the absorption spectrum of Q-sized semiconductor particles, the particles would have to be perfect, monodispersed microcrystals, and this is impossible to achieve. In practice, although increasing evidence of structure in the absorption spectrum is observed with decreasing particle size for most semiconductor materials, it is attenuated by particle size distribution and surface state effects.

Particle quantization will also lead to an increase in the electrostatic attraction between electrons and holes; a coupled electron–hole pair is called an exciton, and evidence of exciton formation can often be seen in the absorption spectrum of the colloid as a sharp peak just below the fundamental absorption edge of the semiconductor.

As a consequence of the blue shift in the absorption edge with decreasing particle size, the redox potentials of the photogenerated electrons and holes in quantized semiconductor particles will be enhanced, i.e. Q particles should be more photoactive than macrocrystalline semiconductor particles. Some work has shown that Q particles are more photoefficient than bulk semiconductor materials. For example, Hoffmann et al. [201] showed that the rates of photoinitiated polymerization of several vinyl monomers by Q-sized particles of CdS, ZnO and TiO<sub>2</sub> increased with decreasing particle size. However, other work has shown that Q particles are less photoefficient than bulk semiconductor materials. For example, Hoffmann et al. [202] showed that the rates of photoinitiated polymerization of methyl methacrylate by Q-sized ZnO colloids decreased with decreasing particle size. It is suggested that the positive effects of quantization of increased overpotential can be offset by unfavourable surface speciation and surface defects, which are in turn associated with the preparation method.

An important aspect of semiconductor photochemistry, in macrocrystalline and microcrystalline material, is the retardation of the electron–hole recombination process through charge carrier trapping. As indicated earlier, in the preparation of semiconductor colloids, ideal crystal lattices are not produced—in many cases, the colloid material can be so disorganized as to appear amorphous to X-ray diffraction. Thus most semiconductor colloid material will have surface and bulk irregularities, i.e. defects, and these can act as electron–hole recombination centres or traps. The presence of such traps can alter significantly the photochemistry associated with the semiconductor colloid. For example, CdS colloids, prepared through the addition of H<sub>2</sub>S to a cadmium salt, usually exhibit a very weak, red luminescence at 600 nm (approximately 0.4 eV below the 515 nm absorption threshold of bulk CdS). This luminescence is due to the radiative recombination of trapped charge carriers, which competes with the dominant process of radiationless recombination. The surface of the CdS colloid particles can be readily modified—the particles are said to be activated—by the addition of 300% Cd<sup>2+</sup> ions and an increase in pH to pH 11 to produce particles which luminesce very brightly (quantum yield, 0.5) around the absorption edge of the CdS material (i.e. 515 nm). It is suggested that the simple surface modification procedure creates a layer of CdOH on the surface of the CdS particles in which Cd<sup>2+</sup> ions bind coordinatively to the surface sulphide anions to form structures which block the surface imperfections responsible for the trapping of charge carriers. As a result of this surface treatment, the stability of the CdS particles towards photoanodic corrosion and OH<sup>•</sup> radical attack is increased by several orders of magnitude [24,197].

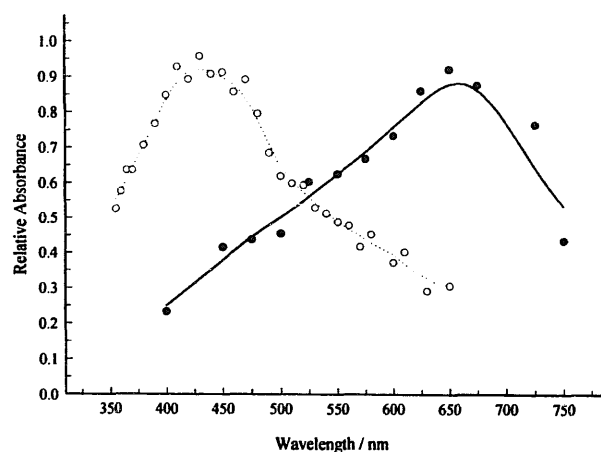


Fig. 19. The transient absorption spectra of photogenerated trapped holes (○) and electrons (●) produced on flash photolysis (347 nm laser light) of a colloid of TiO<sub>2</sub> in the presence of an electron scavenger (PVA or thiocyanate) and a hole scavenger (Pt or methyl viologen) respectively (data from Ref. [203]).

Electron–hole recombination on most semiconductor materials is usually very fast, e.g. typically less than 10 ns for TiO<sub>2</sub> (see Table 6). However, if a hole scavenger is added to a semiconductor colloid, it is possible to remove some of the photogenerated holes and effectively trap the photogenerated electrons for a sufficient time to allow their transient absorption spectrum to be recorded. Similarly, if an electron scavenger is added, the transient absorption spectrum of trapped photogenerated holes can be determined. In a series of simple flash photolysis experiments conducted on TiO<sub>2</sub> colloids, Bahnemann et al. [203] were able to record for a TiO<sub>2</sub> colloid the absorption spectra of trapped photogenerated electrons (using PVA or thiocyanate as the hole scavenging agent) and trapped photogenerated holes (using Pt or methyl viologen as the electron scavenging agent), which live in the microsecond time domain. The absorption spectra of trapped holes and electrons in colloidal TiO<sub>2</sub>, reported by these workers [203], are illustrated in Fig. 19.

The use of electron and hole scavengers in photochemical studies involving semiconductor colloids is widespread and often assumed rather than clearly stated. The most commonly used electron scavenger is dissolved oxygen, and the most commonly used hole scavenger is the PVA added to the colloid dispersion for steric stabilization or an added alcohol, such as isopropanol. Such systems, coupled with time-resolved spectroscopic techniques, such as flash photolysis, allow the reactions of photogenerated holes and electrons at the semiconductor surface to be studied independent of one another. Table 13 [204–212] provides a few examples of reported studies in which TiO<sub>2</sub> colloid particles were used as sensitizer.

It is possible to create coupled colloidal structures, in which illumination of one of the semiconductors produces a response in the other semiconductor or at the interface between the two. One colloidal coupled structure which has received more attention than most is that between CdS and TiO<sub>2</sub> colloidal particles. As illustrated in Fig. 20, with such

Table 13

Examples of time-resolved studies of photo-oxidation and photoreduction reactions sensitized by colloidal TiO<sub>2</sub>

Substrate	Scavenger	$E^0(\text{substrate})$ (V) <sup>a</sup>	Reference
<b>Photo-oxidation reactions</b>			
Methyl orange	Dissolved O <sub>2</sub>	–	[204]
Iodide	Dissolved O <sub>2</sub>	1.0	[205]
Thiocyanate	Dissolved O <sub>2</sub>	1.3	[206]
<b>Photoreduction reactions</b>			
Methyl viologen	PVA	–0.44	[207,208]
Methyl orange	PVA	–0.01	[209]
Thionine	Isopropanol <sup>b</sup>	0.064	[210]
Methylene blue	Isopropanol <sup>b</sup>	0.01	[210]
Phenosafrin	Isopropanol <sup>b</sup>	0.25	[211]
Tetraisoethane	Isopropanol	–	[212]

<sup>a</sup> $E^0(\text{substrate})$  is  $E^0(\text{X}_2^-/2\text{X})$  for  $\text{X} = \text{I}$  and  $\text{SCN}^-$  and  $E^0(\text{X}/\text{X}^-)$  for all other substrates vs. normal hydrogen electrode (NHE).<sup>b</sup>TiO<sub>2</sub> colloid in acetonitrile, rather than water.

a structure, it should be possible to irradiate the CdS colloid with light of lower energy than that needed to excite electronically the TiO<sub>2</sub> particles, with the result that a photogenerated electron can be injected from the CdS particle to the TiO<sub>2</sub> particle while a hole remains in the CdS particle.

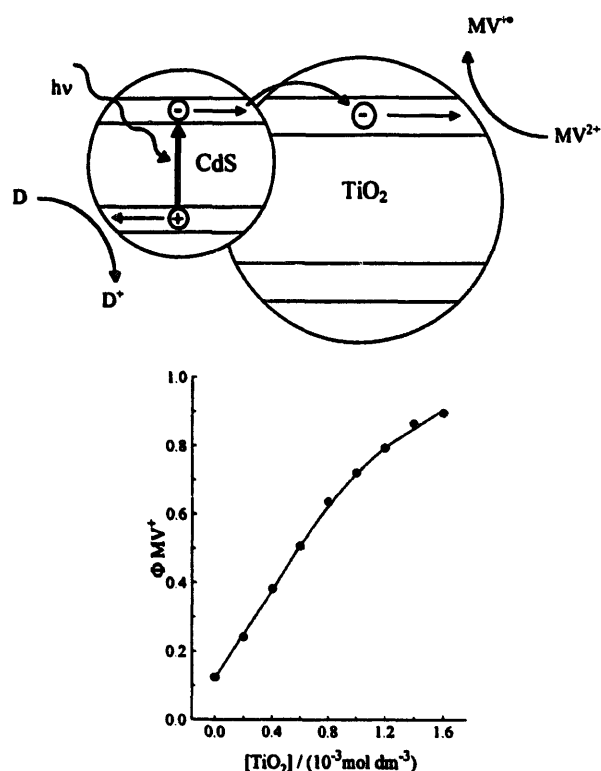


Fig. 20. Schematic illustration of the photoinduced charge injection process which occurs on excitation of the CdS component of a CdS/TiO<sub>2</sub> colloidal combination in the presence of a sacrificial electron donor D and electron scavenger (methyl viologen, MV<sup>2+</sup>). The bottom diagram refers to the measured [213] variation in the quantum yield of reduced methyl viologen production as a function of the amount of TiO<sub>2</sub> colloid present; the latter determines the number of CdS/TiO<sub>2</sub> combination colloids present. In this work, 436 nm monochromatic light was used and the initial solution contained  $2 \times 10^{-4}$  mol dm<sup>-3</sup> activated CdS colloid,  $2 \times 10^{-4}$  mol dm<sup>-3</sup> (NaPO<sub>3</sub>)<sub>6</sub> (electrostatic supporting agent),  $2 \times 10^{-4}$  mol dm<sup>-3</sup> methyl viologen (electron scavenger) and 30 vol.% methanol (sacrificial electron donor).

Colloidal CdS–TiO<sub>2</sub> coupled structures form spontaneously when the individual colloids are mixed in the presence of a large excess of Cd<sup>2+</sup> ions in alkaline solution. As noted earlier, CdS colloids at high pH, and with an excess of Cd<sup>2+</sup> ions, form surface-activated, highly fluorescent CdS colloids. Spanhel et al. [213] found that the addition of a TiO<sub>2</sub> colloid to this surface-activated, highly fluorescent CdS colloid resulted in the quenching of its luminescence, as may be expected if increasing numbers of sandwich CdS–TiO<sub>2</sub> colloids are formed with increasing [TiO<sub>2</sub>]. These workers also found that the quantum yield of photoreduction of methyl viologen sensitized by CdS, using methanol as a hole scavenger, was drastically increased with increasing [TiO<sub>2</sub>], as can be seen from the data illustrated in Fig. 20. However, these workers also noted that, in aerated solution, in which dissolved oxygen acts as an electron scavenger, the CdS colloid was prone to increased photoanodic corrosion with increasing level of TiO<sub>2</sub> present since, in this system, the CdS–TiO<sub>2</sub> structures encourage the accumulation of photogenerated holes on the CdS particles.

### 13. Nanocrystalline photoelectrochemical cells [30–33]

As noted earlier, most photoelectrochemical cells for solar energy conversion need to utilize low bandgap semiconductors, such as *n*-GaAs or *n*-CdSe, rather than large bandgap metal oxide semiconductors, such as TiO<sub>2</sub> or SrTiO<sub>3</sub>. The former semiconductors are prone to photoanodic corrosion and passivation and, in order to minimize electron–hole recombination and maximize photoefficiency, single-crystal semiconductors are required, which are expensive to manufacture. There have been many attempts over the years to develop photoelectrochemical cells in which a dye is adsorbed onto the surface of the semiconductor, usually a large bandgap metal oxide, in order to improve the solar energy conversion efficiency of the cell.

The basic processes associated with such dye-sensitized photoelectrochemical cells are illustrated in Fig. 21. Thus the

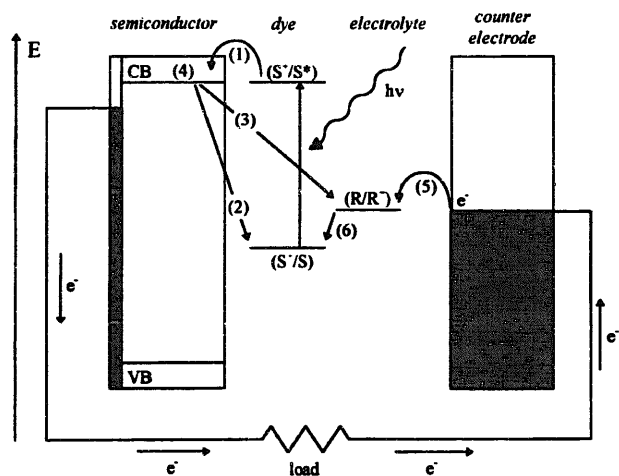


Fig. 21. General features of a dye-sensitized nanocrystalline semiconductor photoelectrochemical cell. Following electronic excitation of the dye sensitizer, i.e.  $S \rightarrow S^*$ , the charge injection (process (1)) can occur very rapidly, although back reaction, via processes (2) and (3), represents an efficiency-lowering step. The percolation of the injected charge to the back contact (process (4)) is usually slow. The movement of the photoinjected electrons through the external circuit is driven by the photopotential developed by the system. At the dark counter electrode, reduction of the oxidized form of the redox relay  $R^+$  occurs (process (5)); at the photoanode, the photo-oxidized dye  $S^+$  is reduced to  $S$  by the reduced form of the redox relay  $R$  (process (6)) (diagram after Ref. [30]).

adsorbed dye is electronically excited and, provided that it has a sufficiently negative redox potential, it can transfer an electron into the conduction band of the semiconductor (process (1) in Fig. 21). Undesirable recombination processes include the reaction of the injected electron with the oxidized form of the dye sensitizer ( $S^+$ ) and the oxidized form of the redox relay ( $R^+$ ), i.e. processes (2) and (3) respectively in Fig. 21. Instead, for the photoelectrochemical cell to work efficiently, the injected electron must move to the back contact (process (4) in Fig. 21). This latter process is efficient in photoelectrochemical cells using single-crystal semiconductors, because of the well-established electric field present over the space charge region; however, in colloidal semiconductor particles, the degree of band bending is small and this process will be much slower as a consequence. At the back contact, the electron is driven through the external circuit, through a load resistance, by the photogenerated potential difference between the semiconductor photoanode and the dark counter electrode. At this electrode, the oxidized form of the redox relay ( $R^+$ ) is rapidly reduced to  $R$  and, at the photoanode, the oxidized form of the dye ( $S^+$ ) is reduced to  $S$  by  $R$ , i.e. processes (5) and (6) respectively in Fig. 21. In order for such a cell to be efficient, process (1) must be more rapid than the lifetime of the electronically excited state of  $S$ , the rates of the recombination processes (2) and (3) must be slower than process (4), the vectorial displacement of the photoinjected electron, and the dye in all its forms, i.e.  $S$ ,  $S^*$  and  $S^+$ , must be very stable.

In most of the early examples of dye-sensitized photoelectrochemical cells, it was found that only the first monolayer of the adsorbed dye was efficient in photoinjecting an electron

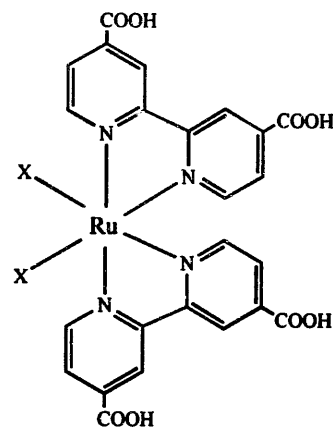


Fig. 22. Structure of *cis*- $X_2$ bis(2,2'-bipyridyl-4,4'-dicarboxylate)-ruthenium(II) dyes (where  $X \equiv CN^-$  or  $SCN^-$ ), which have recently been used with great success to sensitize thin films of nanocrystalline  $TiO_2$  in thin layer, dye-sensitized, nanocrystalline photoelectrochemical sandwich solar cells [31].

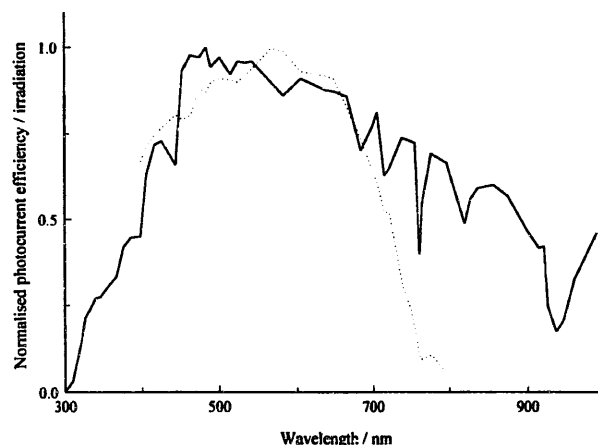


Fig. 23. Measured relative photocurrent efficiency (broken line) of a thin layer, dye-sensitized, nanocrystalline photoelectrochemical sandwich solar cell, using the dye in Fig. 22 ( $X \equiv SCN^-$ ), and relative illumination intensity of sunlight at AM 1.5 (full line) as a function of wavelength [33].

into the semiconductor, and the light-harvesting efficiency at any wavelength  $\lambda$  ( $LHE_{\lambda}$ ) of a single dye monolayer was very small. Attempts to use multilayers of dyes were usually thwarted by problems of self-quenching and inefficient exciton/electron transfer. In addition, there appeared to be few dyes efficient in sensitizing the photoinjection of electrons into semiconductor materials and stable in their oxidized form. In recent years, interest in dye-sensitized photoelectrochemical cells has been reinvigorated with the introduction of nanocrystalline semiconductor materials, most notably nanocrystalline  $TiO_2$ , and the discovery [30–33] of a type of dye (see Fig. 22) which is very stable in all its forms and has a broad visible absorption spectrum (see Fig. 23). The components of the two major types of dye-sensitized nanocrystalline photoelectrochemical cell, namely transparent (I) [32] and reflecting (II) [33] thin layer sandwich solar cells, are listed in Table 14, together with relevant details; the major processes which occur in such cells, as illustrated in Fig. 21, together with current estimates of their timescales, are given in Table 15 [30,33].

Table 14

Components and preparation of dye-sensitized, nanocrystalline, thin layer, sandwich solar cells [32,33]

## (I) Transparent, dye-sensitized, nanocrystalline, thin layer, sandwich solar cells [32]

## (a) Conducting glass support substrate

The glass substrate has a conducting ( $7\text{--}8\ \Omega/\square$ ), fluorine-doped, tin oxide overlayer ( $0.7\ \mu\text{m}$  thick) with a haze, or roughness factor, of 15% that enhances the multiple reflection and scattering occurring in the subsequent nanocrystalline  $\text{TiO}_2$  layer

(b) Nanocrystalline  $\text{TiO}_2$  film layer

The optically transparent film is prepared by the hydrolysis of titanium isotetrapropoxide, followed by autoclaving for 12 h at  $200\ ^\circ\text{C}$ , to produce particles of approximately  $15\ \text{nm}$ . After concentrating the solution by evaporation, Carbowax M-20000 (40 wt.%  $\text{TiO}_2$ ) is added to the viscous  $\text{TiO}_2$  dispersion (20 wt.%  $\text{TiO}_2$ ) and spread over the conducting glass to give a film of  $10\ \mu\text{m}$  thickness, which is then calcined at  $450\ ^\circ\text{C}$  for 30 min. Before dye coating, a few monolayers of  $\text{TiO}_2$  are electrodeposited onto the nanocrystalline  $\text{TiO}_2$  film from a  $\text{Ti(III)}$  solution, followed by further annealing at  $450\ ^\circ\text{C}$

## (c) Dye sensitizer layer

The dye *cis*-di(cyanato)bis(2,2'-bipyridyl-4,4'-dicarboxylate)ruthenium(II) (see Fig. 22) was coated onto the nanocrystalline  $\text{TiO}_2$  film by soaking the film for at least 3 h in a  $3 \times 10^{-4}\ \text{mol dm}^{-3}$  solution of the ruthenium complex in dry ethanol. This step was carried out directly after the  $\text{TiO}_2$  had been calcined to avoid the rehydration of the film or capillary condensation of water vapour in the pores of  $\text{TiO}_2$ ; both of these processes decrease the charge injection efficiency of the dye. The electrode was dipped into the dye solution whilst still hot ( $80\ ^\circ\text{C}$ ), withdrawn under a stream of dry air or argon and stored in dry ethanol or used immediately. The visible absorption maximum of the dye is  $493\ \text{nm}$  ( $\epsilon = 1.45 \times 10^4\ \text{dm}^3\ \text{mol}^{-1}\ \text{cm}^{-1}$  in ethanol; lifetime of 166 ns in ethanol-methanol (90 : 10, v/v))

## (d) Electrolyte layer

Fills the gap between the photoanode and the dark counter electrode by capillary action, which are then clamped together. The thickness of this layer is not specified. Typically, the electrolyte comprises  $0.04\ \text{mol dm}^{-3}\ \text{I}_2$  and  $0.5\ \text{mol dm}^{-3}$  tetrapropylammonium iodide in a mixture of ethylene carbonate (80% by volume) and acetonitrile. The use of lithium, rather than tetrapropylammonium cations, improves the performance of the cell

## (e) Counter electrode

Conducting glass coated with a few monolayers of platinum

## (f) Performance characteristics

Using AM 1.5 simulated sunlight ( $83\text{--}75\ \text{mW cm}^{-2}$ ): (a) open-circuit voltage,  $0.66\text{--}0.68\ \text{V}$ ; (b) short-circuit current,  $13\text{--}11.5\ \text{mA cm}^{-2}$ ; fill factor,  $0.76\text{--}0.684$ ; overall solar energy efficiency  $\eta$ ,  $0.079\text{--}0.0713$

## (g) Cell longevity

Tested for 2 months, in which time  $62000\ \text{C cm}^{-2}$  of charge was generated with less than 10% loss in photocurrent. From these values, it is possible to estimate the number of electrons transferred over the 2 month period ( $3.87 \times 10^{23}\ \text{cm}^{-2}$ ) using a film with  $1.3 \times 10^{-7}\ \text{mol cm}^{-2}$  dye (i.e.  $7.83 \times 10^{16}$  molecules of dye  $\text{cm}^{-2}$ ), from which a turnover number for the dye of greater than  $(3.87 \times 10^{23}/7.83 \times 10^{16}) = 4.9 \times 10^6$  can be calculated

## (II) Reflecting, dye-sensitized, nanocrystalline, thin layer, sandwich solar cell [33]

## (a) Conducting glass support substrate

As above

(b) Nanocrystalline  $\text{TiO}_2$  film layer

Two different methods have been used to produce more strongly light scattering, white films of nanocrystalline  $\text{TiO}_2$  in which the particle size is typically greater than  $15\ \text{nm}$  with some particles greater than  $100\ \text{nm}$ . In the first method, the same procedure as above was used, except that an autoclave temperature of  $230\text{--}240\ ^\circ\text{C}$  was employed. In the second method, Degussa P25  $\text{TiO}_2$  was used, and the aggregates were broken up into separate ( $25\ \text{nm}$ ) particles by grinding in a porcelain mortar with a small amount of water containing acetylacetone. The final paste was diluted with water, and a detergent (Triton X-100) was added to facilitate spreading of a layer approximately  $40\ \mu\text{m}$  thick on the conducting glass substrate. The film was annealed for 30 min at  $450\text{--}550\ ^\circ\text{C}$  to produce a  $12\ \mu\text{m}$  thick film. The sensitivity of the film was further enhanced by depositing a thin layer of  $\text{TiO}_2$  from an aqueous solution of titanium tetrachloride; the whole system was further annealed at  $450\text{--}550\ ^\circ\text{C}$  for 30 min. The latter process results in the nucleation of nanometre-sized  $\text{TiO}_2$  particles on the  $\text{TiO}_2$  film, which have a low impurity content thought to favour higher efficiencies than the base, slightly impure (with Fe) Degussa P25  $\text{TiO}_2$  particles

## (c) Dye sensitizer layer

The dye *cis*-di(thiocyanato)bis(2,2'-bipyridyl-4,4'-dicarboxylate)ruthenium(II) (see Fig. 22) was coated onto the nanocrystalline  $\text{TiO}_2$  film as described above. After dye coating, the film was treated with 4-tert-butylpyridine as this increases the open-circuit voltage ( $0.38$  to  $0.66\ \text{V}$ ) and fill factor ( $0.37$  to  $0.63$ ) by suppressing process (3) in Fig. 21, i.e.  $\text{I}_3^- + 2\text{e}^-_{\text{CB}} \rightarrow 3\text{I}^-$ . The 4-tert-butylpyridine at the  $\text{TiO}_2$  surface is thought to block the surface states which are active as intermediates in the above process; calculations indicate that the rate of this process is reduced by as much as a factor of  $5.5 \times 10^4$ . The visible absorption maximum of the dye is  $534\ \text{nm}$  ( $\epsilon = 1.42 \times 10^4\ \text{dm}^3\ \text{mol}^{-1}\ \text{cm}^{-1}$  in ethanol; lifetime of 50 ns in ethanol-methanol (90 : 10, v/v))

## (d) Electrolyte layer

Fills the gap between the photoanode and the dark counter electrode by capillary action, which are then clamped together. The thickness of this layer is not specified. Typically, the electrolyte comprises  $0.04\ \text{mol dm}^{-3}\ \text{I}_2$  in  $0.5\ \text{mol dm}^{-3}$  lithium iodide in acetonitrile

## (e) Counter electrode

Conducting glass coated with a  $2\ \mu\text{m}$  thick platinum mirror deposited by sputtering. Apart from reflecting the light that passes through the semiconductor film, the Pt serves to catalyse the reduction of  $\text{I}_3^-$ , i.e. process (5) in Fig. 21

## (f) Performance characteristics

Using AM 1.5 simulated sunlight ( $96.4\ \text{mW cm}^{-2}$ ): (a) open-circuit voltage,  $0.72\ \text{V}$ ; (b) short-circuit current,  $18.3\ \text{mA cm}^{-2}$ ; fill factor,  $0.73$ ; overall solar energy efficiency  $\eta$ ,  $0.10$

## (g) Cell longevity

Tested for more than 10 months, in which time more than  $10^5\ \text{C cm}^{-2}$  of charge was generated with less than 10% loss in photocurrent. The thiocyanato dye complex was present at a level of  $10^{-7}\ \text{mol cm}^{-2}$ ; thus a turnover number for the dye of more than  $1 \times 10^7$  can be calculated, recently reported as  $5 \times 10^7$

Table 15

Major processes in the modern nanocrystalline TiO<sub>2</sub> photoelectrochemical cell sensitized by *cis*-X<sub>2</sub>bis(2,2'-bipyridyl-4,4'-dicarboxylate)ruthenium(II) (X ≡ CN<sup>−</sup> or SCN<sup>−</sup>) [30,33]

Process	Reaction and comments
(1)	$S^* + \text{TiO}_2 \rightarrow S^+ + \text{TiO}_2(e_{\text{CB}}^-)$ . Photoinduced electron transfer from the electronically excited photosensitizer, adsorbed on the surface of the TiO <sub>2</sub> nanocrystal, to TiO <sub>2</sub> . Studies carried out using <i>cis</i> -X <sub>2</sub> bis(2,2'-bipyridyl-4,4'-dicarboxylate)ruthenium(II) (X ≡ H <sub>2</sub> O) show that this is a very fast process (less than 7 ps) and, given the lifetime of S* (166–50 ns) (see Table 14), the quantum yield of this process is likely to be approximately 100%
(2)	$S^+ + \text{TiO}_2(e_{\text{CB}}^-) \rightarrow S + \text{TiO}_2$ . The back reaction, which is usually slow, typically 1 μs. One reason why process (2) is slow is that the process will be associated with a large driving force, possibly placing it in the Marcus inverted region, where the rate of reaction decreases with increasing exothermicity. In addition, the injected electron will be delocalized over many conduction band states and, if there is only one S <sup>+</sup> available, the back reaction will be associated with a large entropy decrease which will render it unfavourable
(3)	$2\text{TiO}_2(e_{\text{CB}}^-) + \text{I}_3^- \rightarrow 3\text{I}^-$ . The exchange current density for this process is low ( $10^{-11}$ – $10^{-9}$ A cm <sup>−2</sup> ) and, as a result, the photogenerated charge carriers TiO <sub>2</sub> (e <sub>CB</sub> <sup>−</sup> ) can percolate through the nanostructured film without undergoing significant loss through this recombination process, giving a near-quantitative charge collection
(4)	$\text{TiO}_2(e_{\text{CB}}^-) \rightarrow \text{Pt}(e^-)$ . Movement of the photogenerated electron to the back contact ( $1$ – $10^{-3}$ s) is a slow process as there is no/little space charge region; however, it is efficient because of the even slower nature of process (3), although process (2) would render it inefficient if it was not for the super-scavenging action of iodide in process (6) which reduces S <sup>+</sup>
(5)	$2\text{Pt}(e^-) + \text{I}_3^- \rightarrow 3\text{I}^-$ . A very labile process, with an exchange current of 0.1–0.01 A cm <sup>−2</sup>
(6)	$2S^+ + 3\text{I}^- \rightarrow 2S + \text{I}_3^-$ . A very fast process ( $10^{-8}$ s)

Nanocrystalline semiconductor electrodes have high surface area to volume ratios, and therefore a thin layer will provide a much larger surface area for a monolayer of dye to adsorb to than a flat, single-crystal semiconductor electrode, resulting in a larger LHE<sub>λ</sub>. An expression for the latter term is as follows

$$\text{LHE}_\lambda = 1 - 10^{I\sigma(\lambda)R} \quad (20)$$

where  $I$  is the number of moles of dye sensitizer in a monolayer per square centimetre of flat surface,  $\sigma(\lambda)$  is the absorption cross-section of the sensitizer (cm<sup>2</sup> mol<sup>−1</sup>) and  $R$  is the roughness factor for the surface. In a typical modern, dye-sensitized nanocrystalline photoelectrochemical cell [32], the sensitizers used have areas of approximately 1 nm<sup>2</sup>; thus  $I \approx 1.66 \times 10^{-10}$  mol cm<sup>−2</sup> and  $\sigma(\lambda)$  at  $\lambda_{\text{max}}$  is equal to approximately  $1.9 \times 10^7$  cm<sup>2</sup> mol<sup>−1</sup>. Substituting these values for  $I$  and  $\sigma(\lambda)$  in Eq. (20), it follows that, if the dye is adsorbed onto the surface of a perfectly flat single crystal of the semiconductor ( $R = 1$ ), the best LHE<sub>λ</sub> value expected will be 0.0072, which is very inefficient. The roughness factor  $R$  for a nanocrystalline film of the semiconductor can be crudely estimated by assuming that the semiconductor particles of diameter  $d$  are stacked on top of each other to create an overall film of thickness  $b$ . Under these conditions

$$R = \pi b/d \quad (21)$$

In a typical nanocrystalline film (see Table 14),  $b = 10$  μm and  $d = 15$  nm; thus  $R = 2094$  and LHE<sub>λ</sub> ≈ 1, i.e. a much more efficient and viable photoelectrochemical cell than that based on a single-crystal semiconductor. In practice, not all the surface area appears to be utilized by the dye, and roughness factors of 780–1000 are usually reported; however, even under these conditions, the value for LHE<sub>λ</sub> will be greater than 0.99.

The sintering process, i.e. heating the semiconductor film to 450–550 °C, described for both the transparent and reflecting dye-sensitized nanocrystalline photoelectrochemical cells in Table 14, produces electronic contact not only between particles, but also between the particles and the conducting glass support. This electronic contact allows the photoinjected electrons to percolate through the films to the back contact. The result is a sponge-like structure, which is highly porous (typically 50% porous) and has a high surface area to volume ratio. A crude estimate of the degree of porosity ( $P$  (%)) in a nanocrystalline film can be gained by considering it to comprise spherical particles stacked on top of one another. Under these conditions,  $P$  (%) =  $1 - \pi/6 = 0.48$ , regardless of the film thickness. The pores between the particles are interconnected and filled with electrolyte so that the semiconductor–electrolyte interface is accessible throughout the whole film.

The dye at the heart of these new dye-sensitized nanocrystalline sandwich solar cells is *cis*-X<sub>2</sub>bis(2,2'-bipyridyl-4,4'-dicarboxylate)ruthenium(II) [31] where, for the most efficient solar cells, X ≡ CN<sup>−</sup> (for the transparent cells) and SCN<sup>−</sup> (for the most efficient ( $\eta = 10\%$ ) reflecting solar cells); the general structure of these complexes is illustrated in Fig. 22. This class of dye has, for a long time, been ignored, largely because of the much shorter lifetimes (typically less than 200 ns) compared with the more famous trisbipyridyl analogues (typically greater than 600 ns). However, in photoelectrochemistry, charge injection can be much more rapid than even the short lifetime of the *cis*-X<sub>2</sub>bis(2,2'-bipyridyl-4,4'-dicarboxylate)ruthenium(II) compounds and, as a result, these complexes can be very efficient sensitizers (see Table 15, process (1)). The four-ligand complex adsorbs onto the surface of TiO<sub>2</sub> through two of the carboxylate groups, which also provide a strong electronic coupling between the charge transfer excited state of the dye and the

conduction band of the semiconductor. This coupling helps to ensure that the photoinduced electron injection step, process (1) in Table 15, is very rapid, with a quantum yield close to unity [30,33].

When adsorbed onto nanocrystalline  $\text{TiO}_2$ , the visible absorption edge is shifted by about 200 mV. Thus the *cis*-di(thiocyanato)bis(2,2'-bipyridyl-4,4'-dicarboxylate)ruthenium(II) complex has an absorption edge at 708 nm in ethanolic solution, which is shifted to 800 nm when the dye is adsorbed onto  $\text{TiO}_2$ . Fig. 23 illustrates the action spectrum of the nanocrystalline  $\text{TiO}_2$  photoelectrochemical cell using *cis*-di(thiocyanato)bis(2,2'-bipyridyl-4,4'-dicarboxylate)ruthenium(II) as dye sensitizer. Comparing the action spectrum of the *cis*-di(thiocyanato)bis(2,2'-bipyridyl-4,4'-dicarboxylate)ruthenium(II)-sensitized nanocrystalline  $\text{TiO}_2$  photoelectrochemical cell with the spectral profile of sunlight (AM 1.5), as illustrated in Fig. 23, the degree of overlap is striking. The action spectrum is broader than the actual absorption spectrum of the dye, because of the high roughness factor, coupled with the high molar absorptivity of the dye at many wavelengths in the visible; the result is a light-harvesting efficiency of approximately unity at many wavelengths. If the absorption edge of the *cis*- $\text{X}_2$ bis(2,2'-bipyridyl-4,4'-dicarboxylate)ruthenium(II) dye is shifted by 200 mV, it might be expected that the absorption maxima will also be shifted to the same extent, i.e. from 534 nm in ethanolic solution to 584 nm on  $\text{TiO}_2$  for the *cis*- $\text{X}_2$ bis(2,2'-bipyridyl-4,4'-dicarboxylate)ruthenium(II) complex for example.

Although the action spectra of the *cis*- $\text{X}_2$ bis(2,2'-bipyridyl-4,4'-dicarboxylate)ruthenium(II) dye-sensitized nanocrystalline  $\text{TiO}_2$  photoelectrochemical cells have been reported in some detail, the actual visible absorption spectra of the dyes in the cells initially and as a function of time have not been reported. From the literature [30–33] on this cell, we know that the absorption spectrum of the dye is shifted by 200 mV; however, when adjusted for this shift, it is not clear if it is the same shape. A change in shape of the absorption spectrum of the dye might give an indication of the formation of dimers, trimers, etc., and any change in nature with prolonged use might provide an insight into the major dye degradation processes which operate, albeit inefficiently. Although the *cis*- $\text{X}_2$ bis(2,2'-bipyridyl-4,4'-dicarboxylate)ruthenium(II) dye-sensitized nanocrystalline  $\text{TiO}_2$  photoelectrochemical cells appear to have an excellent useful working life, there are some indications that the photocurrent drops initially (by 20%–30%) if simulated sunlight of  $\lambda > 390$  nm is used, although light of  $\lambda > 420$  nm appears to be less effective in reducing the initial cell output. This initial loss in performance is associated with UV excitation of the  $\text{TiO}_2$  nanocrystals and water contamination. After 2–20 days, no significant changes in the cell performance are observed and the photocurrent is stable for months. The observed changes in the visible absorption spectrum of the sensitizer with use, if any, may go some way to identifying in more detail the nature of these processes.

In general, the *cis*-di(thiocyanato)bis(2,2'-bipyridyl-4,4'-dicarboxylate)ruthenium(II) dye sensitizers used in the new photoelectrochemical cells are considered to be very photostable. Although photoinduced ligand substitution is known for these complexes in solvents such as *N,N*-dimethylformamide (DMF), the rates are much slower ( $1.4 \times 10^7$  times slower) than charge injection (approximately  $1.4 \times 10^{11} \text{ s}^{-1}$ ). There appears to be no evidence of ligand substitution in the visible absorption spectrum of the dye after prolonged use. The oxidized form of the sensitizing dye ( $\text{S}^+$ ) may also undergo an internal self-destruction redox reaction; however, cyclic voltammetry studies indicate that this process will be very slow, on the 1 s timescale, whereas the reduction of  $\text{S}^+$  by  $\text{I}^-$  will occur on the  $10^{-8}$  s timescale, as revealed by laser photolysis experiments [33].

In conclusion, the new nanocrystalline photoelectrochemical cells appear to have excellent characteristics as solar to electrical energy conversion devices, with efficiencies of 10% and predicted working lifetimes of 10 years of natural sunlight [30] (the report of “a lifetime consistent with about 108 turnovers for each dye molecule” for such cells is presumably a mistake and should, possibly, read “ $10^8$  turnovers”) [31]. If the high efficiencies for this type of cell and high dye turnover number can be validated by other research groups, and if the production costs are not too high, this type of cell will represent a real challenge to existing solid state photovoltaic cells.

## 14. Conclusions

The field of heterogeneous photocatalysis is very diverse although most work in this area falls under one, or more, of the themes in Scheme 1. Some of the earlier work on semiconductor photosystems has proved to be highly irreproducible; this has not helped the subject to develop as rapidly as it might have done and may have generated some degree of scepticism in the scientific community about subsequent developments in the field. However, as the research has moved away from systems which *might* work in the hands of specific research groups to those which *do* work in the hands of all research groups, a number of research themes have emerged which offer real potential for commercial development and merit much greater research. Of particular promise are the areas of:

1. semiconductor particles as photocatalysts for the removal of organic pollutants [12–20];
2. semiconductor particles and films as sensitizers for the destruction of gaseous and thin film organic pollutants [24,25];
3. semiconductor particles as sensitizers for the photo-destruction of bacteria and viruses [19,25–28];
4. dye-sensitized nanocrystalline photoelectrochemical cells [30–33].

The field of semiconductor photocatalysis is vibrant and involves many research groups throughout the world; it is



one of the fields in photochemistry to be working in and, after a shaky start, appears to be going from strength to strength.

## References

- [1] E. Becquerel, C.R. Acad. Sci. 9 (1839) 561.
- [2] A. Perret, J. Chim. Phys. 23 (1926) 97.
- [3] A. Fujishima, K. Honda, Nature (London) 238 (1972) 37.
- [4] M.S. Wrighton, Acc. Chem. Res. 12 (1979) 303.
- [5] A.J. Bard, Science 207 (1980) 139.
- [6] M. Grätzel (Ed.), Energy Resources Through Photochemistry and Catalysis, Academic Press, New York, 1983.
- [7] S. Licht, Sol. Energy Mater. Sol. Cells 38 (1995) 305.
- [8] B. Parkinson, Acc. Chem. Res. 17 (1984) 431.
- [9] M.X. Tan, P.E. Laibinis, S.T. Nguyen, J.M. Kesselman, C.E. Stanton, N.S. Lewis, in: K.D. Karlin (Ed.), Progress in Inorganic Chemistry, Vol. 41, Wiley, New York, 1994, pp. 21–144.
- [10] K. Kalyanasundaram, M. Grätzel, Coord. Chem. Rev. 69 (1986) 57.
- [11] A. Mills, in: F. Hartley (Ed.), Chemistry of the Platinum Group Metals: Recent Developments, Elsevier, New York, 1991.
- [12] N. Serpone, E. Pelizzetti (Eds.), Photocatalysis: Fundamentals and Applications, Wiley, New York, 1989.
- [13] M.A. Fox, M.T. Dulay, Chem. Rev. 93 (1993) 341.
- [14] P.V. Kamat, Chem. Rev. 93 (1993) 267.
- [15] A. Mills, R.H. Davies, D. Worsley, Chem. Soc. Rev. 22 (1993) 417.
- [16] M.R. Hoffmann, S.T. Martin, W. Choi, D.W. Bahnemann, Chem. Rev. 95 (1995) 69.
- [17] A.L. Linsebigler, G. Lu, J.T. Yates, Chem. Rev. 95 (1995) 735.
- [18] M. Grätzel, Heterogeneous Photochemical Electron Transfer, CRC Press, Boca Raton, 1989.
- [19] D. Ollis, H. El-Akabi (Eds.), Photocatalytic Purification and Treatment of Water and Air, Elsevier, New York, 1993.
- [20] M. Sciavello (Ed.), Photocatalysis and Environment: Trends and Applications, Kluwer Academic Publishers, Dordrecht, 1988.
- [21] J.A. Davies, D.L. Boucher, J.G. Edwards, in: D.C. Neckers, D.H. Volman, G. von Bülow (Eds.), Adv. Photochem. 19 (1995) 235–309.
- [22] M.A. Fox, Acc. Chem. Res. 16 (1983) 314.
- [23] M.A. Fox, Top. Curr. Chem. 142 (1987) 72.
- [24] A. Heller, Acc. Chem. Res. 28 (1995) 503.
- [25] R. Cai, K. Hashimoto, K. Itoh, Y. Kubota, A. Fujishima, Bull. Chem. Soc. Jpn. 64 (1991) 1268.
- [26] R. Cai, Y. Kubota, T. Shuin, H. Sakai, K. Hashimoto, A. Fujishima, Cancer Res. 52 (1992) 2346.
- [27] T. Matsunaga, R. Tomoda, T. Nakajima, H. Wake, FEMS Microbiol. Lett. 29 (1985) 211.
- [28] T. Matsunaga, R. Tomoda, T. Nakajima, N. Nakamura, T. Komine, Appl. Environ. Microbiol. 54 (1988) 1330.
- [29] A. Henglein, Chem. Rev. 89 (1989) 1861.
- [30] A. Hagfeldt, M. Grätzel, Chem. Rev. 95 (1995) 49.
- [31] A.J. McEvoy, M. Grätzel, Sol. Energy Mater. Sol. Cells 32 (1994) 221.
- [32] M. Grätzel, B. O'Regan, Nature (London) 353 (1991) 737.
- [33] M.K. Nazeruddin, A. Kay, I. Rodicio, R. Humphry-Baker, E. Müller, P. Liska, N. Vlachopoulos, M. Grätzel, J. Am. Chem. Soc. 115 (1993) 6382.
- [34] P. Suppan, Chemistry and Light, Royal Society of Chemistry, Cambridge, 1994, p. 5.
- [35] G. Porter, in: J.D. Coyle, R.R. Hill, D.R. Roberts (Eds.), Light, Chemical Change and Life: a Source Book in Photochemistry, Open University Press, Milton Keynes, 1982, p. 355.
- [36] P. Pichat, M.N. Mozzanega, H. Courbou, J. Chem. Soc., Faraday Trans. 1 83 (1987) 697.
- [37] E. Borgarello, R. Harris, N. Serpone, Nouv. J. Chim. 9 (1985) 74.
- [38] T. Kawai, T. Sakata, Nature (London) 286 (1980) 474.
- [39] W.H. Brattain, C.G.B. Garret, Bell. Syst. Tech. J. 34 (1955) 129.
- [40] E. Keidel, Furben Zeitung 34 (1929) 1242.
- [41] C.F. Goodeve, J.A. Kitchener, Trans. Faraday Soc. 34 (1938) 570, and references cited therein.
- [42] S.P. Fappas, R.M. Fischer, J. Paint Technol. 46 (1974) 65.
- [43] H. Gerischer, in: H. Eyring, D. Henderson, W. Jost (Eds.), Physical Chemistry—An Advanced Treatise, Academic Press, New York, 1970, pp. 463–542.
- [44] V.A. Myamlin, Y. Pleskov, Electrochemistry of Semiconductors, Plenum, New York, 1967.
- [45] Y.V. Pleskov, Y.Y. Gurevich, Semiconductor Photoelectrochemistry, Plenum, New York, 1986.
- [46] Y.V. Pleskov, Solar Energy Conversion, Springer-Verlag, Berlin, 1990.
- [47] M.S. Wrighton, A.B. Ellis, P.T. Wolczanski, D.L. Morse, H.B. Abrahamson, D.S. Ginley, J. Am. Chem. Soc. 98 (1976) 2774.
- [48] G.S. Calabrese, M.S. Wrighton, J. Am. Chem. Soc. 103 (1981) 6273.
- [49] C.R. Dickson, A.J. Nozik, J. Am. Chem. Soc. 100 (1978) 8007.
- [50] A. Nozik, Nature (London) 257 (1975) 383.
- [51] M. Halman, Nature (London) 275 (1975) 113.
- [52] B.J. Tufts, I.L. Abrahams, G.P. Santangelo, G.N. Ryba, L.G. Casagrande, N.S. Lewis, Nature (London) 326 (1987) 861.
- [53] A. Heller, B. Miller, F.A. Thiel, Appl. Phys. Lett. 38 (1981) 282.
- [54] G. Kline, K. Kam, D. Cranfield, B.A. Parkinson, Sol. Energy Mater. 6 (1982) 337.
- [55] S. Licht, D. Peramunage, Nature (London) 345 (1990) 330.
- [56] G. Hodes, Nature (London) 285 (1980) 29.
- [57] A. Heller, H. Lewerenz, B. Miller, Ber. Bunsenges. Phys. Chem. 84 (1980) 592.
- [58] M.A. Russak, J. Reichman, C. Creter, J. DeGaro, 5th Photoelectrochemical Cell Contractors Review S.E.R.I., Golden, Colorado, June 15–16, 1982.
- [59] T. Sakata, T. Kawai, Nouv. J. Chim. 5 (1981) 279.
- [60] P. Pichat, M.N. Mozzanega, J. Disdier, J.M. Herrmann, Nouv. J. Chim. 6 (1982) 559.
- [61] A. Mills, G. Porter, J. Chem. Soc., Faraday Trans. 1 78 (1982) 3659.
- [62] P. Cruendet, K.K. Rao, M. Grätzel, D.O. Hall, Biochimie 68 (1986) 3659.
- [63] D.H.M.W. Thewissen, K. Timmer, E.A. Zouwen-Assink, A.H.A. Tinnemans, A. Mackor, J. Chem. Soc., Chem. Commun. (1985) 1485.
- [64] J.S. Curran, J. Domenech, N. Jaffrezic-Renault, R. Phillipe, J. Phys. Chem. 89 (1985) 957.
- [65] J. Darwent, A. Mills, J. Chem. Soc., Faraday Trans. 2 78 (1982) 359.
- [66] N.M. Dimitrijevic, S. Li, M. Grätzel, J. Am. Chem. Soc. 106 (1984) 6565.
- [67] I. Lauermaun, D. Meissner, R. Memming, J. Electroanal. Chem. 228 (1987) 45.
- [68] A.V. Bulatov, M.L. Khidkel, Izv. Akad. Nauk SSSR Ser. Khim. (1976) 1902.
- [69] D. Duonghong, E. Borgarello, M. Grätzel, J. Am. Chem. Soc. 103 (1981) 4685.
- [70] J.M. Lehn, J.P. Sauvage, Nouv. J. Chim. 4 (1980) 623. K. Sayama, H. Arakawa, J. Chem. Soc., Chem. Commun. (1992) 150.
- [71] E. Borgarello, K. Kalyanasundaram, D. Duonghong, M. Grätzel, Angew. Chem. Int. Ed. Engl. 20 (1981) 987.
- [72] M.M. Taqui Khan, R.C. Bhardwaj, C.M. Jadhav, J. Chem. Soc., Chem. Commun. (1985) 1690.
- [73] L. Milgrom, New Scientist, 2nd February (1984) 26.
- [74] A.L. Pruden, D.F. Ollis, J. Catal. 82 (1983) 404.
- [75] C.Y. Hsiao, C.L. Lee, D.F. Ollis, J. Catal. 82 (1983) 418.
- [76] R.W. Matthews, J. Catal. 97 (1986) 565.
- [77] K. Okamoto, Y. Yamamoto, H. Tanaka, A. Itaya, Bull. Chem. Soc. Jpn. 58 (1985) 2023.
- [78] S. Morris, Photocatalysis for water purification, Ph.D. Thesis, University of Wales, 1992, Chapter 1.

- [79] E. Pelizzetti, C. Minero, V. Maurino, *Adv. Colloid Interface Sci.* 32 (1990) 271.
- [80] A. Mills, P. Sawunyama, *J. Photochem. Photobiol. A: Chem.* 84 (1994) 305.
- [81] N. Serpone, G. Sauve, R. Koch, H. Tahiri, P. Pichat, P. Piccinini, E. Pelizzetti, H. Hidaka, *J. Photochem. Photobiol. A: Chem.* 94 (1996) 191.
- [82] H. Gerischer, A. Heller, *J. Phys. Chem.* 95 (1991) 5261.
- [83] H. Gerischer, A. Heller, *J. Am. Chem. Soc.* 114 (1992) 5230.
- [84] J.M. Kesselman, G.A. Shreve, M.R. Hoffmann, N.S. Lewis, *J. Phys. Chem.* 98 (1994) 13 385.
- [85] S. Le Hunte, PGM's in semiconductor photocatalysis, M. Phil. Thesis, University of Wales, 1995.
- [86] C.S. Turchi, D.F. Ollis, *J. Catal.* 122 (1990) 178.
- [87] M. Bideau, B. Claudel, C. Dubien, L. Faure, H. Kazouan, *J. Photochem. Photobiol. A: Chem.* 91 (1995) 137.
- [88] C.S. Turchi, D.F. Ollis, *J. Phys. Chem.* 92 (1988) 6852.
- [89] A. Mills, R. Davies, *J. Photochem. Photobiol. A: Chem.* 85 (1995) 173.
- [90] M. Abdullah, G.K. Low, R.W. Matthews, *J. Phys. Chem.* 94 (1990) 6820.
- [91] J.R. Bolton, R.G. Bircher, W. Tumas, C.A. Tolman, *J. Adv. Oxid. Technol.* 1 (1996) 13.
- [92] N. Serpone, R. Terzian, D. Lawless, P. Kennepohl, G. Sauve, *J. Photochem. Photobiol. A: Chem.* 73 (1993) 11.
- [93] M. Sciavello, V. Augugliaro, L. Palmisano, *J. Catal.* 127 (1991) 332.
- [94] T. Watanabe, T. Takizawa, K. Honad, *J. Phys. Chem.* 81 (1977) 1845.
- [95] R.W. Matthews, S.R. McEvoy, *J. Photochem. Photobiol. A: Chem.* 66 (1992) 355.
- [96] A. Mills, S. Morris, R. Davies, *J. Photochem. Photobiol. A: Chem.* 70 (1993) 183.
- [97] A. Mills, S. Morris, *J. Photochem. Photobiol. A: Chem.* 71 (1993) 75.
- [98] Y. Hori, A. Nakatsu, S. Susuki, *Chem. Lett.* (1985) 1429.
- [99] S.N. Frank, A.J. Bard, *J. Phys. Chem.* 81 (1977) 1484.
- [100] J.M. Herrmann, J. Disdier, P. Pichat, *J. Catal.* 113 (1988) 72.
- [101] S.N. Frank, A.J. Bard, *J. Am. Chem. Soc.* 99 (1977) 303.
- [102] H. Hidaka, T. Nakamura, A. Ishizaha, M. Tsuchiya, J. Zhao, *J. Photochem. Photobiol. A: Chem.* 66 (1992) 367.
- [103] E. Borgarello, R. Harris, N. Serpone, *Nouv. J. Chim.* 9 (1985) 741.
- [104] J.M. Herrmann, C. Guillard, P. Pichat, *Catal. Today* 17 (1993) 7.
- [105] K. Tanaka, K. Harda, S. Murata, *Sol. Energy* 36 (1986) 159.
- [106] A. Lozano, J. Garcia, X. Domenech, J. Casado, *J. Photochem. Photobiol. A: Chem.* 69 (1992) 237.
- [107] A.A. Krasnovskii, G.P. Brin, V.V. Nikandrov, *Dokl. Akad. Nauk. SSSR* 229 (1976) 990.
- [108] Y. Oosawa, *Chem. Lett.* (1982) 423.
- [109] A. Mills, A. Belghazi, D. Rodman, *Water Res.* 30 (1996) 1973.
- [110] H. Mozzanega, J.M. Herrmann, P. Pichat, *J. Phys. Chem.* 83 (1979) 2251.
- [111] J.M. Herrmann, J. Disdier, P. Pichat, in: P. Grange, P.A. Jacobs, G. Poncet (Eds.), *Preparation of Catalysts IV*, Elsevier, Amsterdam, 1987, p. 285.
- [112] N. Serpone, Y.K. Ah-You, T.P. Tran, R. Harris, *Sol. Energy* 39 (1987) 491.
- [113] E. Borgarello, N. Serpone, G. Emo, R. Harris, E. Pelizzetti, C. Minero, *Inorg. Chem.* 25 (1986) 4499.
- [114] N. Serpone, E. Borgarello, M. Barbeni, E. Pelizzetti, P. Pichat, J.M. Herrmann, M.A. Fox, *J. Photochem.* 36 (1987) 373.
- [115] G.N. Schrauzer, T.D. Guth, *J. Am. Chem. Soc.* 99 (1977) 7189.
- [116] J.G. Edwards, J.A. Davies, D.L. Boucher, A. Mennard, *Angew. Chem. Int. Ed. Engl.* 31 (1992) 480.
- [117] J.G. Edwards, J.A. Davies, *Angew. Chem. Int. Ed. Engl.* 32 (1993) 552.
- [118] D.L. Boucher, J.A. Davies, J.G. Edwards, A. Mennad, *J. Photochem. Photobiol. A: Chem.* 88 (1995) 53.
- [119] V. Augugliaro, J. Soria, *Angew. Chem. Int. Ed. Engl.* 32 (1993) 550.
- [120] L. Palmisano, M. Schiavello, A. Sclafani, *Angew. Chem. Int. Ed. Engl.* 32 (1993) 551.
- [121] J.C. Hemminger, R. Carr, G.A. Somorjai, *Chem. Phys. Lett.* 57 (1978) 100.
- [122] B. Moore, T.A. Webster, *Proc. R. Soc. London, Ser. B* 87 (1913) 163.
- [123] N.R. Dhar, E.V. Sechacharyubu, S.K. Mukerji, *Ann. Agron.* 11 (1941) 83.
- [124] G.N. Schrauzer, N. Strampach, L.N. Hui, M.R. Palmer, J. Salehi, *Proc. Natl. Acad. Sci. USA* 80 (1983) 3873.
- [125] W.W. Dunn, Y. Aikawa, A. Bard, *J. Am. Chem. Soc.* 103 (1981) 6893.
- [126] R.A. Kerr, *Science* 219 (1980) 42.
- [127] B. Kraeutler, A.J. Bard, *J. Am. Chem. Soc.* 100 (1978) 2239.
- [128] B. Kraeutler, A.J. Bard, *Nouv. J. Chim.* 3 (1979) 31.
- [129] M.A. Fox, A.A. Abdel-Wahab, Y.S. Kim, M. Dulay, *J. Catal.* 126 (1990) 693.
- [130] M.A. Fox, C.C. Chen, *J. Am. Chem. Soc.* 103 (1981) 6757.
- [131] D. Worsley, A. Mills, K. Smith, M.G. Hutchings, *J. Chem. Soc., Chem. Commun.* (1995) 1119.
- [132] H. Kasturirangan, V. Ramakrishnan, J.C. Kuriacose, *J. Catal.* 69 (1981) 216.
- [133] B. Ohtani, T. Watanabe, K. Honda, *J. Am. Chem. Soc.* 108 (1986) 308.
- [134] F.H. Hussein, G. Pattenden, R. Rudham, J.J. Russell, *Tetrahedron Lett.* 25 (1984) 3363.
- [135] R.S. Davidson, J.E. Pratt, *Tetrahedron Lett.* 24 (1983) 5903.
- [136] M.A. Fox, C.C. Chen, K.H. Park, J.H. Younathan, *Am. Chem. Soc. Symp. Ser.* 278 (1985) 69.
- [137] H. Yamataka, N. Seto, J. Ichihara, T. Hanafusa, S. Teratani, *J. Chem. Soc., Chem. Commun.* (1985) 788.
- [138] S. Lahiry, C. Halder, *Sol. Energy* 37 (1986) 71. H. Ikezawa, C. Kutal, *J. Org. Chem.* 52 (1987) 3299.
- [139] C.M. Wang, T.E. Mallouk, *J. Am. Chem. Soc.* 112 (1990) 2026.
- [140] A. Maldotti, R. Amadelli, C. Bartocci, V. Carassiti, *J. Photochem. Photobiol. A: Chem.* 53 (1990) 263.
- [141] B. Kraeutler, H. Reiche, A.J. Bard, *J. Polym. Sci., Polym. Lett. Ed.* 17 (1979) 535.
- [142] N. Djegheri, S.J. Teichner, *J. Catal.* 62 (1980) 99.
- [143] M.L. Sauer, M.A. Hale, D.F. Ollis, *J. Photochem. Photobiol. A: Chem.* 88 (1995) 169.
- [144] Y. Luo, D.F. Ollis, *J. Catal.* 163 (1996) 215.
- [145] M.R. Nimlos, W.R. Jacoby, D.M. Blake, T.A. Milne, *Environ. Sci. Technol.* 27 (1993) 732.
- [146] W.A. Jacoby, M.R. Nimlos, D.M. Blake, R.D. Nobble, C.A. Koval, *Environ. Sci. Technol.* 24 (1994) 1661.
- [147] S. Yamazaki-Nishida, K.J. Nagano, L.A. Phillips, S. Cervera-March, M.A. Anderson, *J. Photochem. Photobiol. A: Chem.* 70 (1993) 95.
- [148] J.M. Herrmann, J. Disdier, M.N. Mozzanega, P. Pichat, *J. Catal.* 60 (1979) 369.
- [149] N. Djegheri, M. Formenti, F. Juillet, S.J. Teichner, *Faraday Discuss. Chem. Soc.* 58 (1974) 185.
- [150] M. Gratzel, K.R. Thampi, J. Kiwi, *J. Phys. Chem.* 93 (1989) 4128.
- [151] N.R. Blake, G.L. Griffin, *J. Phys. Chem.* 92 (1988) 5697.
- [152] S.A. Larson, J.A. Widegren, J.L. Falconer, *J. Catal.* 157 (1995) 611.
- [153] N. Takeda, T. Torimoto, S. Sampath, S. Kuwabata, H. Yoneyama, *J. Phys. Chem.* 99 (1995) 9986.
- [154] I. Sopyan, M. Watanabe, S. Murasawa, K. Hashimoto, A. Fujishima, *J. Photochem. Photobiol. A: Chem.* 98 (1996) 79.
- [155] M.L. Sauer, D.F. Ollis, *J. Catal.* 149 (1994) 81.
- [156] G.B. Raupp, C.T. Junio, *Appl. Surf. Sci.* 72 (1993) 321.
- [157] A. Pruden, D.F. Ollis, *J. Catal.* 60 (1983) 404.
- [158] W. Holden, A. Marcellino, D. Valic, A.C. Weedon, in: D. Ollis, H. El-Akabi (Eds.), *Photocatalytic Purification and Treatment of Water and Air*, Elsevier, New York, 1993, p. 393.
- [159] S. Sampath, H. Uchida, H. Yoneyama, *J. Catal.* 149 (1994) 189.

- [160] J. Peral, D.F. Ollis, in: D. Ollis, H. El-Akabi (Eds.), Photocatalytic Purification and Treatment of Water and Air, Elsevier, New York, 1993, p. 741.
- [161] J. Peral, D.F. Ollis, J. Catal. 136 (1992) 554.
- [162] M.L. Sauer, D.F. Ollis, J. Catal. 163 (1996) 215.
- [163] T. Ibusuki, T. Takeuchi, Atmos. Environ. 20 (1986) 1711.
- [164] L.A. Dibble, G.B. Raupp, Environ. Sci. Technol. 26 (1992) 492.
- [165] M. Primet, J. Basset, M.V. Mothien, M. Prettre, J. Phys. Chem. 76 (1970) 2868.
- [166] S. Sitkiewitz, A. Heller, New J. Chem. 20 (1996) 233.
- [167] W.A. Jacoby, D.M. Blake, R.D. Noble, C.A. Koval, J. Catal. 157 (1995) 87.
- [168] K. Suzuki, in: D. Ollis, H. El-Akabi (Eds.), Photocatalytic Purification and Treatment of Water and Air, Elsevier, New York, 1993, p. 421.
- [169] T. Watanabe, A. Kitamura, E. Kojima, C. Nakayama, K. Hashimoto, A. Fujishima, in: D. Ollis, H. El-Akabi (Eds.), Photocatalytic Purification and Treatment of Water and Air, Elsevier, New York, 1993, p. 747.
- [170] I. Sopyan, S. Murasawa, K. Hashimoto, A. Fujishima, Chem. Lett. (1994) 723.
- [171] N. Negishi, T. Iyoda, K. Hashimoto, A. Fujishima, Chem. Lett. (1995) 841.
- [172] T. Ibusuki, S. Kutsuna, K. Takeuchi, in: D. Ollis, H. El-Akabi (Eds.), Photocatalytic Purification and Treatment of Water and Air, Elsevier, New York, 1993, p. 375.
- [173] Chem. Br. 33 (1997) 18.
- [174] N.B. Jackson, C.M. Wang, Z. Luo, J. Schwitzgebel, J.G. Ekerdt, J.R. Brock, A. Heller, J. Electrochem. Soc. 138 (1991) 3660.
- [175] Y. Paz, Z. Luo, L. Rabenberg, A. Heller, J. Mater. Chem. 10 (1995) 2842.
- [176] A. Heller, M. Nair, L. Davidson, Z. Luo, J. Schwitzgebel, J. Norrell, J.R. Brock, S.E. Lindquist, J.G. Ekerdt, in: D. Ollis, H. El-Akabi (Eds.), Photocatalytic Purification and Treatment of Water and Air, Elsevier, New York, 1993, p. 139.
- [177] A. Heller, J. Schwitzgebel, M. Pishko, J.G. Ekerdt, in: T.L. Rose, O. Murphy, E. Rudd, B.E. Conway (Eds.), Proceedings of Environmental Catalysis (Waste Water Treatment). Vol. 94-19, The American Electrochemical Society, Pennington, NJ, 1994, p. 1.
- [178] J. Schwitzgebel, J.G. Ekerdt, H. Gerischer, A. Heller, J. Phys. Chem. 99 (1995) 5633.
- [179] G.A. Russell, J. Am. Chem. Soc. 79 (1957) 3871.
- [180] E.C. Butler, A.P. Davis, J. Photochem. Photobiol. A: Chem. 70 (1993) 273.
- [181] A. Scafani, L. Palmisano, E. Davi, J. Photochem. Photobiol. A: Chem. 56 (1991) 113.
- [182] R. Bonnett, Chem. Soc. Rev. (1995) 19.
- [183] M. Wainwright, Chem. Soc. Rev. (1996) 351.
- [184] R. Cai, K. Hashimoto, Y. Kubota, A. Fujishima, Chem. Lett. (1992) 427.
- [185] H. Sakai, E. Ito, R. Cai, T. Yoshioka, Y. Kubota, K. Hashimoto, A. Fujishima, Biochim. Biophys. Acta 1201 (1994) 259.
- [186] H. Sakai, R. Baba, K. Hashimoto, Y. Kubota, A. Fujishima, Chem. Lett. (1995) 185.
- [187] T. Saito, T. Iwase, J. Horie, T. Morioka, J. Photochem. Photobiol. B: Biol. 14 (1992) 369.
- [188] J.C. Ireland, P. Klostermann, E.W. Rice, R.M. Clark, Appl. Environ. Microbiol. 59 (1993) 1668.
- [189] C. Wei, W.Y. Lin, Z. Zainal, N.E. Williams, K. Zhu, A.P. Kruzic, R.L. Smith, K. Rajeshwar, Environ. Sci. Technol. 28 (1994) 934.
- [190] P. Zhang, R.J. Scrudato, G. Germano, Chemosphere 28 (1994) 607.
- [191] T. Matsunaga, M. Okochi, Environ. Sci. Technol. 29 (1995) 501.
- [192] J.C. Sjogren, R.A. Sierka, Appl. Environ. Microbiol. 60 (1994) 344.
- [193] R.J. Watts, S. Kong, M.P. Orr, G.C. Miller, B.E. Henry, Water Res. 29 (1995) 95.
- [194] T. Ogawa, T. Saito, K. Unno, K. Hasegawa, Y. Yoshioka, N. Tsubochi, S. Hosoi, T. Katayama, A. Fujishima, K. Hashimoto, Japanese Patent 07000462, January 6th, 1995.
- [195] D. Duonghong, J. Ramsden, M. Grätzel, J. Am. Chem. Soc. 104 (1982) 2977.
- [196] J. Moser, M. Grätzel, J. Am. Chem. Soc. 105 (1983) 6547.
- [197] L. Spanhel, M. Haase, H. Weller, A. Henglein, J. Am. Chem. Soc. 109 (1987) 5649.
- [198] C. Kormann, D.W. Bahnemann, M.R. Hoffmann, J. Phys. Chem. 92 (1988) 5196.
- [199] A.J. Nozik, in: D. Ollis, H. El-Akabi (Eds.), Photocatalytic Purification and Treatment of Water and Air, Elsevier, New York, 1993, p. 39.
- [200] H. Weller, H.M. Schmidt, U. Koch, A. Fojtik, S. Baral, A. Henglein, W. Kunath, K. Weiss, E. Dieman, Chem. Phys. Lett. 124 (1986) 557.
- [201] A.J. Hoffmann, G. Mills, H. Yee, M.R. Hoffmann, J. Phys. Chem. 96 (1992) 5546.
- [202] A.J. Hoffmann, H. Yee, G. Mills, M.R. Hoffmann, J. Phys. Chem. 96 (1992) 5540.
- [203] D. Bahnemann, A. Henglein, J. Lilie, L. Spanhel, J. Phys. Chem. 88 (1984) 709.
- [204] G.T. Brown, J.R. Darwent, J. Phys. Chem. 88 (1984) 4955.
- [205] R.B. Draper, M.A. Fox, Langmuir 6 (1990) 1396.
- [206] R.B. Draper, M.A. Fox, J. Phys. Chem. 94 (1990) 4628.
- [207] D. Duonghong, J. Ramsden, M. Grätzel, J. Am. Chem. Soc. 104 (1982) 2977.
- [208] G.R. Brown, J.R. Darwent, J. Am. Chem. Soc. 107 (1985) 6446.
- [209] G.R. Brown, J.R. Darwent, J. Chem. Soc., Faraday Trans. 1 80 (1984) 1631.
- [210] P.V. Kamat, J. Chem. Soc., Faraday Trans. 1 81 (1985) 509.
- [211] K.R. Gopidas, P.V. Kamat, Langmuir 5 (1985) 22.
- [212] A. Henglein, Ber. Bunsenges. Phys. Chem. 86 (1982) 24.
- [213] L. Spanhel, H. Weller, A. Henglein, J. Am. Chem. Soc. 109 (1987) 6632.